

**Scalable Xeno-Free Expansion of Human  
Pluripotent Stem Cells in Stirred-  
Suspension Vessels and Their  
Differentiation into Pancreatic Progenitor  
Cells**

A dissertation submitted by

**Yongjia Fan**

in partial fulfillment of the requirements for the degree of

Doctor of Philosophy

in

Chemical Engineering

Tufts University

February 2016

Advisor: Emmanuel S. Tzanakakis

## **Abstract**

Recent advances on human pluripotent stem cells (hPSCs), including human embryonic stem cells (hESCs) and induced pluripotent stem cells (hiPSCs) have brought us closer to the realization of their clinical potential. Nonetheless, tissue engineering and regenerative medicine applications will require the generation of hPSC products well beyond the laboratory scale. This also mandates the production of hPSC therapeutics in fully-defined, xeno-free systems and in a reproducible manner.

In this work, we first showed that hPSCs can be propagated on peptide-conjugated/poly-L-lysine (pLL)-treated microcarriers in spinner flasks for long-term while maintaining their pluripotency, normal karyotype, proliferation and differentiation capacity. Mesoderm differentiation of cells can be integrated as a single process with expansion of hPSCs on the microcarriers without compromising differentiation efficiency.

Considering the specific gravity of the peptide-conjugated microcarriers and the complexity in the preparation, we developed another approach to engineer polystyrene microcarriers with vitronectin, human serum albumin (HSA) and UV irradiation. In this way, we were able to prepare xeno-free VN-HSA-UV microcarriers for long-term cultivation of hPSCs observing yields comparable to those in cultures with peptide-conjugated microcarriers. Preparation of the VN-HSA-UV beads however was significantly shorter and more straightforward.

On the other side, a differentiation protocol to coax hPSCs into insulin-expressing pancreatic progenitor cells was developed under completely xeno-free conditions.

All xenogeneic components were eliminated or substituted with xeno-free reagents. The specification strategy was optimized based on both the differentiation and the maintenance of cell viability.

In conclusion, this work provides a step forward to the development of bioprocessing of hPSCs integrating expansion and directed pancreatic differentiation of human stem cells for the production of therapeutically useful pancreatic cell progeny.

## **Acknowledgement**

First of all and most importantly, I would like to thank my advisor, Dr. Tzanakakis, for his patience, insightful guidance and endless support throughout my Ph.D. study. His hard work and passion to science is an inspiration to me. His deep and broad knowledge of scalable cell culture in bioreactors, pancreatic cell biology, and molecular biology techniques provides me great help during my graduate research life.

I also would like to thank my committee members: Dr. Kyongbum Lee, Dr. Qiaobing Xu and Dr. Laertis Ikonou for their invaluable advice and help on my Ph.D. dissertation.

Next I would like to thank my previous and current lab colleagues: Dr. Lye Theng Lock, Dr. Donghui Jing, Dr. Abhirath Parikh, Dr. Jincheng Wu, Michael Hsiung, Roofya Rahmati, Preeti Ashok and Fan Zhang. Their support and friendship will always be one of the most memorable parts during my Ph.D. study. My appreciation is also extended to our collaborator Prof. Chong Chen from SUNY Buffalo on the generation of microcarriers using surface peptide conjugation.

Lastly, I cannot finish this work without my family's support. My parents and my husband are always there for me during my long journey of Ph.D. study. It is hard for me to express how much I love and owe them.

# Table of Contents

Abstract.....	ii
Acknowledgement .....	iv
Table of Contents.....	v
List of Figures.....	x
Introduction and Background .....	1
1.1 Motivation .....	1
1.2 Xeno-free culture of hPSCs .....	3
1.2.1 Xeno-free media for maintaining undifferentiated hPSCs.....	4
1.2.2 Xeno-free extracellular matrices (ECM) for the maintenance of undifferentiated hPSCs .....	8
1.3 Large-scale cultivation of hPSCs.....	14
1.3.1 Cell encapsulation.....	16
1.3.2 Microcarriers.....	18
1.4 Differentiation of human pluripotent stem cells towards pancreatic progenitors .....	23
1.4.1 Diabetes and stem cell-based therapy .....	23
1.4.2 Pancreatic differentiation strategy .....	25
2 Peptide-conjugated microcarrier expansion and differentiation of hPSCs ...	28
2.1 Introduction .....	28

2.2	Materials and Methods .....	30
2.2.1	Human pluripotent stem cell culture .....	30
2.2.2	Microcarrier seeding and passaging .....	31
2.2.3	Preparation of microcarriers with peptide conjugation and pLL treatment .....	32
2.2.4	RT-PCR and quantitative PCR .....	33
2.2.5	Flow cytometry .....	35
2.2.6	Immunocytochemistry .....	36
2.2.7	Karyotyping .....	37
2.2.8	Embryoid body formation .....	37
2.2.9	Definitive endoderm, mesoderm, and neuroectoderm differentiation .	38
2.2.10	Statistical Analysis .....	39
2.3	Results .....	40
2.3.1	Single dispersed hESC seeding on Matrigel-coated microcarriers for stirred suspension culture .....	40
2.3.2	Multi-passage suspension culture of hPSCs seeded as dispersed cells on Matrigel-coated microcarriers .....	43
2.3.3	Culture of hPSCs on peptide-conjugated microcarriers .....	46
2.3.4	Human PSC expansion on peptide-conjugated, pLL-treated microcarriers .....	48

2.3.5 Directed differentiation of hPSCs on CP+pLL microcarriers in stirred-suspension culture .....	54
2.4 Discussion .....	56
3 Scalable xeno-free microcarrier cultivation of human pluripotent stem cells in stirred suspension.....	62
3.1 Introduction .....	62
3.2 Materials and Methods .....	63
3.2.1 Human pluripotent stem cell culture.....	63
3.2.2 Microcarrier preparation .....	63
3.2.3 Microcarrier seeding and passaging.....	64
3.2.4 RT-PCR and quantitative PCR .....	65
3.2.5 Flow cytometry .....	65
3.2.6 Immunocytochemistry .....	66
3.2.7 Embryoid body formation.....	66
3.2.8 Definitive endoderm, mesoderm, and neuroectoderm differentiation .	67
3.2.9 Statistical Analysis.....	69
3.3 Results .....	69
3.3.1 Treating microcarrier surface with vitronectin, HSA, and UV irradiation.....	69
3.3.2 Human PSC expansion on Plastic Plus and Plastic microcarriers coated with vitronectin and HSA, and treated with UV .....	72

3.3.3	Multi-passage suspension culture of hESCs seeded on VN-HSA-UV microcarriers .....	75
3.4	Discussion .....	78
4	Xeno-Free Differentiation of hPSC towards Pancreatic Progenitor Cells....	81
4.1	Introduction .....	81
4.2	Materials and Methods .....	82
4.2.1	Human PSC culture and differentiation.....	82
4.2.2	Reverse transcription and quantitative PCR .....	83
4.2.3	Flow cytometry .....	84
4.2.4	Immunocytochemistry .....	85
4.3	Results .....	85
4.3.1	Effects of different basal medium on the cell viability of DE differentiation stage .....	85
4.3.2	Differentiation of hPSCs into PGT cells.....	89
4.3.3	Directed differentiation of hPSCs into <i>PDX1</i> -expressing pancreatic progenitor cells.....	89
4.3.4	Differentiation of hPSCs into insulin-producing pancreatic progenitor cells .....	92
4.4	Discussion .....	93
5	Conclusion and Future Work .....	95
5.1	Impact of the work .....	95

5.2 Outlook and future work .....	96
Bibliography .....	98

## List of Figures

<b>Figure 1.1</b> Bioprocessing of hPSCs for use in therapeutic applications. ....	2
<b>Figure 1.2</b> Schematic demonstration of microenvironment faced by hPSCs including soluble factors, mechanical forces, interaction between cell and extracellular matrix and cell-cell interaction .....	4
<b>Figure 1.3</b> Different culture modes of hPSCs in stirred suspension flasks (A) Human ESCs cultured in alginate encapsulation without liquefied core. (B) Human ESCs cultured after encapsulation in alginate and core liquefaction. (C) Human ESCs cultured on vitronectin coated microcarriers and live cells stained with fluorescein diacetate (FDA). (D) Human ESCs cultured as aggregates. Live cell staining with fluorescein FDA is shown. ....	15
<b>Figure 2.1</b> Seeding H9 cells onto Matrigel-coated microcarriers (A) Seeding efficiency comparison between seeding with single cells (white bars) vs. seeding with cell clusters (grey bars) after either 4 hours or overnight. (B) Colonization percentage comparison between seeding with single cells vs. seeding with cell clusters after overnight. (* $p < 0.05$ ). Fluorescein diacetate acid (FDA) staining of H9 cells seeded on Matrigel-coated microcarriers as single cells (C) or small cell clusters (D) (* represents microcarriers which were either empty or populated with far few cells). (E) Growth profile of H9 cells seeded on Matrigel-coated microcarriers in spinner flasks with 4 hours (dashed curve) or overnight (solid curve) treatment of ROCK inhibitor (* $p < 0.05$ ). ....	42
<b>Figure 2.2</b> Seeding IMR90 cells onto Matrigel-coated microcarriers (A) Seeding efficiency comparison between seeding with single cells (white bars) vs. seeding	

with cell clusters (grey bars) after either 4 hours or overnight. (B) Colonization percentage comparison between seeding with single cells vs. seeding with cell clusters after overnight (\* $p < 0.05$ )..... 43

**Figure 2.3** Continuous culture of H9 cells on Matrigel-coated microcarriers for 5 passages. (A) Live cells on beads were stained with FDA showing their distribution and expansion over time. (B) Growth profile and viability. (C) Cumulative LDH activity. Expression of pluripotency markers were checked by qPCR (D, normalized to first passage), flow cytometry (E) and immunostaining (F, Passage 5). Data from a representative experiment are shown. .... 45

**Figure 2.4** Peptide surface density of microcarriers and seeding efficiency of hPSCs. (A) Surface peptide density versus the total amount of peptide used in amidation reaction. (B) Seeding efficiencies of IMR90 cells on microcarriers conjugated with different amount of peptides. Cells were cultured in TeSR2 medium. (C) IMR90 cells seeded on CP beads and cultured in spinner flasks failed to spread on the beads and formed aggregates. Scale bar: 200  $\mu\text{m}$ . .... 47

**Figure 2.5** Coating of peptide-conjugated microcarriers with poly-L-lysine (pLL) for hPSC culture in xeno-free medium. (A) Seeding efficiency of IMR90 (hiPSCs) and H9 (hESCs) on microcarriers featuring different surface treatments: CP+pLL: beads with conjugated peptide and pLL coating; CP: beads with conjugated peptide; FP+pLL: beads with free (unconjugated) peptide and pLL coating; pLL: beads with pLL coating only, N-(3-Dimethylaminopropyl)-N'-ethylcarbodiimide hydrochloride (EDC)/N-hydroxysuccinimide (NHS): beads subjected to the coupling reaction without peptide; Untreated: plain beads without any treatment.

(\*P<0.05: CP + pLL versus pLL and CP + pLL versus FP + pLL, #P<0.05: CP versus EDC/NHS and CP versus untreated. Mean values are compared among different microcarriers for the same cell type (H9 or IMR90)). (B) FDA-stained Live IMR90 cells grown on CP+pLL beads right after the seeding phase (left, Day 0) and during the spinner flask culture (right, Day 3). (C) Time course of the concentration and viability of IMR90 cultured on CP + pLL beads in stirred suspension. (D) Relative expression of NANOG and OCT4 in IMR90 cells cultured for 6 days in a microcarrier suspension (spinner flask). The corresponding gene expression of IMR90 cells maintained in dishes is also shown. (E) Analysis of cultured cells (day 6) by flow cytometry for the expression of stem cell markers. Values are shown as mean  $\pm$  SD (n  $\geq$  3). (F) Immunostaining of cells after 6 days of expansion on CP + pLL beads in the spinner flask. Cells in (A–F) were cultured in TeSR2 medium. Scale bars in (B): 200  $\mu$ m, (F): 50 $\mu$ m. 49

**Figure 2.6** Human PSCs cultured on CP + pLL microcarriers for multiple passages in stirred-suspension vessels. (A) Growth profile, viability and (B) cumulative LDH activity of IMR90 hiPSCs cultured for five passages on microcarriers in spinner flasks. After each passage, the expression of pluripotency markers was characterized by (C) qPCR and (D) flow cytometry. (E) After the last passage, cells were plated and stained for pluripotent markers (scale bar: 50  $\mu$ m). (F) Karyotyping results for IMR90 cells after their culture for five passages in spinner flasks. .... 51

**Figure 2.7** Embryoid body (EB) formation and germ layer differentiation of IMR90 cells cultured on CP+pLL microcarriers after 5 passages. (A) Gene

expression of germ layer markers of EBs checked by qPCR (expression normalized to that of undifferentiated IMR90 cells). Definitive endoderm (DE) marker (SOX17 and FOXA2) expression of IMR90-derived DE cells was checked by qPCR (B) and immunostaining (E). Mesoderm (MS) marker (KDR and MEOX1) expression of IMR90-derived MS cells was checked by qPCR (C) and immunostaining (F). Neuroectoderm (NE) marker (TUBB3 and NES) expression of IMR90-derived NE cells was checked by qPCR (D) and immunostaining (G). Gene expression was normalized to IMR90 cells differentiated in basal medium without any growth factors. .... 53

**Figure 2.8** Directed differentiation of hPSCs cultured on CP + pLL microcarriers in a stirred-suspension bioreactor. (A) Expression of MS genes after IMR90 hiPSC differentiation in the bioreactor. Gene expression was normalized to hiPSCs differentiated in basal medium without factors. (B) Immunostaining of differentiated cells on beads. Stars denote the position of microcarriers. Scale bars: 100  $\mu$ m. (C) Flow cytometric analysis of KDR expression. A flow cytometry graph is shown from a representative experiment. Curves correspond to samples of negative control (black), cells in dishes incubated in basal media without differentiation factors (green; dish control), cells differentiated in dishes (red) and cells differentiated in microcarrier suspension culture (blue). The gate excludes 99% of the negative control cells. Results are summarized in the bar graph (n = 3) as mean  $\pm$  SD..... 55

**Figure 3.1** Seeding efficiency of microcarriers treated with different coatings in static conditions. (A). VN: 5  $\mu$ g/ml vitronectin for 1 hr; HSA: 0.01 g/ml (1%)

recombinant human serum albumin, 30 min; UV: shortwave 254 nm, 75 W UV lamp, 40 min. (B) A schematic demonstration of how to prepare VN-HSA-UV microcarriers. .... 71

**Figure 3.2** Comparison of cell attachment on VN-HSA-UV microcarrier with VN-UV microcarrier under agitation (45 rpm). Live cells were stained with FDA. Bar = 200  $\mu$ m. .... 72

**Figure 3.3** H9 hESCs cultured on Plastic and Plastic Plus microcarriers coated with VN-HSA-UV under agitation at 45 rpm for 6 days in E8 (without F-68).... 73

**Figure 3.4** H9 cells cultured on plastic coated microcarriers coated with VN-HSA-UV under agitation for 6 days in E8 with 0.02% F68. (A) Cell growth profile and viability. (B) Expression level of pluripotency markers OCT4 and SSEA-4 in cells harvested from VN-HSA-UV coated microcarriers. Red curve: E8 with 0.02% F-68 (99% OCT4 positive, 92% SSEA-4 positive), Blue curve: E8 only (97% OCT4 positive, 91% SSEA-4 positive), Black curve: control. (C) FDA staining of live H9 cells attached on VN-HSA-UV coated microcarriers on Day 2, Day 4 and Day 6. .... 74

**Figure 3.5** H9 (hPSCs) cultured on VN-HSA-UV microcarriers for multiple passages in stirred-suspension vessels. (A) Growth profile and viability. After each passage, the expression of pluripotency markers was characterized by (B) qPCR, and (C) flow cytometry. PX is the passage number (e.g. P3: passage number 3). .... 76

**Figure 3.6** Germ layer differentiation of H9 (hESCs) cells harvested from VN-HSA-UV microcarriers after 5 passages of expansion. Definitive endoderm (DE)

marker (SOX17 and FOXA2) expression of H9-derived DE cells was probed by qPCR (A) and immunostaining (D). Mesoderm (MS) marker (KDR and MEOX1) expression of H9-derived MS cells was checked by qPCR (B) and immunostaining (E). Neuroectoderm (NE) marker (TUBB3 and NES) expression of H9 NE cells was checked by qPCR (C) and immunostaining (F). Gene expression was normalized to H9 cells differentiated in basal medium without any differentiation stimuli..... 77

**Figure 4.1** Scheme of step-wise pancreatic differentiation protocol of hPSCs under xeno-free conditions. Activin A: 100 ng/ml; B27XF: Xeno-free B27 supplement; CYC: 0.25  $\mu$ M KAAD-cyclopamine; KGF: 50 ng/ml; RA: 2  $\mu$ M Retinoic Acid; NOG: 50 ng/ml noggin. .... 86

**Figure 4.2** H9 cells (hESCs) differentiated in different basal medium towards DE. Initial seeding:  $2 \times 10^6$  cells/10 cm<sup>2</sup>. Cell number was counted after 4 days of differentiation. (A) cell viability. (B) Level of co-expression of SOX17 and FOXA2. \*p<0.05. (C) Co-staining of SOX17 and FOXA2 of DE stage cells with RPMI supplemented with B27XF..... 87

**Figure 4.3** H9 cells (hESCs) differentiated with RPMI with 1% B27XF and 100 ng/ml Activin A on vitronectin-coated dish co-stained with SOX17 and CXCR4 (A) and SOX17 + CKIT (B). Bar = 50  $\mu$ m..... 88

**Figure 4.4** IMR90 cells (hiPSCs) differentiated into DE cells on VN-coated dishes with RPMI containing 1% B27XF and 100 ng/ml Activin A were co-stained with SOX17 and FOXA2 (A). The co-positive percentage is shown in (B). ..... 88

**Figure 4.5** Immunostaining of HNF4A and HNF1B of PGT stage cells differentiated in RPMI medium with B27XF and KGF on VN-coated dishes. (A) H9 hESC-derived and (B) IMR90-Clone 4 hiPSC-derived cells. Bar = 50  $\mu\text{m}$ . .. 89

**Figure 4.6** H9 differentiated on VN-coated dishes to PF stage. (A) Flow cytometry results of differentiation with different combinations of growth factors. (B) Immunostaining of H9 cells differentiated with NOG, CYC, RA condition. 91

**Figure 4.7** Effect of different basal media on the induction of PDX1. (A) Comparison of cell concentration using different media. \* $p < 0.05$ . (B) Differentiation efficiency determined by flow cytometry. RPMI: RPMI with 1% B27XF; DMEM: DMEM with 1% B27XF. In both cases the culture was supplemented with NOG, CYC and RA. .... 92

**Figure 4.8** IMR90 hiPSCs were differentiated into PF cells with DMEM containing 1% B27XF and supplemented with NOG, CYC and RA on VN-coated dishes. (A) Cells were stained for PDX1. (B) The PDX1<sup>+</sup> cell fraction is shown. Bar = 50  $\mu\text{m}$ . .... 92

**Figure 4.9** Immunostaining of H9 hESCs (A) and IMR90 hiPSCs (B) coaxed toward pancreatic cells in DMEM with B27XF on VN-coated dishes co-expressing INS and C-peptide after 19 days of differentiation. .... 93

# Introduction and Background

## 1.1 Motivation

Since their isolation and derivation in 1998 [1], human embryonic stem cells (hESCs) have been considered a promising inexhaustible cellular source for treating currently incurable degenerative diseases such as diabetes, Parkinson and heart failure. Human ESCs exhibit two fundamental attributes: extensive self-renewal ability and the potential for differentiation into all types of somatic cells. Ethical concerns relating to the derivation of hESCs from fertilized eggs have largely abated with the reprogramming of differentiated adult cells to stem cells termed induced pluripotent stem cells (iPSCs) [2-4]. Human iPSCs and hESCs (collectively termed human pluripotent stem cells or hPSCs) share many key properties including pluripotency and prolonged self-renewal under appropriate conditions making feasible their propagation in traditional static culture as well as scalable stirred-suspension vessels [5, 6]. These cells also provide a way toward patient-specific therapies and disease model development [7, 8].

Therapeutic use of hPSCs necessitates their expansion and efficient differentiation in large-scale under well-defined conditions. Scalable production is required for most current and under development cell therapy protocols requiring  $10^8$ - $10^{10}$  cells per patient [5]. For example, myocardial infarction results in the damage or ablation of at least  $1$ - $2 \times 10^9$  myocytes [9] and approximately  $1.3 \times 10^9$   $\beta$ -cells are required for insulin independence in diabetes patients [10]. Stirred-suspension bioreactor systems affording densities of  $10^6$ - $10^7$  cells/ml are appealing for

generating stem cell therapeutics, especially given the limitations for scale-up of traditional dish cultures.

Large-scale production of hPSC derivatives goes hand in hand with the development of xeno-free environments excluding animal-derived products such as serum and cytokines commonly used in traditional mammalian cell culture [11] but also feeder cells. The promise of stem cells for regenerative medicine and the rapid advances in recent years have intensified efforts toward the development of xeno-free scalable systems for stem cell products. Yet such advances are contingent upon addressing hPSC survival, proliferation, and differentiation, issues whose exact dependencies on intracellular signals and extrinsic factors require further elucidation. A simplified scheme of bioprocessing of hPSCs used for therapeutic applications is shown in **Figure 1.1**.

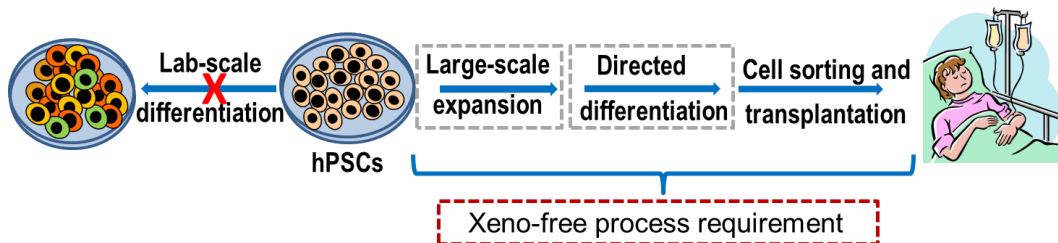


**Figure 1.1** Bioprocessing of hPSCs for use in therapeutic applications.

Therefore, before the successful therapeutic application of hPSCs, at least two challenges need to be tackled. One is the development of defined, xeno-free and scalable culture system for generating large quantities of hPSCs and their derivatives that can meet the requirement of clinical demands which cannot be met using lab-scale dish culture. In this dissertation, we aim to establish a stirred suspension microcarrier system for expansion of hPSCs at a large scale under

fully defined and xeno-free conditions. Furthermore, we aim to develop an efficient and xeno-free differentiation protocol to coax hPSCs into insulin-producing cells. Combining the two, the microcarrier culture system may serve as a step forward in the development of bioprocesses integrating expansion and directed differentiation of human stem cells for the production of therapeutically useful pancreatic progeny.

## **1.2 Xeno-free culture of hPSCs**

Limiting the aberrant differentiation of cultured hPSCs is a key consideration as the cells self-renew or their fate is directed along particular lineages. Our knowledge basis for appropriate conditions supporting hPSC self-renewal has been obtained from heterologous systems of development, mainly of the mouse embryo. A significant body of studies on hPSC signaling during culture has extended our understanding of the dependence of self-renewal on extracellular parameters. The microenvironment – commonly referred to as the niche – imposes its effects mainly through soluble factors, cell-cell and/or cell-matrix contacts and mechanotransduction (**Figure 1.2**). Here we summarize first the development of defined xeno-free media, extracellular matrices and synthetic substrates, which are the main microenvironmental considerations while establishing culture systems for the maintenance of uncommitted hPSCs on 2 dimensional (2D) surfaces. We will also study the progress and challenges faced by scalable culture systems for hPSCs under defined conditions.

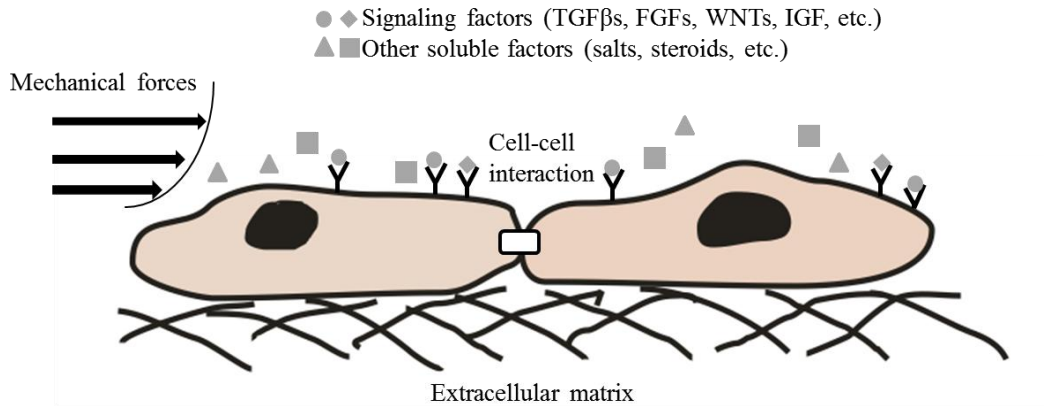


**Figure 1.2** Schematic demonstration of microenvironment faced by hPSCs including soluble factors, mechanical forces, interaction between cell and extracellular matrix and cell-cell interaction

### 1.2.1 Xeno-free media for maintaining undifferentiated hPSCs

It is well documented that the pluripotency of hESCs is controlled through common genetic networks of transcriptional factors [12-14]. Examples of such factors include Nanog, Pou5f1 (also known as Oct4) and Sox2. Cooperative interactions among them underline the maintenance or loss of pluripotent state [15] early in embryonic development and *in vitro* [13, 16].

Multiple signaling pathways such as the transforming growth factor-beta (TGF-β) super family-activated cascades, receptor tyrosine kinase (RTK) signaling (downstream of the basic fibroblast growth factor (bFGF) also known as FGF-2), canonical Wnt signaling [12, 17], and insulin or insulin-like growth factors (IGFs) [18, 19] regulate pluripotency gene levels [20, 21]. Based on signaling studies, a key approach to develop media for hPSCs is to identify and supply extrinsic growth factors which work through signaling pathways impacting hPSC pluripotency. Bone morphogenetic proteins (e.g. BMP4) and the leukemia

inhibitory factor (LIF; a JAK/STAT signaling activator) are sufficient to preserve the undifferentiated state of cultured mouse ESCs [22] even in serum-free conditions [23] but not of hESCs [1, 24]. The hPSC pluripotent state mainly depends on TGF $\beta$  signaling [25] with TGF $\beta$ 1, Activin A and Nodal directly activating Nanog expression via a promoter site for SMAD2/3 binding [26, 27]. Because these molecules are produced by hPSCs to varying degrees, they are not part of all medium formulations.

Basic FGF though is a universal supplement which is critical for sustaining hESC self-renewal *in vitro* [28, 29]. For hPSC culture on mouse embryonic fibroblast (mEF) feeder layers [30] or in mEF-conditioned medium [31], the bFGF concentration (4 ng/ml) is lower than in feeder free cultures (40-100 ng/ml) [28, 32, 33]. The BMP antagonist noggin supports the growth of undifferentiated hESCs in unconditioned medium with 40 ng/ml bFGF but does not appear to have an effect when bFGF is increased to 100 ng/ml [34].

Canonical Wnt/ $\beta$ -catenin signaling has also been implicated in hPSC self-renewal [35, 36]. Even so, others reported that recombinant Wnt3a is not sufficient to maintain hESCs undifferentiated without feeder cells and  $\beta$ -catenin-mediated transcriptional activity is up-regulated during differentiation [37]. The effects of Wnt signaling in hESC pluripotency have been difficult to unravel because different hPSC lines exhibit disparate levels of endogenous Wnt activity. Further, Wnt has been implicated in the specification of stem and progenitor cells along multiple and often developmentally distant lineages suggesting that exposure of hPSCs to Wnt ligands should be finely customized.

These and other -often unidentified- factors are traditionally provided through supplementation of the medium with fetal bovine serum (FBS). Nonetheless, the use of non-human components (e.g. Neu5Gc; [38]) is incompatible with clinical applications and drives efforts to design xeno-free culture systems for hPSCs and their products. Serum replacement products (e.g. knockout serum replacer (KSR)) [39] have proprietary composition and may also contain animal-derived components such as bovine serum albumin (BSA).

Media composed of chemically defined, non-xenogeneic compounds for the propagation and differentiation of hPSCs are highly desirable [20, 40-42]. Approaches to develop defined media for hPSCs consist of identifying both a suitable basal medium and additional signaling factors promoting cell growth and preservation of pluripotency or induction of (directed) differentiation. Basal media such as DMEM and DMEM/F12 provide mainly glucose, vitamins and salts (at appropriate osmolarity) to cells whereas factors (e.g. bFGF) eventually de/activate genetic programs for hPSC self-renewal or specification. For example, a defined medium based on DMEM/F12 with 100 ng/ml bFGF and components such as TGF $\beta$ , LiCl, insulin, GABA and BSA or human serum albumin (HSA) is extensively used in hPSC cultivation [43, 44]. DMEM/F12 with 20 ng/ml bFGF and B27, N2 and BSA has been used to maintain hESCs for over 27 passages. And in the absence of BSA, DMEM/F12 combined with N2, B27 and high concentration of bFGF (40 ng/ml or 100 ng/ml) is adequate for hESC maintenance. The X-Vivo 10 medium supplied with recombinant bFGF, stem cell factor, LIF and flt3 ligand has also been successfully used to maintain hESCs.

Nonetheless, the aforementioned media typically contain bovine albumin or the more expensive human serum albumin. Recently, a fully defined medium (E8) containing 8 factors (including bFGF) but no BSA was described for the long-term propagation of hPSCs [45].

Despite the significant advances in the development of defined and xeno-free media, there are still unresolved issues. For instance, side-by-side comparison by our laboratory and others of the performance of commercially available xeno-free media indicates differences in the fold-expansion of cells, particularly over multiple passages. Although the root(s) of such discrepancies are unclear, the quality of supplements used in these medium formulations may be a suspect. The generation even of recombinant growth factors and other proteins (e.g. recombinant albumin) requires separation steps (e.g. isolation from bacterial cultures, purification etc.) which do not always result in impurity-free preparations. Traces of impurities may affect the propagation of cells and their long-term potential.

Moreover, almost all current protocols for hPSC culture require daily medium replacement increasing the cost and associated labor. Fluctuation of growth factor levels in the medium contributes to the variability of hPSC cultivation. Soluble human or zebrafish bFGF loses most of its activity in culture after 24 hours [46]. This may be circumvented with the controlled release of bFGF (or other factors) in culture. Basic FGF-loaded PLGA microspheres added to hPSC cultures reduce the frequency of medium from daily to every three days or biweekly [47].

Hence, creating supplements with extended shelf life while keeping the cost low are highly desirable. Small molecules promoting hPSC self-renewal have been suggested as candidates that may fit the bill. Using high-content screening methods, small molecules such as trimipramine and ethopropazine which can penetrate multi-layer cells easily and have much longer degradation times have been reported to maintain the self-renewal of hESCs replacing bFGF [48, 49].

### **1.2.2 Xeno-free extracellular matrices (ECM) for the maintenance of undifferentiated hPSCs**

Despite the availability of chemically defined media for hPSC cultivation, the quest for relevant xeno-free substrates, particularly for large-scale production has yet to yield widely utilized products. Beyond the obvious requirement for promoting cell adhesion, the design of defined surfaces is subjected to a unique constraint for unimpeded hPSC self-renewal and differentiation. Efforts in this direction are hampered by the incomplete knowledge of how human stem and progenitor cell fate decisions are regulated within complex niches in vivo.

Traditionally, hPSCs have been maintained on layers of inactivated mEFs, which secrete factors supporting hPSCs. Thus, early efforts focused on feeder cell surrogates of human origin including human fetal foreskin fibroblasts [50-53], adult epithelial cells [54], bone marrow cells [55, 56] and placenta-derived feeder cells [57, 58]. Apparent difficulties in the sourcing –including variability due to donor age and condition [59], derivation, preparation and preservation of human feeder cells limit their use in stem cell culture. Importantly, co-culturing hPSCs

with feeder cells adds a requirement for separation and removal of the latter thereby imposing significant technical and economic burdens on the bioprocess.

The introduction of the extracellular matrix protein (ECM) mixture (Matrigel) produced by Engelbreth-Holm-Swarm mouse sarcoma led to successful expansion of stem cells without the need for feeder cells. Matrigel contains laminin, collagen type IV, heparan sulfate, proteoglycans, and nidogen [1, 60], and its use as an hPSC substrate is fairly straightforward and fast. However, its undefined composition precludes its use in applications calling for the xeno-free production of stem cell progeny.

Natural ECM glycoproteins such as laminin, fibronectin, vitronectin, entactins, tenascins and collagen influence adhesion, survival, growth and differentiation [61] through their interactions with cell surface moieties. Each ECM component exhibits distinct domains for binding to surface receptors (e.g. integrins) mediating adhesion and triggering signaling cascades linked to cell fate decisions [62, 63]. Along this vein, the use of ECM proteins and peptides from tissue isolates or in recombinant form has been investigated extensively for the culture of hPSCs.

The integrin-interacting arginine-glycine-aspartic acid ('RGD') motif is shared by various ECM proteins including laminin, vitronectin and fibronectin [64] [65] while RGD mutations result in greatly reduced cell adhesion [66]. A mixture of recombinant human collagen IV, vitronectin, fibronectin and laminin supports the derivation and growth of undifferentiated hESCs over multiple passages [43].

Among the 24 different known integrin heterodimers,  $\alpha3\beta1$ ,  $\alpha6\beta1$ ,  $\alpha6\beta4$ , and  $\alpha7\beta1$  in various cell types have been reported to bind laminin [67]. The  $\alpha6\beta1$  integrin is expressed by hESCs and plays a significant role in adhesion [60] suggesting that laminin is a critical ECM protein for supporting hESC proliferation. Indeed, natural or recombinant laminin in lieu of Matrigel maintained the growth and pluripotency of hESCs in mEF-conditioned medium [60, 68]. However, human placenta-derived laminin could only support hESC self-renewal for 3 passages in chemically defined medium [69]. Over more than 10 passages, hESCs grew significantly more slowly with evident spontaneous differentiation and poor adhesion [70]. The presence of ECM molecules (besides laminin) secreted by feeder cells may be a potential explanation for the discrepancy in the results reported in the aforementioned studies. Yet, laminin-511 (but not laminin-332) was reported to support the culture of multiple hESC lines under xeno-free conditions [71]. Interestingly, laminin peptides did not support hESC attachment and growth according to the results of a concurrent study [72].

Like laminin, vitronectin has been investigated as a substrate for culturing hPSCs. Vitronectin mediates hPSC adhesion through  $\alpha V\beta5$  integrins as shown in integrin-blocking antibody experiments [70]. The proliferation of three hESC lines in mTESR1 medium was supported by vitronectin in a manner comparable to that of Matrigel. This is in contrast to fibronectin (acting through the  $\alpha5\beta1$  integrin) coated surfaces on which hESCs grew only in feeder cell-conditioned (but not defined) medium. Conversely, Liu *et al.* reported that cultured hESCs could not

be maintained on vitronectin for more than 7 days [73] in defined medium containing bFGF, N2 and B27 supplements. These results illustrate the complexity of pinpointing suitable matrix components supporting hPSC culture and emphasize the need for considering multiple aspects of the culture system including the medium used for hPSC maintenance.

Vitronectin from human plasma also promotes self-renewal (>20 passages) without compromising the potential of hPSCs for differentiation [74]. Notably, a threshold surface density of 250 ng of vitronectin/cm<sup>2</sup> was estimated for successful hPSC culture. This value applies to whole-molecule vitronectin and should be adjusted when utilizing vitronectin derivatives or fragments. In fact, variants of vitronectin exhibit differential support of hPSCs in culture [45]. For hESCs grown in E8 medium, two truncated vitronectin molecules (amino acids 62-398 and 62-478) promoted initial attachment and survival of hESCs as single cells (with ROCK inhibitor or blebbistatin) and as clumps. A chimeric glycoprotein of vitronectin and IGF1 was also reported for hESC maintenance in defined medium [63].

Fibronectin also features the RGD domain which interacts with  $\alpha 5\beta 1$ ,  $\alpha 8\beta 1$ ,  $\alpha \nu\beta 1$ ,  $\alpha \nu\beta 3$ ,  $\alpha \nu\beta 5$ , and  $\alpha \nu\beta 6$  integrins [75, 76]. Based on available reports on the role of fibronectin in stem cell adhesion and culture is still debatable. Human plasma fibronectin was shown to promote hESC proliferation and pluripotency in defined medium for at least 10 passages [69] or 13 passages [73]. Yet, cultivation of hESCs failed on fibronectin-coated surfaces with mTeSR1 but not with mEF-conditioned medium as mentioned above [70] noting that cell attachment on

fibronectin is mediated by RGD interaction with the  $\alpha 5\beta 1$  integrin. As with vitronectin, a threshold density of  $80 \text{ ng/cm}^2$  of plasma-fibronectin was determined for hESC culture in a serum-free medium [77]. This density also applied to the 120 kDa fragment of fibronectin with the central cell-binding domain containing the RGD motif (1–10 type III repeats), while other fibronectin fragments did not support the maintenance of hESCs.

Capitalizing on the central role of the RGD domain of ECM molecules on hPSC adhesion, various groups implemented an approach of building ECM substrata with synthetic RGD-containing peptides [72, 78]. A cyclic RGD peptide covalently bound to tissue culture surface at  $10\text{-}30 \text{ fmol/cm}^2$  was used to culture hESCs in conditioned medium (10 passages) or mTeSR1 (5 days) [79]. Such substrata are required to promote not only hPSC adhesion but self-renewal and unhindered differentiation as well. For example, one peptide featuring the YIGSR domain promotes hESC adhesion but cultured cells display significantly reduced OCT4 and SSEA4 expression [80] in contrast to other integrin-binding peptides (e.g. GKKQRFHRNRKG, FHRRIKA and GWQPPARARI). Peptides derived from the bone sialoprotein and vitronectin (but not from fibronectin) and covalently attached onto acrylate-coated surfaces facilitate the adhesion of hESCs [81]. Thus, although the presence of binding (e.g. RGD) domains of natural ECM molecules may point to candidate peptides for hPSC culture, additional optimization of the whole peptide sequences is necessary for the development of appropriate substrata.

Findings reviewed thus far pertain mostly to flat surfaces coated with ECM or synthetic molecules for the culture of hPSCs. Considerable efforts however have been geared toward the design of three-dimensional (3D) scaffolds, some of which mimic natural stem/progenitor cell niches. Hydrogels are commonly used to create 3D environment for stem cell culture. For example, such scaffolds synthesized with 2.4% (w/v) alginate and 2.4% (w/v) chitosan mixture by lyophilization [82] support BG01V hESCs over 21 days of culture. Human H1 ESCs encapsulated in alginate beads and cultured in dishes maintain their undifferentiated state expressing OCT4, NANOG, SSEA-4, TRA-1-60 and TRA-1-81 after 260 days [83]. Scaffolds of alginate and chitin support HUES7, BG01V/hOG and hFib2-iPS4 cells for 10 passages [84]. Human ESCs in 3D alginate capsules differentiated into midbrain dopamine neurons faster than in 2D cultures [85]. Defined hydrogels consisting of hyaluronic acid, which is present during early embryo development, have also been used to maintain and differentiate hESCs [86]. Hydrogels composed of alginate and poly( $\gamma$ -glutamic acid) ( $\gamma$ -PGA) and coated with nerve growth factor (NGF) promote neural differentiation of iPSCs [87].

In addition to the composition, the scaffold ultrastructure affects stem cell growth. Fibrous scaffolds support the proliferation of stem cells (H1, H9 hESCs) cultured for 14 days in poly(desaminotyrosyl tyrosine ethyl ester carbonate) (pDTEc) matrices coated with poly-D-lysine. The cells were subsequently differentiated into neuronal, smooth muscle, and hepatic-like lineages [88]. Along the same vein, hESCs (HES3, Endeavour-1, Envy) adhere to 3D PLGA cylindrical matrix slices

(2 mm thick) coated with laminin [89]. Two days after seeding, the cells within the scaffold can be coaxed to mesoderm. Poly(methacrylic acid)-coated carbon nanotubes, which are similar in scale to collagen and laminin moieties, promote neuronal differentiation of hESCs [90, 91].

### **1.3 Large-scale cultivation of hPSCs**

The development of xeno-free culture media and substrates is driven largely by the therapeutic applications envisioned for hPSCs and their progeny. The generation of large quantities of cells under strictly defined conditions and in a reproducible fashion is a prerequisite for the use of hPSC products in the clinic. Moreover, the production of larger batches of cells is more economical motivating scale-up of stem cell cultivation.

Different designs of bioreactors, which have been utilized for the culture of stem cells, offer alternatives for the large-scale culture of hPSC products [92-94]. Stirred suspension bioreactors are a popular choice in large-scale cultures due to the homogenous environment and ease of operation and monitoring of culture. This bioreactor type affords multiple culture modes including the cultivation of cells encapsulated, on microcarriers or as aggregates. **Figure 1.3** shows hPSCs cultured under the different stir-suspension-bioreactor culture modes. All of those modes have been demonstrated for the culture of hPSCs and will be discussed below in the context of xeno-free generation of stem cells.

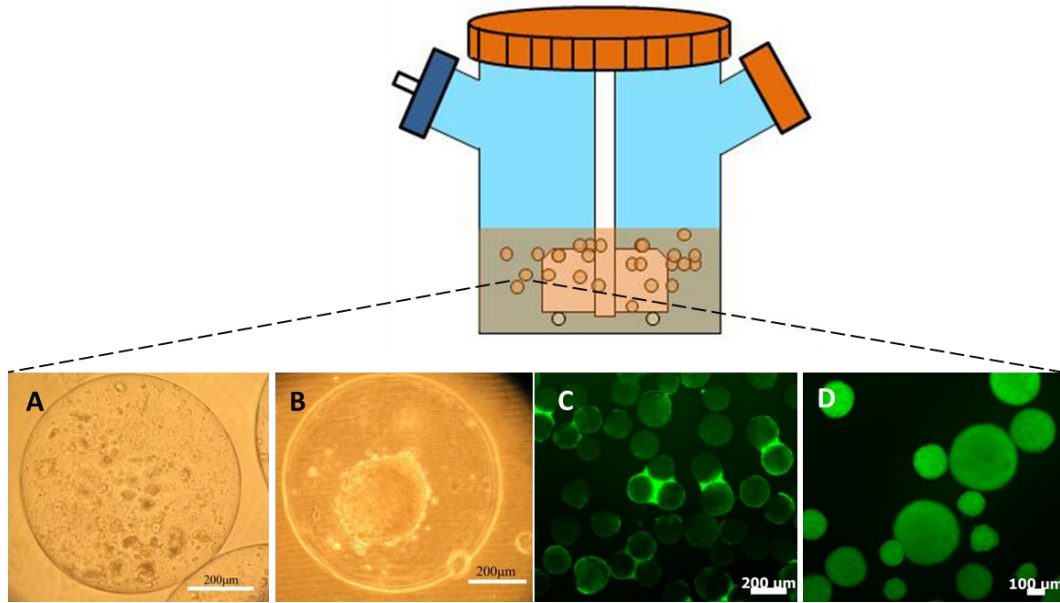


**Figure 1.3** Different culture modes of hPSCs in stirred suspension flasks (A) Human ESCs cultured in alginate encapsulation without liquefied core. (B) Human ESCs cultured after encapsulation in alginate and core liquefaction. (C) Human ESCs cultured on vitronectin coated microcarriers and live cells stained with fluorescein diacetate (FDA). (D) Human ESCs cultured as aggregates. Live cell staining with fluorescein FDA is shown.

It should be noted that selecting biomaterials for scalable application, for example, by mere translation of materials used in static cultivation might not be straightforward and requires caution. In stirred suspension, both cells and scaffolds face a different hydrodynamic environment than that in static culture. Agitation is necessary to keep cells and scaffold suspended and ensures a homogeneous environment. However, stirring exposes cells and scaffolds to shear stresses. Apparently, biomaterials should bear certain mechanical properties for preservation of structural integrity under flow in the bioreactor. Shear stress

induces cell removal from surfaces and reduces cell viability [11]. In one of our previous studies, we found that a peptide-conjugated polystyrene matrix which supported attachment and proliferation of hiPSCs under static condition was not sufficient to achieve the same goal under agitation [6]. In another report, hESCs cultured on vitronectin coated microcarrier showed reduced growth rate compared to cells cultured on dishes coated with the same protein [95]. Besides the consideration of mechanical properties, affordable, biocompatible and biodegradable materials are highly preferred considering the needs of large scale bioprocessing and future clinical application.

### **1.3.1 Cell encapsulation**

Cells cultivated in stirred suspension after their encapsulation in matrices (typically hydrogels) are protected from hydrodynamic shear and excessive agglomeration of clusters. The materials employed for encapsulation allow control of their permeability and therefore of the molecules exchanged between cells and the culture environment. For example, tight control of the permeability of encapsulation materials aims to allow the transport of oxygen and nutrients while blocking the penetration of immune cells and antibodies. These cell-laden scaffolds may be transplanted directly with minimum immunological rejection [96] serving as a basis for scalable systems intended for expansion and differentiation of hPSCs to therapy-grade cells.

The general procedure of encapsulation entails the formation of cell-gel droplets and gel cross-linking. In this respect, biocompatible materials requiring mild

cross-linking conditions are advantageous. Alginate is the most common material used for encapsulation [97] with appealing attributes such as biocompatibility, inertness toward cells [98] and a relatively straightforward protocol for generating micron-size capsules laden with cells under mild conditions. A cell suspension (a few million cells per milliliter) of sodium alginate solution (normally 1-2% (w/v)) is dispersed in droplets, which solidify upon contact with a  $\text{CaCl}_2$  solution [99]. Cells can be maintained in solid or liquefied-core capsules with external coating. Encapsulated mouse and human stem cells have been successfully cultured in bioreactors for expansion and differentiation. We previously demonstrated that both mESCs and hESCs can be entrapped in alginate beads coated with poly-L-lysine (pLL) and cultured in spinner flasks [100]. The pLL coat allows the liquefaction of the bead core using  $\text{Ca}^{+2}$ -chelating agents thereby facilitating the controlled aggregation of the cells. Besides enhancing the mechanical strength of the beads, the pLL layer is also permeable to soluble differentiation factors (e.g. Wnt3a, Activin A, BMP4) as shown with the coaxing of encapsulated hESCs to cardiomyocyte-like cells. Combining alginate microencapsulation with microcarriers allowed the hESC expansion in spinner flasks for two weeks noting a 20-fold increase in concentration and a 3-fold improvement of post-thawing viability after cryopreservation [101]. Alginate can also be mixed with other materials for stem cell entrapment. For example, mESCs encapsulated in a mixture of 1.1% (w/v) alginate and 0.1% (v/v) gelatin have been cultured in a rotary high-aspect-ratio vessel (HARV) [102]. Mouse ESCs cultured in rotary

bioreactors have been induced to cardiomyocytes [103] and osteogenic lineages [104].

Besides alginate, agarose is another (hydrogel) material used for ESC encapsulation. Mouse ESCs encapsulated in size-controlled agarose capsules were cultured in stirred suspension at high density and were shown to become hematopoietic cells [105]. Agarose-encapsulated mESCs propagated in 250 ml spinner flasks were differentiated into cardiomyocytes [106].

Despite all the advantages that cell encapsulation offers, it hinders the transfer of oxygen and nutrients. Such limitations may present obstacles in controlling cell proliferation and/or the differentiation along particular lineages. If cell purification is required, the separation and harvesting of cells from the scaffolding material(s) not only increases the cost of the process but potentially contributes to the reduction in cell number and viability. Moreover, the use of UV for cross-linking certain gels after cell loading is another concern.

### **1.3.2 Microcarriers**

Microcarrier bioreactors have been utilized since the early 1970's for the large-scale culture of different (particularly anchorage-dependent) cell types intended to generate a wide gamut of products including, viruses, vaccines and proteins [107, 108]. Microcarriers afford distinct advantages such as high surface-to-volume ratio and flexibility in accommodating the adhesion needs of various cells via surface modification [109] in addition to the benefits of stirred suspension bioreactors such as real-time monitoring and controlling of the culture

environment. Microcarrier culture usually holds a higher volume fraction (ratio of cells to medium). Considering an average volume of  $2000 \mu\text{m}^3$  per human cell [110][114] and based on data from our lab, the volume fraction in microcarrier suspension culture is about 0.4% (roughly 2 million cells/ml) after a 6-day culture when initially 0.1 million cells/ml are seeded compared to 0.2%-0.3% in dish culture (6-day culture when cells reached confluency with the same seeding density compared to suspension). Compared to bioreactor aggregate cultures, hPSCs attached on microcarriers are also exposed more readily and uniformly to the medium bulk concentrations of oxygen, nutrients and factors.

Current embodiments of the microcarrier culture systems however, require the separation of cells from the beads unless secreted metabolites or other non-cell products are desired. This requirement increases the downstream processing time and overall cost while reducing the recovery of cellular products. Moreover, high levels of agitation-induced shear are detrimental to cells while the effects of stress from lower stirring speeds especially on stem cells are still unsettled. It should be noted that compared to other cell types (e.g. CHO or Vero cells) traditionally cultured on microcarriers, hPSCs exhibit a more pronounced tendency for cell-cell aggregation. Thus, multi-bead cell clusters may be formed at low agitation speeds. The presence of shear in microcarrier bioreactors hampers the direct application of xeno-free substrates from 2D to 3D environments [6]. Indeed, much of the discussion in the previous sections centered upon xeno-free matrices developed for hPSC cultured on flat surfaces (e.g. dishes) but there are significant differences between 2D and 3D substrata with respect to curvature and elasticity

affecting stem cell shape, spreading, and ultimately specification. For example, the growth rate of mesenchymal stem cells cultured on peptide-modified alginate beads is inversely related to the diameter of the beads resulting from differences in shear stresses acting on cells [111]. Proliferation of hESCs was reportedly hampered on vitronectin (full molecule)-coated microcarriers compared to tissue culture dishes coated with the same protein [95]. Attachment and proliferation of hESCs on microcarriers coated with laminin-111, which supports hESC growth on dishes, were sensitive to shear [95]. Human PSCs attach and spread on vitronectin-derived peptide conjugated-microcarriers in static culture. However, cells readily peel off of microcarriers and form aggregates in agitated suspension [6]. Taken together these findings demonstrate that surface modifications for 2D hPSC cultures do not translate directly to dynamic 3D cultures.

The composition of microcarriers affects the overall surface charge and functional group availability for cell adhesion thereby dictating largely their suitability for cultivation of particular cell types. Various commercially available microcarrier types have been tested in multiple reports for hPSC culture [95, 112]. Microcarriers layered with Matrigel exhibit consistent performance in stirred suspension bioreactors but the matrix's undefined composition and animal origin prevent its use in clinical-grade hPSC products.

Microcarriers with positive surface charges perform better than those with negative or neutral charge [95, 113]. Indeed, microcarriers with surface-conjugated peptides supported hPSC attachment and growth under agitation, only after coating with pLL, which is a positively charged synthetic polymer. Despite

the lower seeding efficiency than on Matrigel-coated microcarriers (38% vs. 77%), a similar fold-increase (23.3 vs. 20.7) was achieved for hPSCs on pLL-coated, peptide microcarriers over 6 days. The cells maintained a normal karyotype and consistent expression of pluripotency genes and proteins (Nanog, OCT4 and SSEA4) during 5 consecutive passages while subsequently formed embryoid bodies (EBs) and directed their specification to all three germ layers [6].

In the future, functional modifications of microcarriers will aim to not only support the expansion of uncommitted hPSCs but also their lineage-specific differentiation so that the two culture segments can be integrated into a single process. To better meet the needs of clinical applications, materials should be utilized for microcarrier construction which is biocompatible and biodegradable allowing direct transplantation to patients while eliminating expensive downstream processing steps. Certain clinical applications, for example, may call for particular degradation rates, which can be adjusted by controlling the biomaterial composition, for better integration of the implanted cells with the host tissue. Obviously, such considerations should be viewed in conjunction with the overall bioprocess cost.

### **1.3.3 Cell aggregates**

Undifferentiated hPSCs aggregate forming EBs on non-adhesive surfaces or in suspension. Methods for EB formation include suspension in low-affinity culture dishes and hanging drops [114] although control of the aggregate size can be challenging. Conversely, cells can be cultured in microwells of specific size [115]

or microchannel devices [116] resulting in aggregates with a narrow size distribution. The scalability of most of these methods for producing large quantities of EBs for bioreactor culture is debatable. This issue may be addressed with the use of rotary orbital suspension culture systems yielding EBs which are homogeneous in size and shape [117]. Yet, single dispersed hPSCs can be seeded directly into suspension bioreactors [11, 118] in the presence of ROCK inhibitor Y-27632 [119]. Since then, several reports emerged of hPSCs successfully expanded as aggregates in stirred suspension [120-122].

A major advantage of culturing hPSCs as aggregates in stirred suspension is the absence of extraneous scaffolds. This reduces the downstream separation steps for obtaining pure cell populations and make the whole process easy to setup and economic. However, aggregates formed by hPSCs are usually heterogeneous in sizes, which can be caused by initial heterogeneous aggregate formation as well as agglomeration during culture. As EBs increase in size, cells near the aggregates' core are subjected to limited transport of nutrients and oxygen. The spatial gradients of nutrients and oxygen may modulate the propensity of stem cells for proliferation, differentiation and apoptosis [106, 123]. Shear stress faced by aggregates when cultured under agitation play a role during cell proliferation and differentiation. It was reported that moderate shear (1.5 to 15 dyne/cm<sup>2</sup>) promoted hematopoietic and endothelial differentiation from hESC [124].

There have been a few reports combining the bioreactor culture of hPSC aggregates with materials for structural support of the clusters and for promoting cell adhesion, self-renewal and differentiation. During normal embryogenesis,

progenitor cells form complex 3D structures and differentiate along disparate lineages. To that end, the EB system may serve as an *in vitro* platform of stem cells differentiation mimicking aspects of *in vivo* development when the early (pre-gastrulation) development happened spontaneously [125]. Microparticles (10-15  $\mu\text{m}$  in diameter) can be incorporated into cell aggregates to affect cell fate decisions via controlled release of soluble factors. Such localized delivery of cues promotes differentiation by altering their local concentration. Incorporation of gelatin microparticles loaded with BMP4 and thrombopoietin (TPO) promoted mesoderm differentiation of hESCs compared to the traditional medium supplementation with soluble stimuli [126]. Microparticles made from different materials including agarose, PLGA and gelatin were embedded within mESC aggregates. When mESC clusters were cultured with retinoic acid (RA)-releasing PLGA beads, the fate and organization of the cells changed compared to aggregates without the particles [127]. Vascular differentiation was also enhanced by PLGA microparticles (diameter of 0.24-25  $\mu\text{m}$ ) releasing vascular endothelial growth factor (VEGF), placental growth factor (PGF) and bFGF [128].

## **1.4 Differentiation of human pluripotent stem cells towards pancreatic progenitors**

### **1.4.1 Diabetes and stem cell-based therapy**

Diabetes mellitus, often mentioned as diabetes, is a chronic disease caused by the loss of insulin-producing  $\beta$ -cells due to autoimmune destruction (Type 1 diabetes), or insulin resistance from muscle, liver, and fat tissue and insufficient insulin

secretion of  $\beta$ -cells (Type 2 diabetes) [129, 130]. Without proper treatment, diabetes patients have high risk of complications including cardiovascular disease, kidney disease and retinal damage. The total number of diabetes patients is expected to reach 380 million by 2025 according to the World Health Organization [131]. The current treatment for diabetes is insulin administration mainly via injection. This method is successful in decreasing the blood glucose level, but it is temporary, hardly mimics the tightly-controlled endogenous insulin release from pancreas, and may cause hypoglycemia while it does not help to fully overcome diabetes side effects. Thus, alternative diabetes therapies or treatments are highly desirable.

Diabetes is an excellent candidate for cell replacement therapy because it is caused by deficiency of mass and/or function of a single, well-defined cell type, the pancreatic islet  $\beta$ -cells. Beta-cells secrete insulin in response to glucose in the blood. Promising results have been obtained by transplantation of whole pancreas or pancreatic islets from donors [132]. However, this approach is limited by the scarce supply of donor tissue and the risk of immune rejection. Patients treated with this therapy have to undergo life-long immunosuppression which may induce complex side-effects. Cell replacement therapy will require a renewable source of glucose-responsive, insulin-secreting  $\beta$ -cells. There are several practical approaches for the generation of  $\beta$ -cells, for example, with the use of adult pancreatic cells, hESCs and hiPSCs.

Human ESCs and iPSCs, which have the ability to infinitely self-renew and differentiate into all kinds of somatic cells, can serve as inexhaustible sources of

islet cell generation for diabetes therapies [2-4]. Human iPSCs are pluripotent stem cells derived from somatic cells by genetic reprogramming the cell through defined factors. The discovery of iPSCs has opened possibilities for patient-specific therapies and disease models [133] [2, 4]. Since iPSCs share many key properties with ESCs including pluripotency, morphology, and self-renewal, it is expected that iPSCs have similar developmental potential and can be coaxed to specific lineages via mimicking embryonic development. Thus, hiPSCs can be used to successfully coax to hormone-expressing and functional  $\beta$ -cells *in vitro* sparking hopes for patient-specific cell therapies for diabetes patients.

#### **1.4.2 Pancreatic differentiation strategy**

Success of stem cell based diabetes therapy relies on the development of efficient differentiation protocols for turning hiPSCs into genetically normal and functional insulin-producing pancreatic islet cells, as well as robust bioprocesses for generating large quantities of therapeutically useful cells under xeno-free, well-defined conditions which meet the standards of clinical applications [134-138].

Recapitulating embryonic development is regarded as the most efficient approach to generate certain differentiated cell types *in vitro*. Therefore, in order to develop efficient protocols for pancreatic differentiation, the fundamental processes involved in the development of embryonic pancreas must be well understood. Embryonic pancreas development is a step-wise and complex process which involves many different signaling pathways. Although the individual effects of growth factors and pathways in pancreatic differentiation are well-characterized,

their combinatorial effects and interactions are often overlooked. Success in developing efficient differentiation protocol calls for systematically analysis and optimization of the effects of a set of growth factors that involved in different signaling pathways during pancreas development.

Based on literature studies, embryonic pancreas development can be considered as a step-wise process. The first step of pancreas patterning is the definitive endoderm (DE) specification, which is mainly controlled by TGF $\beta$ /Nodal signaling pathway [139] [140-142]. Low concentration (25 ng/ml) of Activin A cannot pattern DE, while high concentration (100 ng/ml) of Activin A alone can successfully induce DE cells [143]. After that, pancreatic progenitors are generated from the portion of DE that gives rise to the gut tube [130] and then foregut/midgut junction [144, 145]. Pancreatic endoderm cells originate from foregut cells and finally turn into insulin-producing  $\beta$ -cells. Several signaling pathways have been shown to be important in the gut tube and foregut/midgut formation, including those activated by retinoic acid [146, 147], Wnt [148-150], FGF [151, 152], hedgehog [141], and epidermal growth factor (EGF) [153]. There is no simple conclusion of pathways involved in the  $\beta$ -cell maturation step, however, nicotinamide [154] was reported to play a role in sustaining PDX1 expression level and therefore induce pancreatic  $\beta$ -cell differentiation.

There are several publications showing that sequential application of growth factors, or small molecules leads to the generation of some insulin/C-peptide-positive cells from hESCs [137, 155, 156] and hiPSCs [138, 157]. However, these protocols were not optimized and the differentiation efficiency of insulin-

producing cells was either not mentioned or very low. Also, none of them were conducted under xeno-free conditions that are critical for clinical use of the cellular products.

## **2 Peptide-conjugated microcarrier expansion and differentiation of hPSCs**

### **2.1 Introduction**

As previously discussed, hPSCs are promising sources of cellular material for regenerative medicine and tissue engineering applications. Despite success in cultivating hPSCs in microcarrier stirred suspension bioreactors (SSBs), the beads utilized in most studies are coated with animal-derived matrices such as Matrigel [112, 158-160] or collagen [161] barring the applicability of this culture method from clinical settings. Considerable progress has been noted in developing chemically defined, xeno-free media for hPSC culture [73, 162-165] some of which are commercially available [45, 166, 167]. Nonetheless, research on three-dimensional (3D) substrates free of xenogeneic factors has still to bear simple solutions for the long-term culture of hPSCs at a reasonable cost. The dissimilar and sometimes conflicting results from comparative analyses of commercially available microcarrier types [168, 169], which are suitable for the culture of non-hPSC lines (e.g. CHO cells, Vero cells etc.), make increasingly clear that these microcarriers are not optimal for the culture of hPSCs. Recent studies on the cultivation of hPSCs on 2D xeno-free surfaces featuring recombinant ECM proteins like fibronectin [163], laminin [71, 162], vitronectin [45, 62], and synthetic polymer- or peptide-conjugated surfaces [72, 80, 170-173] have garnered optimism for the scalable cultivation of stem cells and their progeny. Nonetheless, the fundamental differences between 2D and 3D surfaces (e.g.

substrate curvature and elasticity affecting stem cell shape, spreading and eventually commitment [174-176]), and static versus stirred-suspension cultures (e.g. agitation-induced shear in SSBs) hinder the direct translation of these findings to the hPSC expansion/differentiation in microcarrier SSBs.

Current protocols also rely on seeding hPSCs as clumps on microcarriers for SSB cultivation. This is due to the dramatic decrease in cell viability when hPSC colonies are completely dissociated into single cells. Cluster seeding however creates a bottleneck in the process due to the inefficient attachment of cells and the uneven colonization of the microcarriers. To that end, we set out to investigate the seeding of single dispersed hPSCs on microcarriers thereby boosting the attachment efficiency and the initial number of cells available for cultivation. Enhanced cell survival during the microcarrier ‘loading’ phase was maintained with the use of a Rho-associated kinase inhibitor [119].

More importantly, we demonstrate here the propagation of hPSCs over multiple successive passages and their directed differentiation on xeno-free microcarriers in stirred-suspension cultures with defined media. For this purpose, compact microcarriers were engineered by surface conjugation of a synthetic peptide derived from vitronectin. This peptide was previously shown to support the long-term self-renewal of hESCs and their cardiogenic differentiation on flat surfaces [72]. Our analysis revealed that peptide-conjugated microcarriers supported the growth of hPSCs in static cultures but extensive cell detachment was observed when the beads were suspended in spinner flasks. This was ameliorated upon treatment of peptide-conjugated microcarriers with poly-L-Lysine (pLL), a

synthetic polymer promoting cell attachment onto surfaces. Human PSCs on those microcarriers proliferated consistently over multiple passages without loss of their pluripotency and normal karyotype. Additionally, cells on microcarriers were successfully subjected to differentiation toward mesoderm. These findings evidence the feasibility of cultivating hPSCs in xeno-free microcarrier systems and further support the use of such systems for the scalable generation of therapeutically useful progeny.

## **2.2 Materials and Methods**

### **2.2.1 Human pluripotent stem cell culture**

Human ESCs (H9 (WA09); passages 30-50) and iPSCs (iPSC (IMR90)-4 thereafter IMR90; passages 30-40) were obtained from the WiCell Research Institute (Madison, WI). Cells cultured in dishes coated with Matrigel (BD Biosciences, San Jose, CA) and in mTeSR1 medium (StemCell Technologies, Vancouver, BC) were maintained in 5% CO<sub>2</sub>/95% air at 37 °C. Medium was replaced every day, and the cells were passaged every 5–6 days by enzymatic dissociation with collagenase type IV (Life Technologies, Grand Island, NY).

Viable cells were counted in a hemocytometer after Trypan Blue staining (Sigma-Aldrich, St. Louis, MO). Alternatively, cells were stained with 20 mg/ml fluorescein diacetate (FDA-live cells; Sigma-Aldrich) in PBS for 5 min and after being washed twice with PBS, they were analyzed by fluorescence microscopy or flow cytometry (see below).

Lactate dehydrogenase (LDH) activity was determined in culture samples with a LDH cytotoxicity detection assay (Roche, Indianapolis, IN) according to the manufacturer's instructions as described [158, 177].

### **2.2.2 Microcarrier seeding and passaging**

Collagen-coated polystyrene microcarriers (SoloHill, Ann Arbor, MI) were processed as described [158]. Briefly, beads were equilibrated in PBS for 30 min, autoclaved and coated with Matrigel at room temperature for 1 h. Coated microcarriers were equilibrated in culture medium supplemented with 10  $\mu$ M ROCK inhibitor (Y-27632; Enzo Biochem, Farmingdale, NY) for 1 h before cell seeding. Beads at 0.5 g ( $\sim$ 180 cm<sup>2</sup> surface area)/50 ml medium were used.

Microcarriers subjected to peptide conjugation (see below) were equilibrated in mTeSR1 medium for 30 min before use. The amount of peptide-conjugated microcarriers was adjusted to maintain a constant ratio of bead surface area-to-medium volume among experiments.

Stem cells on Matrigel-coated dishes were treated with 10  $\mu$ M Y-27632 for 1 h before bead seeding. Colonies were dissociated into single cells with Accutase (Innovative Cell Technologies, San Diego, CA). Dispersed hPSCs were transferred with microcarriers (cell-to-bead ratios as stated) to Petri dishes and placed in 5% CO<sub>2</sub>/95% air at 37 °C for the period as noted. Subsequently, the cell-laden beads were transferred to ProCulture spinner flasks (Corning, Corning, NY), the total medium volume supplemented with Y-27632 was brought to 50 ml,

and the agitation rate was set to 60 rpm for the duration of each run after the removal of floating cells. After the first day, the medium was replaced by medium without Y-27632. Subsequent medium changes were performed at half-volume every day. The cultures were maintained at 37 °C in 5% CO<sub>2</sub>/95% air.

After 6-day expansion, hPSCs reached their peak concentration and are ready to be passaged into new spinner flasks. Before passaging, cells on microcarriers in a spinner flask were washed once with PBS and incubated with 10 ml of Accutase for 10-15 min with occasional mixing. After they were detached from microcarriers, cells were harvested by passing the mixture of suspended single cells and microcarriers through a 100 µm mesh strainer (BD Biosciences). Harvested cells were ready to be used in next passages.

### **2.2.3 Preparation of microcarriers with peptide conjugation and pLL treatment**

Polystyrene beads featuring –COOH groups on their surfaces (Rapp-Polymere GmbH, Tuebingen, Germany) were incubated for 30 min with N-(3-dimethylaminopropyl)-N'-ethylcarbodiimide hydrochloride (EDC) and N-hydroxysuccinimide (NHS) (4:1 molar ratio; both from Thermo Scientific) in PBS for –COOH activation. After aspirating the EDC/NHS solution, the microcarriers were incubated with varying amounts of the synthetic peptide AcKGGPQVTRGDVFTMP [72] (GenScript, Piscataway, NJ) derived from vitronectin in PBS for 2 h. The microcarriers were then immersed in

ethanolamine (pH 8.5) for 1 h to quench any unreacted activated ester groups, washed 3 times with PBS and stored in 75% (v/v) aqueous ethanol. Prior to cell culture, peptide-conjugated microcarriers were washed 3 times with sterile deionized water to eliminate traces of ethanol. For poly-L-lysine (pLL) coating, the beads were incubated with sterile 0.01% pLL solution (Sigma) for 5 min and dried.

The peptide density on the bead surface after conjugation and the efficiency of the amidation reaction were quantified using the FluoroProfile Protein Quantification assay (Sigma). Supernatant samples containing unreacted peptide were loaded in triplicates in black-wall 96 well-plates (VWR, Bridgeport, NJ) and fluorescence intensity was measured on a Synergy 4 Hybrid microplate reader (BioTek, Winooski, VT) with the Gen5 software (BioTek).

#### **2.2.4 RT-PCR and quantitative PCR**

Total RNA was isolated using Trizol (Invitrogen, Carlsbad, CA) according to the manufacturer's instructions, and reverse transcription (RT) was performed using the ImPromII reverse transcriptase (Promega, Madison, WI) as described [158]. PCR runs were performed with the resulting cDNA for 35 cycles at an annealing temperature of 58–60 °C depending on the primer set (Table 2.1).

Quantitative PCR (qPCR) was performed on a CFX96 Real-Time PCR machine (Bio-Rad, Hercules, CA) using the DyNAmo™ SYBR Green qPCR Kit (Thermo Scientific, Waltham, MA): Denaturation and polymerase activation at 95 °C for

15 min; amplification for 40 cycles at 94 °C for 10 s, 58–60 °C for 20 s, and 72 °C for 30 s. All reactions were run in triplicates. Amplification specificity was verified by the melting curve method and gel electrophoresis. Relative gene expression was calculated with the BioRad CFX software by normalizing to the endogenous  $\beta$ -actin (*ACTB*) expression. The  $C_T$  for the housekeeping gene did not vary under different experimental conditions when equal amounts of RNA were used.

Gene	Forward primer	Reverse primer	Amplicon size (bp)
<i>POU5F1</i>	AAGCTGGAGAAGGAGAA GCTG	AATAGAACCCCCAGGG TGAG	158
<i>NANOG</i>	AGATGCCTCACACGGAGA CT	ACACAGCTGGGTGGAA AGAGA	194
<i>FOXA2</i>	GAAGATGGAAGGGCACG A	CACGTACGACGACATG TTCA	193
<i>SOX17</i>	CTTTCATGGTGTGGGCTA AGG	GTACTTGTAGTTGGGGT GGTCCT	191
<i>PAX6</i>	AACAGACACAGCCCTCAC AAAC	CGGGAAGTTGAACTGG AACTGAC	275
<i>ISL1</i>	GCGGAGTGTAATCAGTAT TTGGA	CACTCGATGTGATACA CCTTGG	184
<i>KDR</i>	CCAGAAGTAAAAGTAATC CCAGATG	CTTTAAAAGTTCTGCTT CCTCACTG	246
<i>MEOX1</i>	AGAGTTTGCCCATCATAA CTACCT	GCTCAGTCCTTAGTCAT TTTTCTC	238
<i>TUBB3</i>	TGTACTCCTTCCTGCTGG	CCCCAACTCTCACTATG	270

	ACTT	TGGAT	
<i>NES</i>	CAGCGTTGGAACAGAGGT TG	GGGAATTGCAGCTCCA GCTT	289
<i>T</i>	TGTACTCCTTCCTGCTGG ACTT	CCCCAACTCTCACTATG TGGAT	270
<i>GATA4</i>	TCATCTCACTACGGGCAC AG	GGGAAGAGGGAAGATT ACGC	233
<i>MIXL1</i>	GGTACCCCGACATCCACT T	GGAGCACAGTGGTTGA GGAT	166
<i>ACTB</i>	CTTCCTGGGCATGGAGTC CT	AGGAGCAATGATCTTG ATCTTC	202

Table 2.1 Primer sequences (shown in 5'-3' orientation) used for PCR and qPCR

### 2.2.5 Flow cytometry

Cells were dissociated from microcarriers by incubation with TrypLE (Life Technologies), passed through 100  $\mu$ m mesh strainers (BD Biosciences) for bead removal, and pelleted by centrifugation at 200xg for 5 min. Cells were then fixed in a 3.7% formaldehyde solution (Sigma-Aldrich) for 10 min, washed with PBS and permeabilized with Cytonin (Trevigen, Gaithersburg, MD) for 30 min before blocking with 3% normal donkey serum (NDS; Jackson ImmunoResearch Laboratories, West Grove, PA) for 20 min. The samples were subsequently incubated with primary antibodies including rabbit anti-OCT4 (Santa Cruz Biotechnology, CA), mouse anti-NANOG (Millipore, Boston MA) and mouse anti-SSEA4 (AbCam, NJ) for 1 h at room temperature. After washing three times with 1% NDS, cells were incubated with appropriate DyLight secondary

antibodies (Jackson Immunoresearch Laboratories, West Grove, PA) for 1 h at room temperature. The samples were washed again three times with PBS and analyzed in a FACS Calibur flow cytometer with the CellQuest software (Becton Dickinson, Franklin Lakes, NJ). Data were further analyzed with the FCS Express V4.0 suite (De Novo Software, Los Angeles, CA). Cells were considered as positive for a particular antigen if their emitted fluorescence level was higher than 99% of that of samples stained only with the corresponding secondary antibodies.

### **2.2.6 Immunocytochemistry**

Cells were fixed with 4% paraformaldehyde (Sigma) in PBS, permeabilized/blocked in PBS with 0.1% Triton X-100 (Mallinckrodt Baker, Phillipsburg, NJ) and 1% bovine serum albumin (BSA; Sigma) for 30 min and incubated overnight at 4 °C with primary antibodies: Mouse anti-SSEA4 (AbCam, NJ), rabbit anti-OCT4 (SantaCruz, CA), goat anti-SOX17 (R&D Systems, MN), rabbit anti-FOXA2 (Cell Signaling Technologies), rabbit anti-MEOX1 (Novus Biologicals), mouse anti-KDR (AbCam, NJ), mouse anti-NESTIN (R&D systems) and rabbit anti-TUBB3 ( $\beta$ III-tubulin; Sigma-Aldrich). After three washes with PBS, cells were incubated with DyLight secondary antibodies (Jackson Immunoresearch Laboratories) for 1 h at room temperature. Nuclear DNA was stained with DAPI (Vectashield, Vector Laboratories, Burlingame, CA). Images were acquired with an inverted microscope with epifluorescence (Zeiss Axio Observer D1; Carl Zeiss, Thornwood, NY) connected to a digital camera (Zeiss AxioCam MRm).

### **2.2.7 Karyotyping**

Cells harvested from microcarrier cultures were replated on T-75 flasks and allowed to grow until ~70% confluence before treatment with 30 ng/ml of KaryoMAX Colcemid Solution (Gibco, Grand Island, NY) for 4 h at 37 °C. Cells were then harvested, transferred to 15 ml conical tubes, centrifuged for 5 min at 250xg and gently resuspended in cell hypotonic solution (CHS; 40 mM KCl, 20 mM HEPES, 0.5 mM EGTA and 9 mM NaOH) for 1 h of incubation at 37 °C. After centrifugation of the cell/CHS suspension at 250xg, the supernatant was removed and the cells were fixed with 1:3 (v/v) acetic acid-methanol solution. G-banding analysis was performed in the SKY/FISH facility at the Roswell Park Cancer Institute (Buffalo, NY).

### **2.2.8 Embryoid body formation**

Single dispersed hPSCs were cultured in AggreWell plates (StemCell Technologies) according to a manufacturer's protocol to induce embryoid body (EB) formation. Harvested EBs were transferred to Petri dishes and maintained in Dulbecco's modified Eagle's medium/Ham's F12 medium (DMEM/F12) (Life Technologies), supplemented with 20% FBS (PAA Laboratories, Dartmouth, MA). Medium was replenished every 2 days until analysis of the EBs.

### **2.2.9 Definitive endoderm, mesoderm, and neuroectoderm differentiation**

Cells harvested from microcarriers were replated on Matrigel-coated dishes. For bioreactor differentiation, the medium used for expansion of hPSCs was exchanged with differentiation medium keeping the total working volume constant. Differentiation to definitive endoderm, mesoderm and neuroectoderm were performed according to previous reports [158, 178-180].

Definitive endoderm (DE) differentiation of IMR90 cells harvested from CP+pLL microcarriers was performed as previously described [158]. Briefly, after 5 passages, cells on microcarriers were disassociated into single cells with Accutase and seeded on Matrigel-coated dishes with mTeSR medium supplied with 10  $\mu$ M Y-27632 and cultured for one day. In the following days, medium replaced daily with mTeSR until cells reached 80% confluence. Differentiation was carried out in RPMI (GIBCO, Grand Island, NY) supplemented with 100 ng/ml activin A (R&D Systems) from days 0 to 4 and various amounts of Knockout Serum Replacer (KSR; GIBCO, Grand Island, NY) as follows: no KSR for Day1, 0.2% KSR for Day 2, and 2% KSR for Day 3-4.

Before mesoderm differentiation, IMR90 cells were harvested from CP+pLL microcarriers and maintained on Matrigel-coated dishes same as that described in definitive endoderm differentiation section. Mesoderm differentiation protocol used here was the same as previously reported [181]. In brief, differentiation was carried out in RPMI medium supplemented various amount of activin A, BMP4 and KSR for 5 days: On Day 1, RPMI was supplemented with 100 ng/ml activin A. On Day 2 and 3, RPMI was supplemented with 0.2% KSR, 10 ng/ml activin A

and 10 ng/ml BMP4 (R&D Systems). On Day 4 and 5, RPMI was supplemented with 2% KSR, 10 ng/ml activin A and 10 ng/ml BMP4.

Before neuroectoderm differentiation, IMR90 cells harvested from CP+pLL microcarriers were cultured on Matrigel-coated dishes until 90% confluence similar as that described in definitive endoderm differentiation. Neuroectoderm differentiation was performed following published protocol [179] with minor changes. On Day 1, mTeSR was replaced by neural induction medium (NIM: DMEM/F12:Neurobasal medium (1:1), 1×N2 supplement, 1×B27 supplement without vitamin A (all from GIBCO) and 2 mM Glutamax (Mediatech, Herndon, VA)). The next day, IMR90 cells were passaged using collagenase IV (GIBCO) and seeded in low-attachment dishes (BD Biosciences) to form embryoid bodies (EBs). EBs were cultured in NIM for 4 days with daily medium change. Then the medium was switched to neural proliferation medium (NPM: DMEM/F12:Neurobasal (1:1), 0.5×N2 supplement, 0.5×B27 supplement, 2 mM Glutamax and 20 ng/mL FGF2 (R&D Systems)) for another 3 days with daily medium change. After that, EBs were replated on Matrigel-coated dishes and cultured for another 2 days before characterization.

#### **2.2.10 Statistical Analysis**

Data are expressed as mean  $\pm$  standard deviation unless stated otherwise. ANOVA and the *post hoc* Tukey test were performed using Minitab (Minitab Inc, State College, PA). P values less than 0.05 were considered as significant.

## 2.3 Results

### 2.3.1 Single dispersed hESC seeding on Matrigel-coated microcarriers for stirred suspension culture

We reported previously that hESCs and hiPSCs seeded as clusters on Matrigel-coated microcarriers can be cultured in stirred-suspension vessels [5, 158]. Although hPSCs in clusters exhibit improved survival, this seeding method results in significant loss of viable cells and attachment efficiency of only ~30%. Therefore, we investigated the seeding of dispersed hPSCs on microcarriers. Human ESCs were cultured with 10  $\mu$ M ROCK inhibitor (which limits dissociation-induced apoptosis [119]) for 1 h on Matrigel-coated plates before harvested as single cells and loaded on Matrigel-coated microcarriers at 25 cells/bead. In parallel, cells were inoculated on Matrigel-coated beads as clusters at the same cell:bead ratio [158]. Of the single hESCs,  $77.0 \pm 7.3\%$  attached on the beads in the presence of ROCK inhibitor within 4 h compared to only  $30.5 \pm 4.8\%$  of cells inoculated as clusters (**Figure 2.1A**,  $p < 0.05$ ). The seeding efficiency was similar whether the cells were incubated with microcarriers for 4 h or overnight. Moreover,  $97.2 \pm 1.8\%$  of beads was colonized with single cells vs. only  $34.7 \pm 8.5\%$  after cell cluster seeding (**Figure 2.1B**). The distribution of hESCs seeded as dispersed cells on the beads was also more even and no large aggregates were observed after six days of culture (**Figure 2.1C-D**). Although ‘bridging’ among beads was noted, the cells grew 25.1-fold (**Figure 2.1E**, solid curve). Similar results were obtained for single dispersed hiPSCs and hiPSC clumps seeded onto Matrigel-coated microcarriers (**Figure 2.2**).

It should be noted that the above results were obtained after cell treatment with the ROCK inhibitor overnight. In contrast, when the inhibitor was removed after 4 h of seeding, cells exhibited a long lag phase and their concentration did not increase substantially (2.8-fold) under the same conditions (**Figure 2.1E**, dashed curve). Keeping the cells with the beads either for 4 h or overnight during the loading phase did not affect the seeding efficiency (**Figure 2.1A**) and this was ruled out as contributing to the difference in the fold expansion of hESCs during their subsequent culture in spinner flasks. We concluded therefore that overnight treatment with ROCK inhibitor was essential for successful expansion on microcarriers in stirred-suspension.

These findings prove that hPSCs can be loaded as single cells on microcarriers with higher seeding efficiency and are distributed uniformly in contrast to cluster seeding. Moreover, subsequent hPSC expansion in stirred-suspension microcarriers is dependent on the interval of hPSC treatment with ROCK inhibitor during and after seeding.

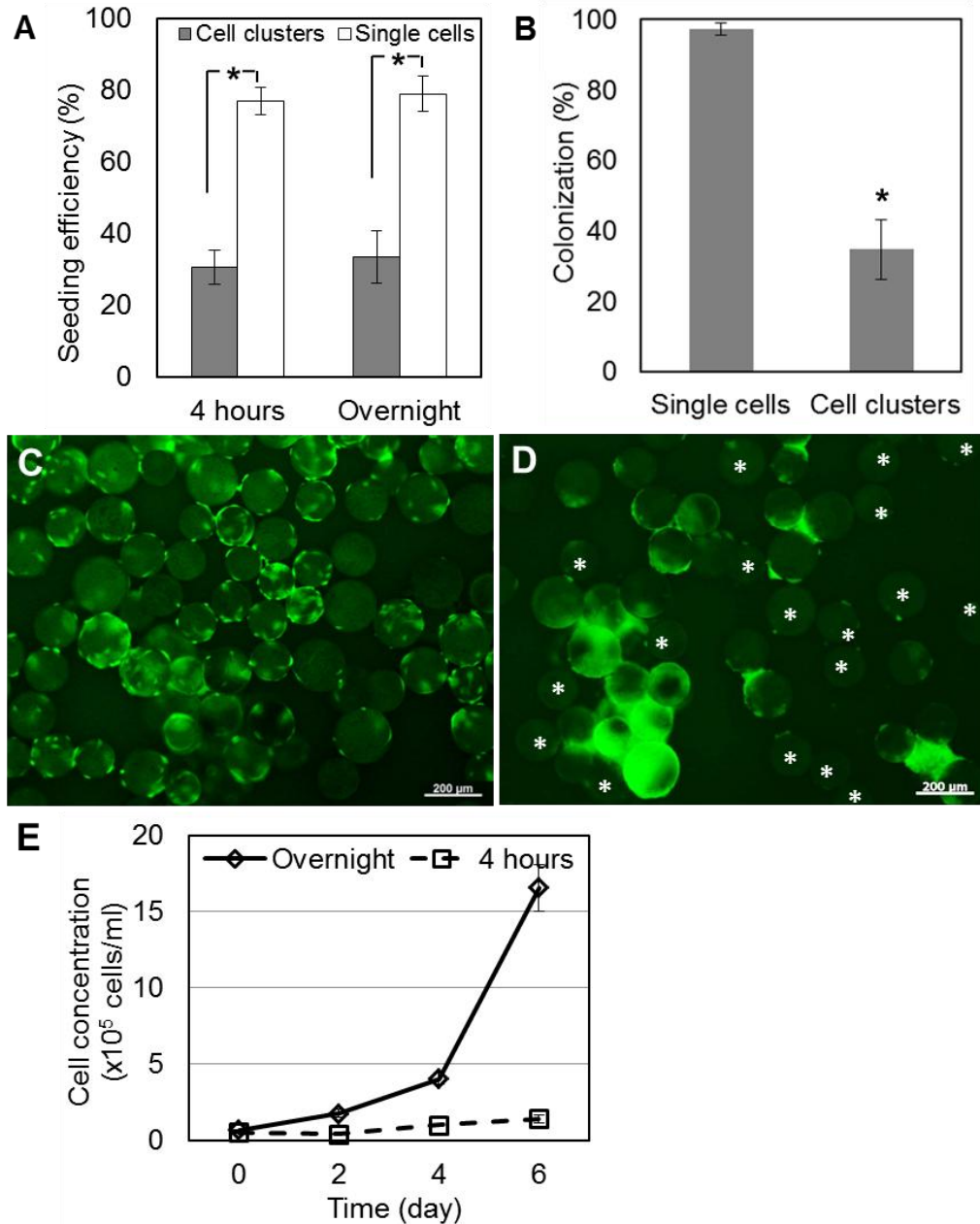


**Figure 2.1** Seeding H9 cells onto Matrigel-coated microcarriers (A) Seeding efficiency comparison between seeding with single cells (white bars) vs. seeding with cell clusters (grey bars) after either 4 hours or overnight. (B) Colonization percentage comparison between seeding with single cells vs. seeding with cell clusters after overnight. (\* $p < 0.05$ ). Fluorescein diacetate acid (FDA) staining of H9 cells seeded on Matrigel-coated microcarriers as single cells (C) or small cell

clusters (D) (\* represents microcarriers which were either empty or populated with far few cells). (E) Growth profile of H9 cells seeded on Matrigel-coated microcarriers in spinner flasks with 4 hours (dashed curve) or overnight (solid curve) treatment of ROCK inhibitor (\*p < 0.05).

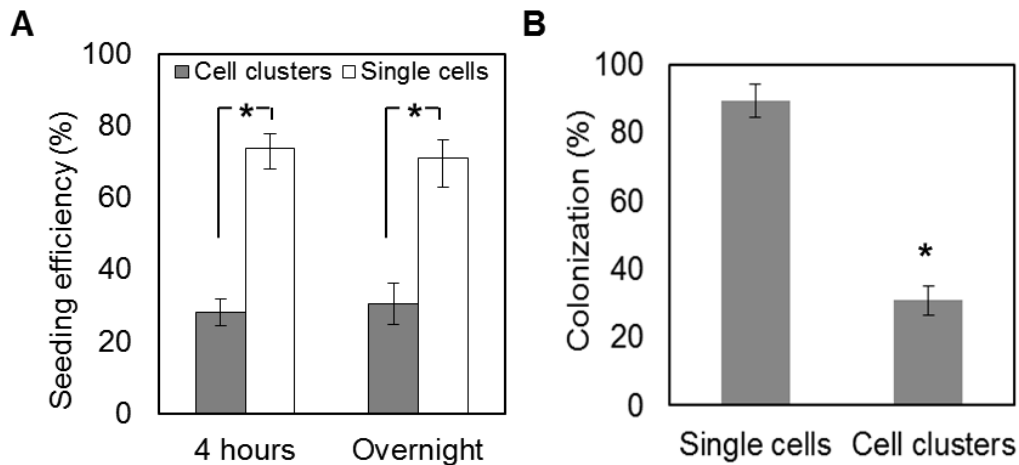


**Figure 2.2** Seeding IMR90 cells onto Matrigel-coated microcarriers (A) Seeding efficiency comparison between seeding with single cells (white bars) vs. seeding with cell clusters (grey bars) after either 4 hours or overnight. (B) Colonization percentage comparison between seeding with single cells vs. seeding with cell clusters after overnight (\*p<0.05).

### 2.3.2 Multi-passage suspension culture of hPSCs seeded as dispersed cells on Matrigel-coated microcarriers

Next, we addressed the question of whether hPSCs seeded as single cells on Matrigel-coated beads can be cultured for multiple passages. Indeed, H9 hESCs were successfully cultured for five 6-day passages on microcarriers. Cell

proliferation was consistent among passages with an average increase of  $20.7 \pm 4.0$ -fold to concentrations of  $1.5\text{-}1.9 \times 10^6$  cells/ml (**Figure 2.3A**). Cumulative LDH activity in the medium was kept at low levels (peak values  $<650$  mU/ml) similar to microcarrier cultures after hESC cluster seeding [158] (**Figure 2.3B**). After each passage, cells harvested from microcarriers were probed for the expression of pluripotency markers by qPCR, flow cytometry and immunostaining. *NANOG* expression was the highest after the second passage and consistently higher in all passages when compared to passage 1 (**Figure 2.3C**). The low expression of *NANOG* after the initial passage may be in part due to the adaptation of cells to the bioreactor environment. When analyzed by flow cytometry, the majority of cells ( $>75\%$ ) also retained the expression of OCT4 and SSEA4 over successive passages (**Figure 2.3D**). These results are corroborated by immunostaining for the same markers of cells harvested from the last passage (**Figure 2.3E**). Taken together, our data indicate that hESCs seeded as single cells with ROCK inhibitor can be propagated on microcarriers in a stirred-suspension vessel without loss of pluripotency marker expression.

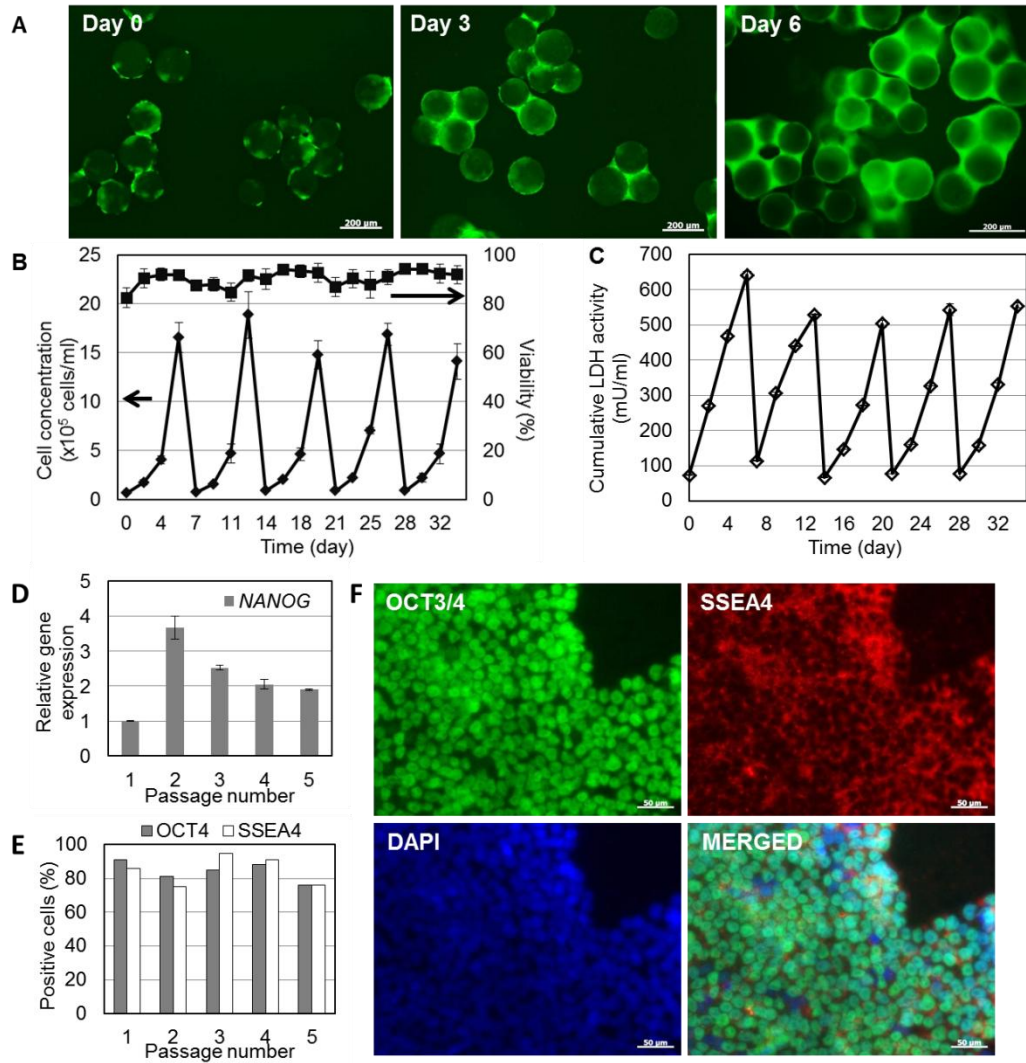


**Figure 2.3** Continuous culture of H9 cells on Matrigel-coated microcarriers for 5 passages. (A) Live cells on beads were stained with FDA showing their distribution and expansion over time. (B) Growth profile and viability. (C) Cumulative LDH activity. Expression of pluripotency markers were checked by qPCR (D, normalized to first passage), flow cytometry (E) and immunostaining (F, Passage 5). Data from a representative experiment are shown.

### 2.3.3 Culture of hPSCs on peptide-conjugated microcarriers

With an improved protocol in place for the efficient seeding of beads with hPSCs, we proceeded to engineer the microcarrier surface by replacing the mouse sarcoma-derived Matrigel matrix with synthetic substrates facilitating the adhesion of hPSCs without affecting their pluripotency. For this purpose, polystyrene microcarriers with surface –COOH groups were decorated with an RGD-containing vitronectin fragment shown to promote hESC adhesion and growth in static cultures [72]. The peptide was conjugated to the –COOH groups via an N-(3-Dimethylaminopropyl)-N'-ethylcarbodiimide hydrochloride/N-hydroxysuccinimide (EDC/NHS) catalyzed amidation reaction. The –COOH concentration was constant (1.09 mmol/g beads) and the amounts of conjugated peptide and peptide used (per gram of beads) in the coupling reaction were proportional (**Figure 2.4A**) allowing for control of the peptide density on the bead surface. Carboxyl group activation by EDC/NHS was critical for the subsequent coupling reaction as no peptide was detected on beads when the EDC/NHS treatment was skipped.

Microcarriers with different peptide surface densities were incubated with IMR90 hiPSCs to evaluate cell attachment. At or above 4 mg peptide/g bead used for the amidation reaction there were no statistically significant differences in seeding efficiency, which was at 30-35% (**Figure 2.4B**). At 0.5 mg peptide/g bead the efficiency decreased to 20%. We therefore selected 4 mg peptide/g bead (600 ng peptide/cm<sup>2</sup>) as the concentration for engineering microcarriers in subsequent

experiments. The cell-to-bead ratio was set to 50 to keep the same number of attached cells on peptide-conjugated and Matrigel-coated microcarriers.

IMR90 cells seeded on peptide-conjugated (CP) beads were cultured in spinner flasks for 6 days. However, cells did not spread on the beads and extensive aggregate formation was observed (**Figure 2.4C**). Hence, despite attachment on CP microcarriers in static culture and in 2D surfaces coated with same peptide [72], the adhesion of cells was not sufficiently strong to maintain them on the beads under stirring.

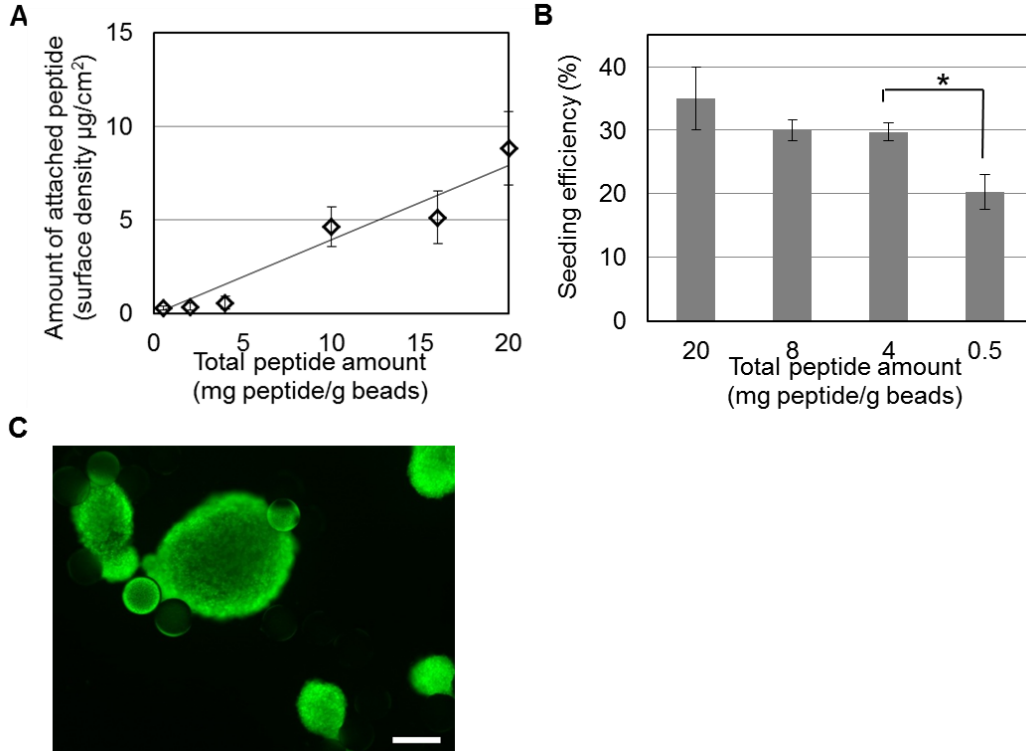


**Figure 2.4** Peptide surface density of microcarriers and seeding efficiency of hPSCs. (A) Surface peptide density versus the total amount of peptide used in amidation reaction. (B) Seeding efficiencies of IMR90 cells on microcarriers conjugated with different amount of peptides. Cells were cultured in TeSR2

medium. (C) IMR90 cells seeded on CP beads and cultured in spinner flasks failed to spread on the beads and formed aggregates. Scale bar: 200  $\mu\text{m}$ .

#### **2.3.4 Human PSC expansion on peptide-conjugated, pLL-treated microcarriers**

The extensive aggregation and loss of surface adhesion observed for hiPSCs cultured on CP microcarriers in stirred-suspension suggested the need for devising ways to strengthen the cell-to-bead attachment. To that end, microcarriers were coated with pLL, which is a positively-charged synthetic polymer enhancing cell attachment [182], and seeded with hPSCs at 50 cells/bead (**Figure 2.5A**). The highest seeding efficiency was measured on CP microcarriers coated with pLL (CP+pLL) at 35.8% compared to 29.8% for peptide-conjugated microcarriers without pLL (CP). Cells seeded on microcarriers coated with only pLL (pLL) or a mixture of pLL and free peptide (without EDC/NHS coupling reaction; FP+pLL), exhibited significantly lower adhesion with efficiencies between 11.7% and 9.2%. Furthermore, microcarriers treated with only EDC/NHS (untreated) displayed poor cell attachment indicating that this step per se does not contribute to the adhesiveness of the bead surface. Of note is that when IMR90 hiPSC clusters were seeded onto CP+pLL beads at the same cell-to-bead ratio, the seeding efficiency was  $16.5\% \pm 3.2\%$ , i.e. significantly lower than inoculating dispersed single cells.

Dispersed hiPSCs were then seeded onto CP+pLL beads and cultured in spinner flask for 6 days. In contrast to forming aggregates when cultured on CP beads,

cells cultured on CP+pLL beads attached and spread and no floating clusters were observed (**Fig. 2.5B**).

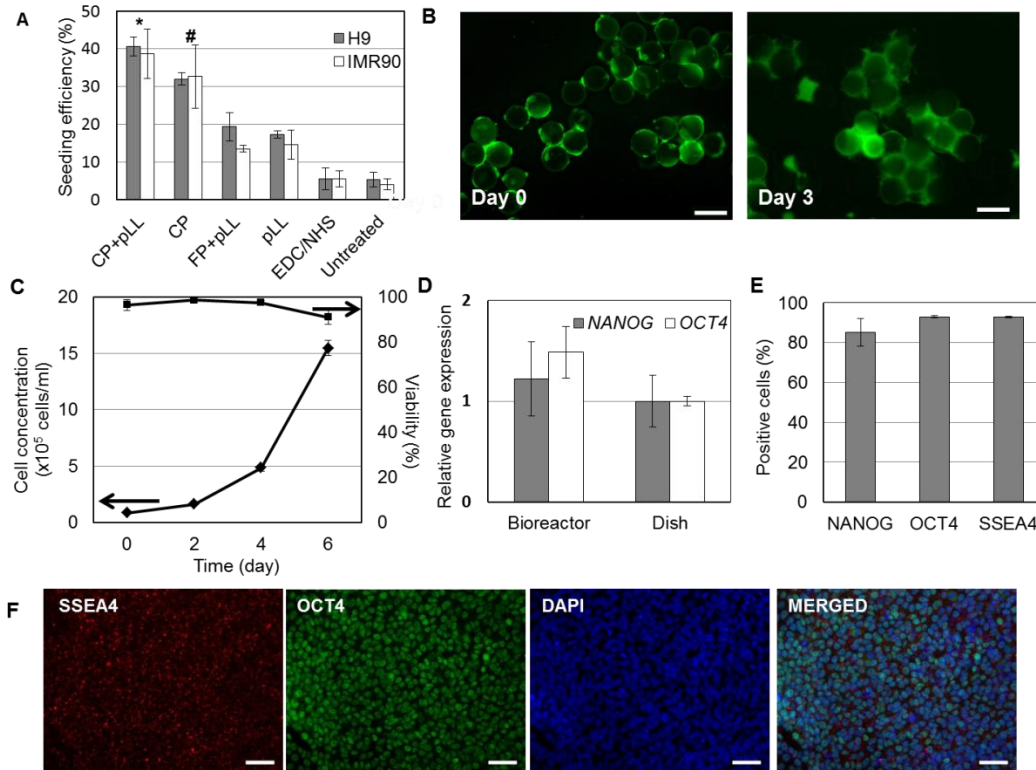


**Figure 2.5** Coating of peptide-conjugated microcarriers with poly-L-lysine (pLL) for hPSC culture in xeno-free medium. (A) Seeding efficiency of IMR90 (hiPSCs) and H9 (hESCs) on microcarriers featuring different surface treatments: CP+pLL: beads with conjugated peptide and pLL coating; CP: beads with conjugated peptide; FP+pLL: beads with free (unconjugated) peptide and pLL coating; pLL: beads with pLL coating only, N-(3-Dimethylaminopropyl)-N'-ethylcarbodiimide hydrochloride (EDC)/N-hydroxysuccinimide (NHS): beads subjected to the coupling reaction without peptide; Untreated: plain beads without any treatment. (\* $P < 0.05$ : CP + pLL versus pLL and CP + pLL versus FP + pLL, # $P < 0.05$ : CP

versus EDC/NHS and CP versus untreated. Mean values are compared among different microcarriers for the same cell type (H9 or IMR90)). (B) FDA-stained Live IMR90 cells grown on CP+pLL beads right after the seeding phase (left, Day 0) and during the spinner flask culture (right, Day 3). (C) Time course of the concentration and viability of IMR90 cultured on CP + pLL beads in stirred suspension. (D) Relative expression of NANOG and OCT4 in IMR90 cells cultured for 6 days in a microcarrier suspension (spinner flask). The corresponding gene expression of IMR90 cells maintained in dishes is also shown. (E) Analysis of cultured cells (day 6) by flow cytometry for the expression of stem cell markers. Values are shown as mean  $\pm$  SD ( $n \geq 3$ ). (F) Immunostaining of cells after 6 days of expansion on CP + pLL beads in the spinner flask. Cells in (A–F) were cultured in TeSR2 medium. Scale bars in (B): 200  $\mu$ m, (F): 50  $\mu$ m.

Cells were then cultured continuously for five 6-day passages. A  $23.3 \pm 5.3$ -fold increase in cell concentration peaking at  $1.4\text{--}1.9 \times 10^6$  cells/ml was noted per passage corresponding to a doubling time of 31 h compared to 34.3 h for Matrigel-coated dish cultures (**Figure 2.6A**). Cells exhibited cumulative LDH release patterns similar to H9 cells cultured on Matrigel-coated beads (**Figure 2.6B**). Moreover, cells maintained the expression of *NANOG*, *POU5F1* (OCT4) and *SSEA4* mRNA and corresponding proteins at each passage (**Figure 2.6 C-D**). After 5 passages, cells plated on Matrigel-coated dishes were positive for pluripotency markers (**Figure 2.6E**). These cells were also karyotypically normal based on G-banding analysis (**Figure 2.6F**).

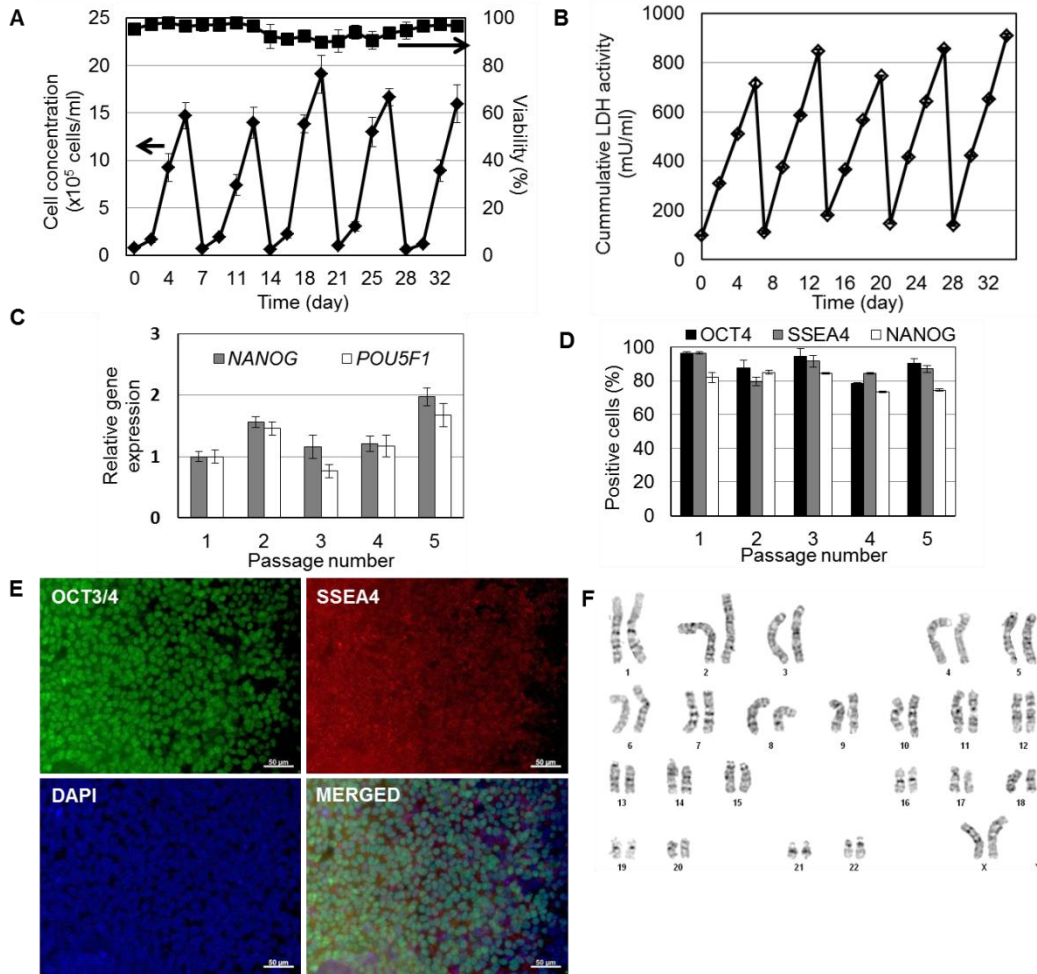


**Figure 2.6** Human PSCs cultured on CP + pLL microcarriers for multiple passages in stirred-suspension vessels. (A) Growth profile, viability and (B) cumulative LDH activity of IMR90 hiPSCs cultured for five passages on microcarriers in spinner flasks. After each passage, the expression of pluripotency markers was characterized by (C) qPCR and (D) flow cytometry. (E) After the last passage, cells were plated and stained for pluripotent markers (scale bar: 50  $\mu$ m). (F) Karyotyping results for IMR90 cells after their culture for five passages in spinner flasks.

Formation of embryoid bodies (EBs) is routinely employed to assess the potential of hPSCs for spontaneous multi-lineage differentiation. Cells propagated for 5 passages on CP+pLL microcarriers in spinner flasks were then cultured as EBs. RNA isolated from these EBs contained transcripts of genes characteristic of the three germ layers: Definitive endoderm (*SOX17*, *FOXA2*)[183, 184], mesoderm (*ISL1*, *MEOX1*) [185, 186] and ectoderm (*PAX6*, *NES*)[179] (**Figure 2.7A**).

Cells cultured for 5 passages in CP+pLL microcarriers were also transferred onto Matrigel-coated dishes and subjected to directed differentiation to definitive endoderm (DE), mesoderm (MS) and neuroectoderm (NE) by applying previously established protocols [158, 178-180]. Differentiation to each lineage was evident by the expression of relevant markers as assessed by qPCR (**Figure 2.7B-D**) and immunostaining (**Figure 2.7E-G**). Cells treated with RPMI media with KSR but without differentiation agents served as controls.

These findings demonstrate that CP+pLL microcarriers support the expansion of hPSCs without adversely affecting their pluripotency and karyotype. Cells are subsequently capable of multi-lineage commitment after application of either spontaneous (EB) or directed differentiation protocols.

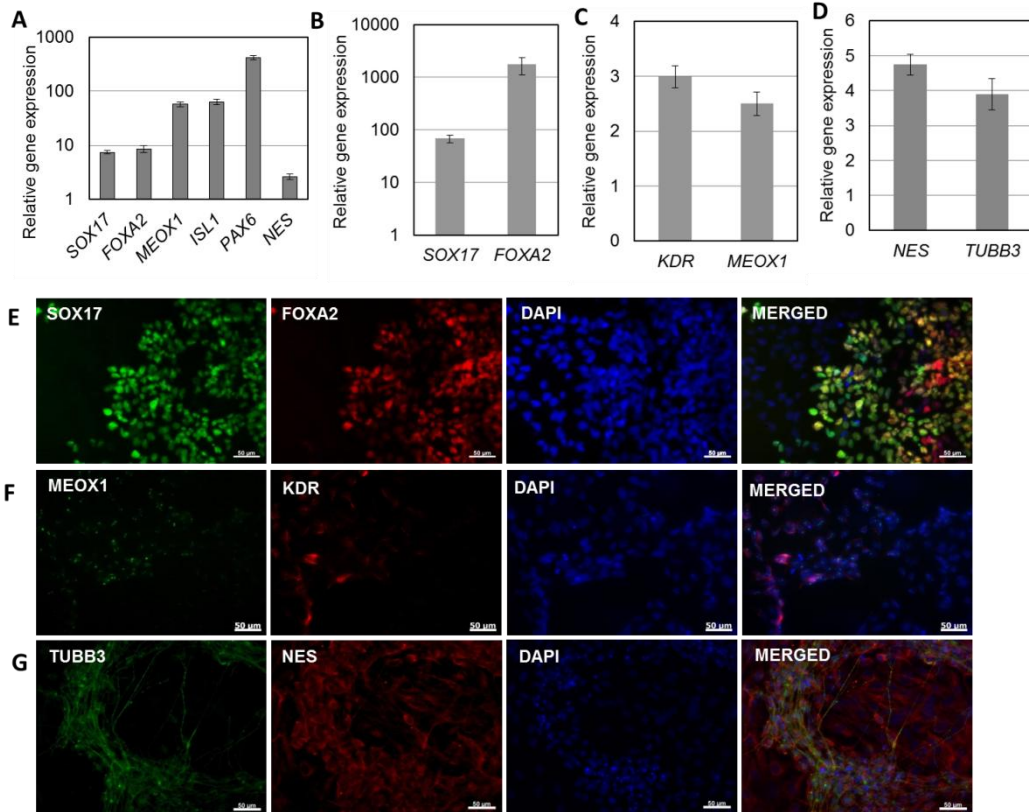


**Figure 2.7** Embryoid body (EB) formation and germ layer differentiation of IMR90 cells cultured on CP+pLL microcarriers after 5 passages. (A) Gene expression of germ layer markers of EBs checked by qPCR (expression normalized to that of undifferentiated IMR90 cells). Definitive endoderm (DE) marker (SOX17 and FOXA2) expression of IMR90-derived DE cells was checked by qPCR (B) and immunostaining (E). Mesoderm (MS) marker (KDR and MEOX1) expression of IMR90-derived MS cells was checked by qPCR (C) and immunostaining (F). Neuroectoderm (NE) marker (TUBB3 and NES) expression of IMR90-derived NE cells was checked by qPCR (D) and immunostaining (G). Gene expression was normalized to IMR90 cells differentiated in basal medium without any growth factors.

### **2.3.5 Directed differentiation of hPSCs on CP+pLL microcarriers in stirred-suspension culture**

Our results showed that hPSCs seeded as dispersed cells on CP+pLL beads can be propagated over multiple passages in a xeno-free stirred suspension culture without loss of their pluripotent state. Then we questioned if the same system can be employed to integrate the expansion of hPSCs with their differentiation in a single scalable process.

For this purpose, stem cells expanded on CP+pLL microcarriers in stirred-suspension were directly subjected to MS differentiation in spinner flasks. In parallel experiments, cells were also dissociated from beads, transferred to dishes and coaxed to MS. After 5 days of differentiation, MS progeny emerged expressing relevant markers as evidenced by qPCR and immunostaining (**Figures 2.8A-B**). The fraction of  $KDR^+$  cells (indicating cardiovascular progenitors [187]) in each culture modality was quantified by flow cytometry as a measure of differentiation efficiency (**Figure 2.8C**). Differentiation in spinner flasks yielded  $52 \pm 8.8\%$   $KDR^+$  cells compared to  $41 \pm 1.29\%$  in dishes whereas cells cultured in medium without differentiation growth factors exhibited  $12 \pm 06\%$   $KDR^+$  cells. It should be noted that the concentration of cells decreased significantly during the first day of commitment both in dish and spinner flask cultures (on average  $\sim 50\%$ ) similar to our previous observations for DE commitment [158]. Taken together, these data support that the xeno-free microcarrier system developed here can accommodate both the expansion and directed differentiation of hPSCs.

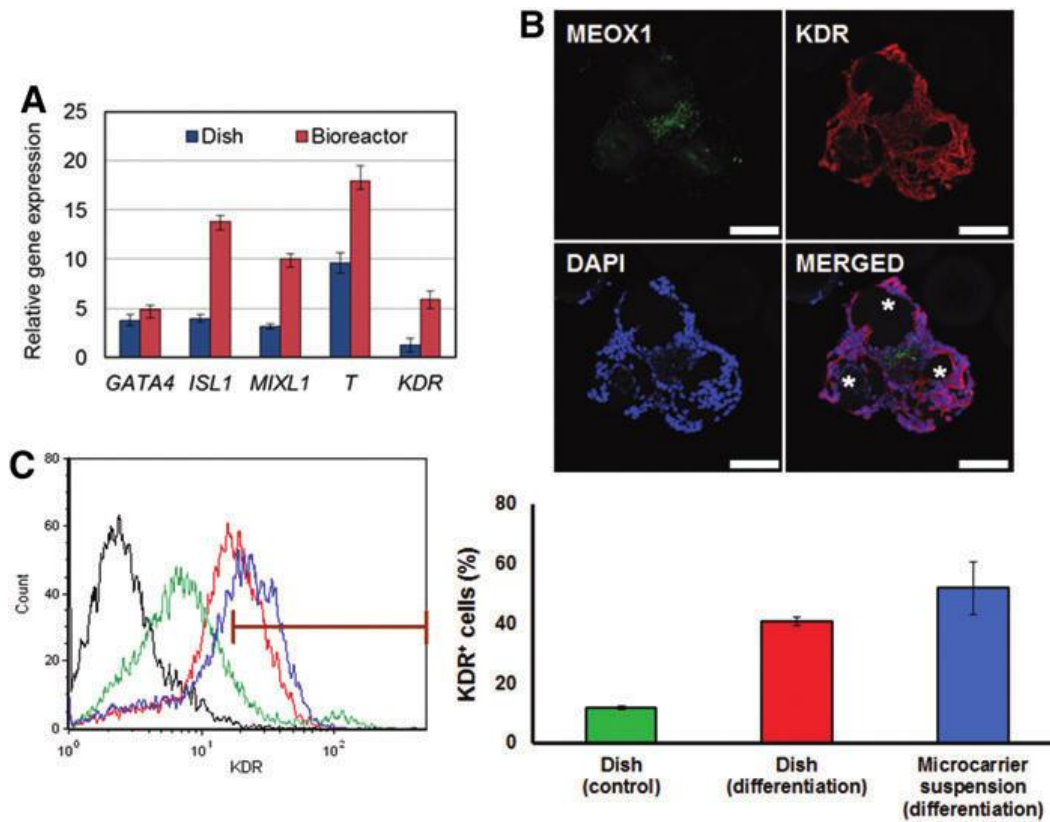


**Figure 2.8** Directed differentiation of hPSCs cultured on CP + pLL microcarriers in a stirred-suspension bioreactor. (A) Expression of MS genes after IMR90 hiPSC differentiation in the bioreactor. Gene expression was normalized to hiPSCs differentiated in basal medium without factors. (B) Immunostaining of differentiated cells on beads. Stars denote the position of microcarriers. Scale bars: 100  $\mu$ m. (C) Flow cytometric analysis of KDR expression. A flow cytometry graph is shown from a representative experiment. Curves correspond to samples of negative control (black), cells in dishes incubated in basal media without differentiation factors (green; dish control), cells differentiated in dishes (red) and cells differentiated in microcarrier suspension culture (blue). The gate excludes 99% of the negative control cells. Results are summarized in the bar graph ( $n = 3$ ) as mean  $\pm$  SD.

## 2.4 Discussion

The development of scalable platforms for the propagation and differentiation of hPSCs is essential for stem cell-based therapies to become a reality. Significant advancements have been made toward culturing stem cells in environments without xenogeneic substrates. The work herein describes the facile engineering of xeno-free microcarriers suitable for the expansion and directed differentiation of hPSCs. Human ESCs and iPSCs on peptide/pLL decorated beads proliferated in mTeSR1 medium at similar or higher levels compared to those for hPSCs grown on commercially available microcarriers coated with Matrigel. Expanded cells maintained a normal karyotype, high viability and the expression of pluripotency markers. When subjected to differentiation either in static culture or stirred-suspension culture, these cells promptly committed to lineages of the three embryonic germ layers.

Defined substrates for supporting the growth of undifferentiated stem cells have been explored in several studies (e.g. [71, 72, 170]). Many of the proposed substrates mimic ECMs to which cell adhesion is mediated via integrins [31, 62]. ECM proteins featuring the integrin-binding arginine–glycine–aspartic acid (RGD) motif [65], such as laminin, fibronectin, collagen, and vitronectin, and derivative peptides have been considered as candidate substrates for hPSC culture. For instance, stem cells have been cultured on RGD-containing ECM proteins/peptides, which were either physically adsorbed or covalently conjugated on 2D surfaces [45, 62, 71, 72, 80, 162, 163, 166]. However, information has been limited on synthetic 3D surfaces supporting hPSC expansion. More importantly, most studies entail static cultures in which the cells are dispensed

from the shear due to agitation experienced in stirred vessels. Indeed, the vitronectin fragment utilized here supports the propagation of undifferentiated hESCs and their differentiation toward cardiac mesoderm on static flat surfaces [72]. We also observed that hPSCs attach and spread well on CP beads in static culture. Yet, the cells come off promptly and/or form aggregates when the beads are placed in agitated suspension. In fact, others also observed reduced hESC growth on (full-length) vitronectin-coated microcarriers compared to flat tissue culture plates layered with the same protein [168]. Therefore, findings based on the culture of cells on microcarriers in static culture do not translate readily to a bioreactor environment.

This also raises caution when screening several microcarrier types in static cultures (e.g. Petri dishes, multi-well plates) and may in part explain conflicting results reported for commonly used microcarriers which best accommodate hPSCs in culture. For example, eight types of commercially available microcarriers were recently tested in static culture [169]. Cytodex 1 beads were among those with the worst performance based on the total amount of hESCs recovered after 72 hours of culture. However, Chen *et al.* [168] examined a cohort of ten different microcarrier types and noted that hESCs attached efficiently during seeding (attachment efficiency ~80% 2 hours post-seeding) and grew to  $\sim 7.7 \times 10^5$  cells/ml after at least two consecutive passages when cultured on Cytodex 1 beads. Coating the microcarriers with Matrigel or purified mouse laminin resulted in higher concentrations of hESCs cultured in mouse embryonic fibroblast-conditioned medium.

The expansion of hPSCs was supported on CP beads in dishes but not in spinner flasks. Increasing the peptide density on the microcarrier surface may strengthen the adhesion and boost the retention of cells under shear but we ruled out this conjecture. First, the seeding efficiency did not increase further with higher peptide densities (and amounts; **Figure 2.4**) on the surface of microcarriers. Second, the density of 600 ng/cm<sup>2</sup> is significantly higher than the threshold density of 250 ng absorbed vitronectin/cm<sup>2</sup> on tissue culture plates to support the growth of undifferentiated hESCs [188]. For the static culture of hESCs on polystyrene beads, a density of 450 ng vitronectin/cm<sup>2</sup> was reported [189] that is closer to the peptide density in our experiments. It should be mentioned that the whole vitronectin molecule (MW~75 kDa or 459 amino acid residues) was used in the studies above in contrast to the smaller decapeptide (MW~1.6 kDa) used here. Hence, the effective density of binding sites was significantly higher than previous reports but the CP beads still did not support cultured stem cells in stirred suspension.

The seeding protocol described here yields higher fractions of attached cells than the current practice of loading hPSCs as clumps on microcarriers for culture. For instance, hESCs are seeded on Matrigel-coated microcarriers as clumps with ~30% efficiency versus almost 80% when seeded as single cells. Moreover, regular culture with the agitation at a set rate can be commenced after 4 hours of inoculating the beads with cells. The nominal loss of cells during the ‘loading phase’ and the reduced preparation time are important from a bioprocess development standpoint. In fact, the protocol timeframe is significantly shorter

than a 3-day seeding preparation reported for hESC clumps on cationic microcarriers (Hillex II, SoloHill, Ann Arbor, MI) with xeno-free medium in spinner flasks [169]. In that study, cells were cultured for a single 11-day passage and therefore the applicability of the method could not be evaluated over longer-term cultivation entailing successive passages. We also found that incubation with the ROCK inhibitor for 24 hours after seeding commences is necessary for the long-term culture of hPSCs in stirred-suspension. During this interval, the inhibitor may curtail apoptosis (e.g. from shear) as the cells adjust to the bioreactor environment.

The use of pLL with the vitronectin-derived RGD peptide for decorating the surface of microcarriers supported the adhesion of hPSCs and their growth under agitation. pLL is a positively-charged synthetic polymer used to facilitate cell attachment while it also promotes the adsorption of ECM proteins to culture surfaces [182]. To our knowledge, there are no reports of pLL alone supporting the maintenance of pluripotent hPSCs in culture. However, pLL enhances the attachment and spreading of mesenchymal stem cells on tissues culture flasks unlike other soluble polymers which are neutral or negatively charged [190]. Correspondingly, microcarriers with positive surface charges are better suited for the culture of hPSCs compared to beads with negative or no outer charge [168, 169]. We posit that the combination of pLL and RGD peptide is effective because the former enhances hPSC attachment by increasing the positive charge on the microcarrier surface while the latter provides proper binding sites for integrin-mediated cell adhesion on beads.

Synthemax microcarrier is a peptide-conjugated microcarrier designed for the culture of hPSCs in stirred suspension. The peptide sequence and conjugation chemistry is derived from Melkounian, Z *et al.*'s work [81]. However, when we tried this microcarrier in our lab, H9 hESCs showed poor attachment and lower proliferation rate compared to the CP + pLL microcarrier.

The fraction of dispersed cells attached on CP + pLL microcarriers was almost 50% of that of cells seeded on Matrigel-coated beads. A similar pattern was noted when comparing the seeding efficiencies of hPSC clusters on the two types of microcarriers. Although CP+pLL beads supported the proliferation and differentiation of IMR90 cells over multiple passages, there is still space for improving the seeding efficiency. Matrigel is a complex protein mixture consisting primarily of entactin, laminin and collagen IV providing sites for cell adhesion [191]. Thus, using an assortment of synthetic peptides featuring distinct cell adhesion sites (e.g. RGD, IKVAV, and YIGSR) rather than a single sequence may enhance the attachment and spreading of hPSCs on microcarriers for stirred-suspension cultivation.

The polystyrene microcarriers with surface –COOH groups were utilized in our study to show that 3D surfaces can be engineered for the scalable culture of hPSCs by employing relatively simple chemistry for peptide conjugation. Going forward however, other microcarriers may be utilized with lower specific gravity (the specific gravity of the CP+pLL microcarriers is about 1.7) or different architecture (e.g. macroporous) to minimize potential effects due to shear-induced agitation.

In conclusion, our study demonstrates the facile engineering of xeno-free microcarriers for long-term scalable culture of hPSCs under defined conditions. Human PSCs were successfully maintained on vitronectin peptide-conjugated/pLL-treated microcarriers in stirred-suspension vessels for multiple passages without compromising their pluripotency, proliferation and karyotype. The microcarrier culture system described here is a step forward in the development of bioprocesses integrating expansion and directed differentiation of human stem cells for the production of therapeutically useful progeny.

### **3 Scalable xeno-free microcarrier cultivation of human pluripotent stem cells in stirred suspension**

#### **3.1 Introduction**

Human pluripotent stem cells (hPSCs) are promising cellular sources for regenerative medicine and tissue engineering. However, before the successful therapeutic application of hPSCs is realized, their large-scale cultivation is critical. Stirred-suspension microcarrier bioreactors [5] are widely-used for large scale mammalian cell culture due to their high surface-to-volume ratio, homogenous environment, plasticity for modification or functionalization of the surface, scalability, and well controlled operation. Human PSCs have been successfully expanded and differentiated to definitive endoderm, cardiomyocytes and neural progenitor cells in stirred-suspension microcarrier vessels [158, 159, 192].

Because of the stringent requirement of hPSCs for attachment substrates, microcarriers used in most hPSC cultivation studies are coated with animal-derived matrices such as Matrigel [112, 158-160] or animal collagen [161]. Those animal originated substrates are not compatible with clinical applications. Vitronectin was reported to be a successful coating matrix for hPSC culture on 2D surfaces [45, 62], however, its application in 3D system has not been fully tested yet.

In this study, we coated microcarriers with recombinant human vitronectin and human serum albumin (HSA) sequentially and then treated the microcarriers with UV irradiation. With these treatments, microcarriers were able to support the

long-term attachment and proliferation of hPSCs in stirred-suspension systems together with commercially available xeno-free medium.

## **3.2 Materials and Methods**

### **3.2.1 Human pluripotent stem cell culture**

Human ESCs (H9 (WA09); passages 30-50) were obtained from the WiCell Research Institute (Madison, WI). Cells cultured in dishes coated with Matrigel (BD Biosciences, San Jose, CA) or recombinant human vitronectin, truncated (Life Technologies, Grand Island, NY) and in TeSR-E8 medium (Stem Cell Technologies, Vancouver, BC) were maintained in 5% CO<sub>2</sub>/95% air at 37 °C. Medium was replaced every day, and the cells were passaged every 5–6 days by enzymatic dissociation with Dispase (Life Technologies, Grand Island, NY) for cells cultured on Matrigel or with Gentle Cell Dissociation Reagent (Stem Cell Technologies).

Viable cells were counted using a hemocytometer after Trypan Blue staining (Sigma-Aldrich, St. Louis, MO). Alternatively, cells were stained with 20 µg/ml fluorescein diacetate (FDA-live cells; Sigma-Aldrich) in PBS for 5 min and after being washed twice with PBS, they were analyzed by fluorescence microscopy or flow cytometry.

### **3.2.2 Microcarrier preparation**

0.5 g plastic microcarriers (Solo Hill, Port Washington, NY) were equilibrated in PBS and autoclaved. 0.1 mg/ml vitronectin was added to the microcarriers/PBS

mixture and mixed well. Incubate for at least 1 hour at room temperature and then add equal volume of 0.01 g/ml to the mixture and incubate for another 30 minutes. Further treat the microcarriers with short wave UV light (254 nm) for up to 40 minutes. These microcarriers were termed VN-HSA-UV microcarriers. The microcarriers were washed with TeSR-E8 media before seeding with cells.

### **3.2.3 Microcarrier seeding and passaging**

Cell colonies were pretreated with 10  $\mu$ M ROCK inhibitor (Y-27632) for 1 hour and then dissociated into single cells using Accutase (Innovative Cell Technologies). Ten million dispersed cells were added to 0.5 g microcarriers and incubated in a 10-cm petri dish with 8 ml of TeSR-E8 medium supplemented with 10  $\mu$ M ROCK inhibitor. The dish was shaken every 15 min for the first 3 hrs to make sure the cells were mixed well with microcarriers. After overnight incubation, the microcarriers were transferred to spinner flask and fresh TeSR-E8 medium was added containing 0.02% Pluronic F-68 to a total of 50 ml. The agitation rate was set at 45 rpm. After the first day, the medium was replaced by medium without Y-27632. Subsequent medium changes were performed at 75% volume every day. The culture was maintained at 37  $^{\circ}$ C in 5% CO<sub>2</sub>/95% air. A sample of 1 ml was taken every other day for cell number counting, viability and LDH activity.

After expansion for 6 days, cells reached a peak concentration and were passaged into new spinner flasks. Before passaging, microcarriers with cells were pretreated with 10  $\mu$ M of ROCK inhibitor. After that, they were washed once with DMEM/F12 and incubated with 10 ml of Accutase for about 15 min with

occasional pipetting. After all the cells were detached from microcarriers, cells were collected by passing the mixture of cells and microcarriers through a 100  $\mu\text{m}$  mesh strainer (BD Biosciences). Collected cells were ready for passaging or characterization.

### **3.2.4 RT-PCR and quantitative PCR**

Total RNA was isolated using Trizol reagent (Life Technologies, Carlsbad, CA) according to the manufacturer's instructions. Reverse transcription was performed using the ImPromII reverse transcriptase (Promega, Madison, WI) as previously described [158]. Quantitative PCR (qPCR) was performed on a Step One™ real-time PCR system (Life Technologies, Grand Island, NY) using the DyNAmo™ SYBR Green qPCR Kit (Thermo Scientific, Waltham, MA). All reactions were run in triplicates. Amplification specificity was verified by the melting curve method. Relative gene expression was normalized to the endogenous  $\beta$ -actin (*ACTB*) expression. All reactions were run in triplicates.

### **3.2.5 Flow cytometry**

Cells detached from the microcarriers were fixed in a 4% paraformaldehyde solution (Sigma-Aldrich) for 10 min. Cells were then washed with PBS and permeabilized with Cytonin (Trevigen, Gaithersburg, MD) for 1 hr and blocked with 3% normal donkey serum (NDS; Jackson ImmunoResearch Laboratories, West Grove, PA) for 20 min. The samples were subsequently incubated with primary antibodies including rabbit anti-OCT4 (Santa Cruz Biotechnology) and mouse anti-SSEA4 (AbCam) for 1 hr at room temperature. After washing three

times with 1% NDS, cells were incubated with appropriate DyLight secondary antibodies (Jackson ImmunoResearch Laboratories) for 1 hr at room temperature. The samples were washed again three times with PBS and analyzed in an Attune flow cytometer (Life Technologies). Cells were considered as positive for a particular antigen if their emitted fluorescence level was higher than 99% of that of samples stained only with the corresponding secondary antibodies.

### **3.2.6 Immunocytochemistry**

Cells were fixed with 4% paraformaldehyde (Sigma) in PBS, permeabilized/blocked in PBS with 0.1% Triton X-100 (Mallinckrodt Baker, Phillipsburg, NJ) and 1% bovine serum albumin (BSA; Sigma) for 30 min and incubated overnight at 4 °C with primary antibodies: Mouse anti-SSEA4 (AbCam) and rabbit anti-OCT4 (Santa Cruz.). After three washes with PBS, cells were incubated with DyLight secondary antibodies (Jackson ImmunoResearch Laboratories) for 1 h at room temperature. Nuclear DNA was stained with DAPI (Vectashield, Vector Laboratories, Burlingame, CA).

### **3.2.7 Embryoid body formation**

Single hPSCs harvested from VN-HSA-UV microcarriers were induced embryoid body (EB) formation. Harvested EBs were transferred to Petri dishes and maintained in Dulbecco's modified Eagle's medium/Ham's F12 medium (DMEM/F12) (Life Technologies), supplemented with 20% FBS (PAA Laboratories, Dartmouth, MA). Medium was replenished every 2 days until analysis of the EBs.

### **3.2.8 Definitive endoderm, mesoderm, and neuroectoderm differentiation**

Cells harvested from microcarriers were replated on Matrigel-coated dishes. For bioreactor differentiation, the medium used for expansion of hPSCs was exchanged with differentiation medium keeping the total working volume constant. Differentiation to definitive endoderm, mesoderm and neuroectoderm were performed according to previous reports [158, 159, 181, 182].

Definitive endoderm (DE) differentiation of H9 cells harvested from UV-HSA-UV microcarriers was performed as previously described [159]. Briefly, after 5 passages, cells on microcarriers were disassociated into single cells with Accutase and seeded on Matrigel-coated dishes with mTeSR medium supplied with 10  $\mu$ M Y-27632 and cultured for one day. In the following days, medium replaced daily with mTeSR until cells reached 80% confluence. Differentiation was carried out in RPMI (GIBCO, Grand Island, NY) supplemented with 100 ng/ml activin A (R&D Systems) from days 0 to 4 and various amounts of Knockout Serum Replacer (KSR; GIBCO, Grand Island, NY) as follows: no KSR for Day1, 0.2% KSR for Day 2, and 2% KSR for Day 3-4.

Before mesoderm differentiation, cells were harvested from microcarriers and maintained on Matrigel-coated dishes same as that described in definitive endoderm differentiation section. Mesoderm differentiation protocol used here was the same as previously reported [183]. In brief, differentiation was carried out in RPMI medium supplemented various amount of activin A, BMP4 and KSR for

5 days: On Day 1, RPMI was supplemented with 100 ng/ml activin A. On Day 2 and 3, RPMI was supplemented with 0.2% KSR, 10 ng/ml activin A and 10 ng/ml BMP4 (R&D Systems). On Day 4 and 5, RPMI was supplemented with 2% KSR, 10 ng/ml activin A and 10 ng/ml BMP4.

Before neuroectoderm differentiation, cells harvested from microcarriers were cultured on Matrigel-coated dishes until 90% confluence similar as that described in definitive endoderm differentiation. Neuroectoderm differentiation was performed following published protocol [182] with minor changes. On Day 1, mTeSR was replaced by neural induction medium (NIM: DMEM/F12:Neurobasal medium (1:1), 1×N2 supplement, 1×B27 supplement without vitamin A (all from GIBCO) and 2 mM Glutamax (Mediatech, Herndon, VA)). The next day, cells were passaged using collagenase IV (GIBCO) and seeded in low-attachment dishes (BD Biosciences) to form embryoid bodies (EBs). EBs were cultured in NIM for 4 days with daily medium change. Then the medium was switched to neural proliferation medium (NPM: DMEM/F12:Neurobasal(1:1), 0.5×N2 supplement, 0.5×B27 supplement, 2 mM Glutamax and 20 ng/mL FGF2 (R&D Systems)) for another 3 days with daily medium change. After that, EBs were replated on Matrigel-coated dishes and cultured for another 2 days before characterization.

### **3.2.9 Statistical Analysis**

Data are expressed as mean  $\pm$  standard deviation unless stated otherwise. ANOVA and the post hoc Tukey test were performed using Minitab (Minitab Inc, State College, PA). P values less than 0.05 were considered as significant.

## **3.3 Results**

### **3.3.1 Treating microcarrier surface with vitronectin, HSA, and UV irradiation**

Recombinant human vitronectin (VN, Life Technologies) was used in 2D surface coating for supporting hPSC attachment and pluripotency. When coating microcarriers with VN alone, the static seeding efficiency was 26% (**Figure 3.1**), but cells quickly detached from the microcarrier surface under stir-suspension conditions. One possible reason is that the VN coating on surfaces is by physical absorption rather than chemical bonding. Therefore, under shear stress in agitated bulk solution, the absorption/desorption balance is different from 2D static culture (dishes) and the amount of VN on microcarriers may not be sufficient to support hPSC attachment. UV irradiation was reported to strengthen the mechanical property of protein membranes by cross-linking individual protein molecules [193] and enhance surface cell-attachment [194]. Therefore, treating VN-coated microcarriers with UV irradiation may be a way to enhance the adsorption of VN on the surface of microcarriers. Besides comparing the performance of hPSC attachment on microcarriers coated with VN vs. microcarriers coated with VN and being UV irradiated (VN-UV), we also studied the effect of a protein carrier,

recombinant human serum albumin (HSA) on supporting cell attachment. As shown in **Figure 3.1A**, in static condition, microcarriers coated with VN and HSA and treated with UV (VN-HSA-UV) showed the highest seeding efficiency (37%), which is comparable to VN-UV (32%) microcarriers and significantly higher than other conditions (VN: 25%  $\pm$ 4%, VN-HSA: 21%  $\pm$ 5%, HSA: 7%  $\pm$ 4%, UV: 5%  $\pm$ 3%). However, VN-UV microcarriers were not able to support long-term cell attachment under stirred suspension condition. As shown in **Figure 3.2**, after 3 days in culture almost all cells on VN-UV microcarriers detached from the surface. In contrast, VN-HSA-UV microcarriers supported cell attachment for 3 days. HSA alone or HSA-UV did not support cell attachment (**Figure 3.1A**), but the inclusion of the HSA coating along with VN is necessary to maintain cell adhesion on microcarriers under agitation. A schematic figure is shown of the preparation of VN-HSA-UV microcarriers (**Figure 3.1B**).

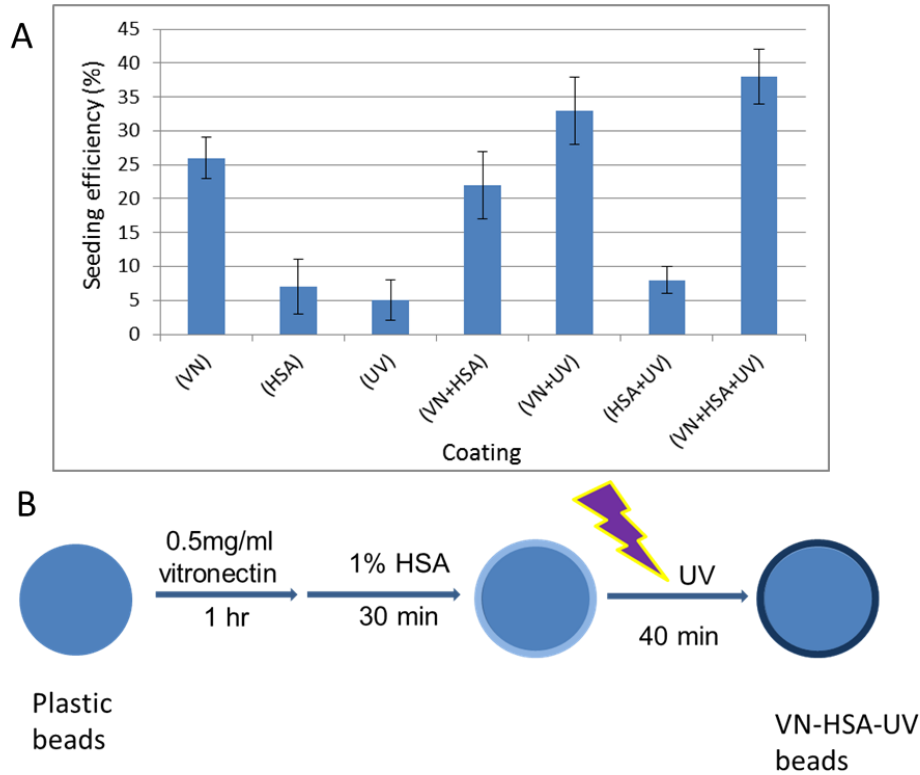


**Figure 3.1** Seeding efficiency of microcarriers treated with different coatings in static conditions. (A). VN: 5  $\mu\text{g/ml}$  vitronectin for 1 hr; HSA: 0.01 g/ml (1%) recombinant human serum albumin, 30 min; UV: shortwave 254 nm, 75 W UV lamp, 40 min. (B) A schematic demonstration of how to prepare VN-HSA-UV microcarriers.

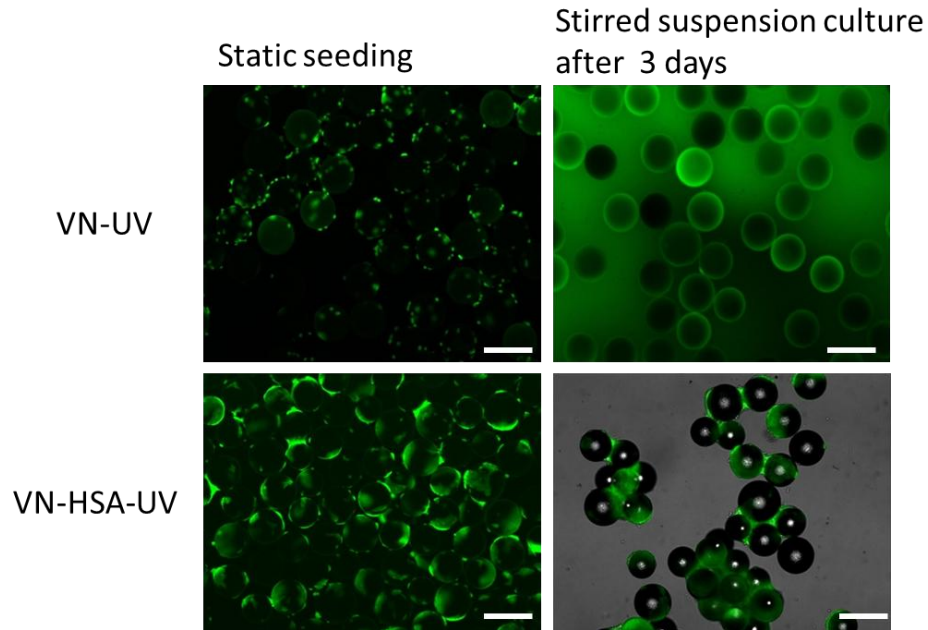


**Figure 3.2** Comparison of cell attachment on VN-HSA-UV microcarrier with VN-UV microcarrier under agitation (45 rpm). Live cells were stained with FDA. Bar = 200  $\mu\text{m}$ .

### 3.3.2 Human PSC expansion on Plastic Plus and Plastic microcarriers coated with vitronectin and HSA, and treated with UV

We tested two types of microcarriers with the VN-HSA-UV treatment to see whether the electric charge affects protein coating and cell attachment. Plastic microcarriers (Solo Hill) are polystyrene beads with neutral charge while Plastic Plus microcarriers are polystyrene beads with positive charge. The two kinds of microcarriers were treated in the same manner and in a 6-day culture in spinner flasks with E8 medium, we found that Plastic microcarriers showed a higher seeding efficiency ( $31.1\% \pm 5.0\%$ ) compared to Plastic Plus ones ( $23.3\% \pm 4.0\%$ ). After 6 days of culture in E8 medium, Plastic microcarriers showed a higher cell

number increase (16.2-fold) compared to Plastic Plus beads (8.7-fold),  $p < 0.05$ . Cell attachment on microcarriers and the growth profiles using the two kinds of beads are shown in **Figure 3.3**.

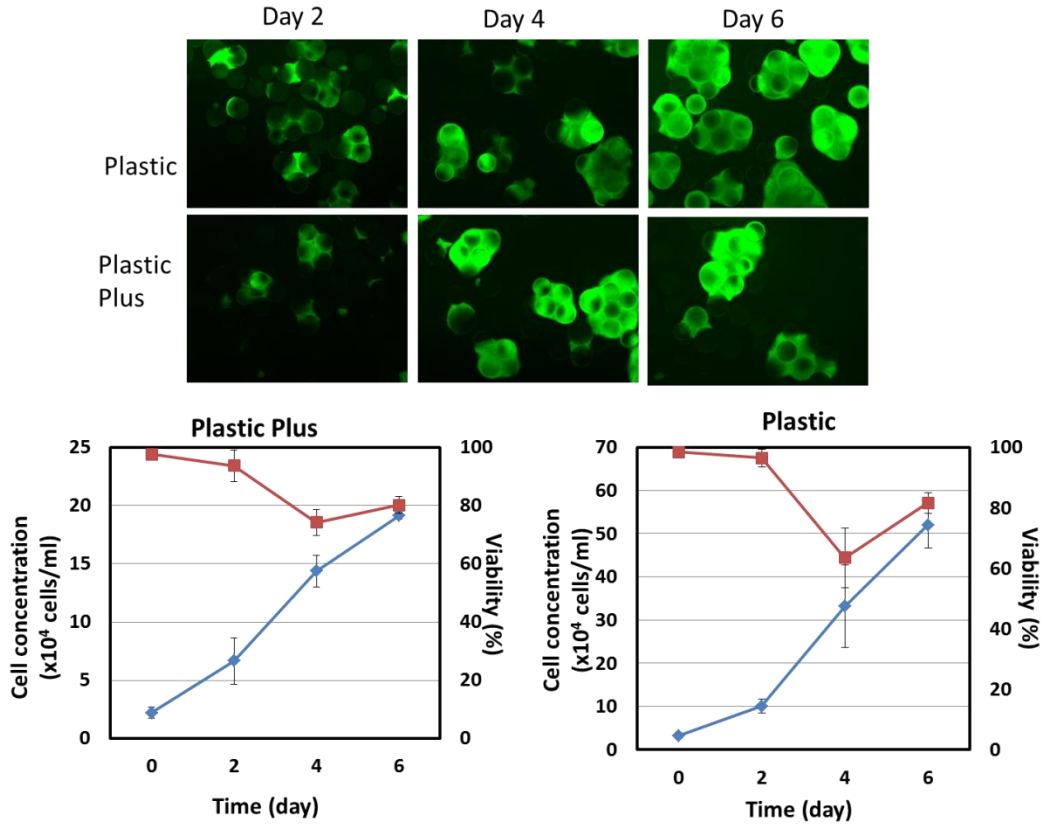


**Figure 3.3** H9 hESCs cultured on Plastic and Plastic Plus microcarriers coated with VN-HSA-UV under agitation at 45 rpm for 6 days in E8 (without F-68).

Another observation is that neither Plastic Plus nor Plastic microcarrier culture showed low cell viability when cultured in E8 medium. This was not observed previously in our lab when cells cultured on Matrigel coated microcarriers with mTeSR1 medium, which is a defined but not xeno-free medium. After comparing the component sheets of E8 and mTeSR1, we found that a key component

protecting cells from shear forces, pluronic F-68, is not present in E8. After supplementing E8 medium with 0.02% F-68, stable and high viability was maintained during a 6-day culture in spinner flasks (**Figure 3.4A**). Supplementation of the medium with F-68 did not affect the pluripotency of cells (**Figure 3.4B**). In both cases, cells harvested from VN-HSA-UV microcarriers showed high expression levels of pluripotency markers OCT4 and SSEA4 (>90%). **Figure 3.4C** showed the distribution of live cells stained with FDA on VN-HSA-UV microcarriers.

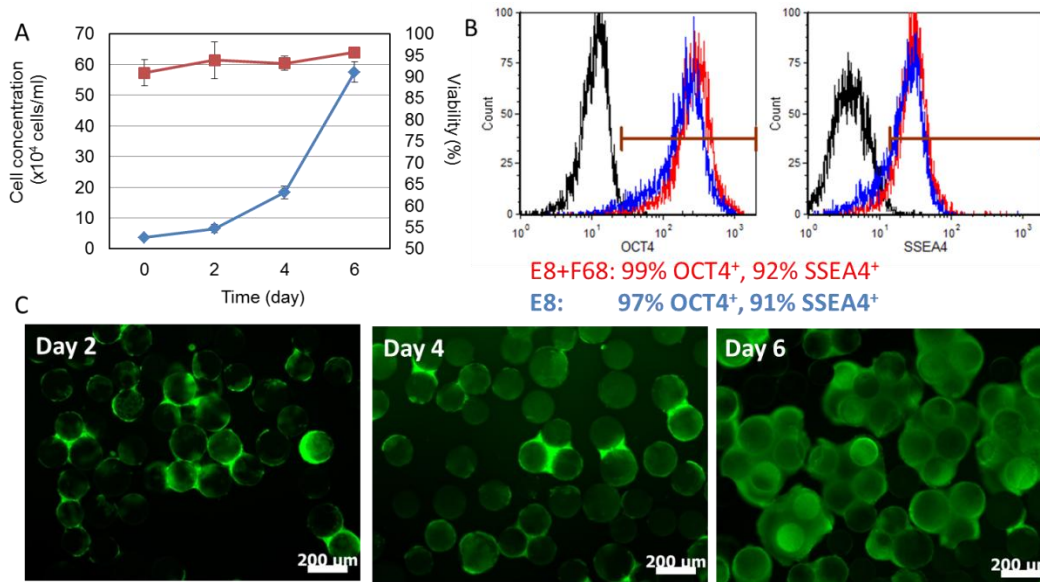


**Figure 3.4** H9 cells cultured on plastic coated microcarriers coated with VN-HSA-UV under agitation for 6 days in E8 with 0.02% F68. (A) Cell growth profile and viability. (B) Expression level of pluripotency markers OCT4 and SSEA-4 in cells harvested from VN-HSA-UV coated microcarriers. Red curve: E8 with 0.02% F-68 (99% OCT4 positive, 92% SSEA-4 positive), Blue curve: E8 only (97% OCT4 positive, 91% SSEA-4 positive), Black curve: control. (C) FDA

staining of live H9 cells attached on VN-HSA-UV coated microcarriers on Day 2, Day 4 and Day 6.

### **3.3.3 Multi-passage suspension culture of hESCs seeded on VN-HSA-UV microcarriers**

Next, we addressed the question of whether hESCs seeded as single cells on VN-HSA-UV beads can be cultured for multiple passages. Indeed, H9 hESCs were successfully cultured for five passages on microcarriers. Cell proliferation was consistent among passages with an average increase of  $20.5 \pm 2.0$ -fold to concentrations of  $1.3\text{-}1.6 \times 10^6$  cells/ml (**Figure 3.5A**). After each passage, cells harvested from microcarriers were collected and characterized for the expression of pluripotency markers by qPCR. The expression levels of pluripotent markers *NANOG*, *POU5F1* and *SSEA4* were consistently high and comparable to the expression level of cells maintained on dishes in all passages (**Figure 3.5B**, normalized to undifferentiated cells maintained on dishes). When analyzed by flow cytometry, the majority of cells (>80%) also retained the expression of OCT4 and SSEA4 over successive passages (**Figure 3.5C**). Taken together, our data indicate that hESCs (H9) seeded as single cells can be propagated on VN-HSA-UV treated microcarriers in a stirred-suspension vessel without loss of pluripotency marker expression for more than 50 days.

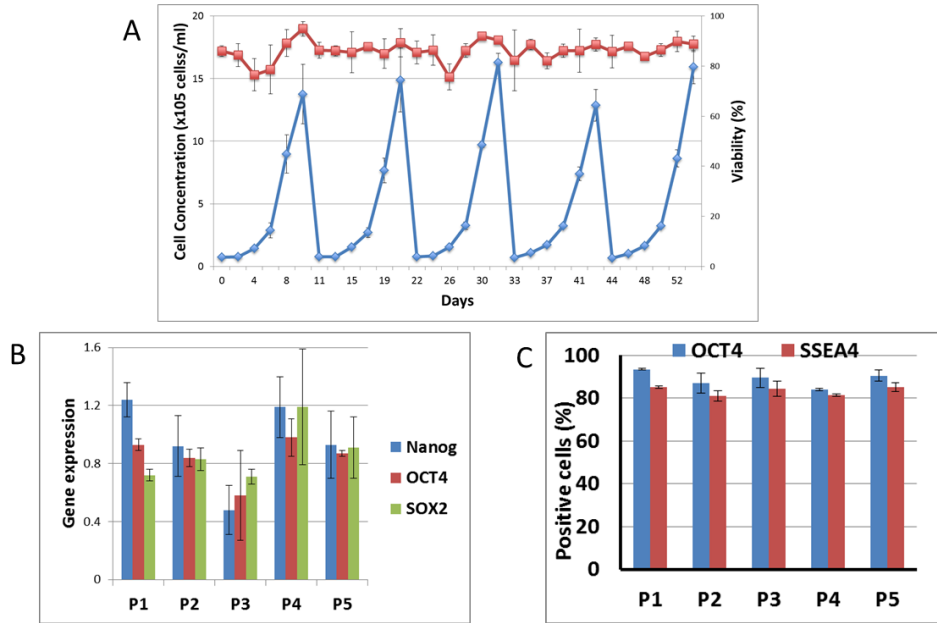


**Figure 3.5** H9 (hPSCs) cultured on VN-HSA-UV microcarriers for multiple passages in stirred-suspension vessels. (A) Growth profile and viability. After each passage, the expression of pluripotency markers was characterized by (B) qPCR, and (C) flow cytometry. PX is the passage number (e.g. P3: passage number 3).

Cells cultured for 5 passages on VN-HSA-UV microcarriers were then harvested from microcarriers, dissociated into single cells and transferred onto Matrigel-coated dishes where they were subjected to directed differentiation to definitive endoderm (DE), mesoderm (MS) and neuroectoderm (NE) by applying previously established protocols [158, 178-180]. Differentiation to each lineage was evident by the expression of relevant markers (DE marker: *SOX17* and *FOXA2*, MS: *KDR* and *MEOX1*, NE: *TUBB3* and *NES*) as assessed by qPCR (**Figure 3.6 A-C**) and immunostaining (**Figure 3.6D-F**). Cells treated with basal media with KSR but without differentiation factors served as controls.

These findings demonstrate that VN-HSA-UV microcarriers support the expansion of hPSCs without adversely affecting their pluripotency and ability for multi-lineage differentiation.

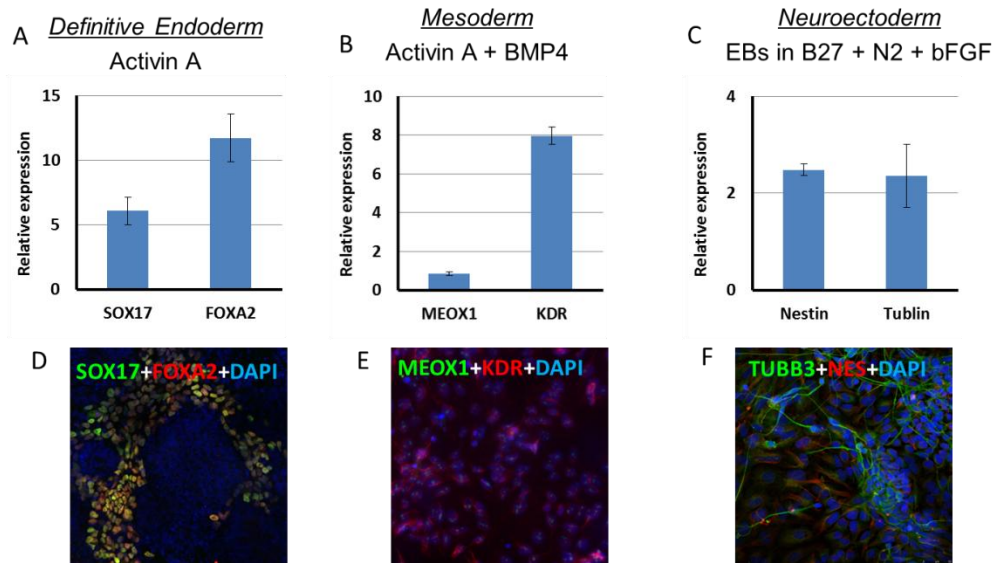


**Figure 3.6** Germ layer differentiation of H9 (hESCs) cells harvested from VN-HSA-UV microcarriers after 5 passages of expansion. Definitive endoderm (DE) marker (SOX17 and FOXA2) expression of H9-derived DE cells was probed by qPCR (A) and immunostaining (D). Mesoderm (MS) marker (KDR and MEOX1) expression of H9-derived MS cells was checked by qPCR (B) and immunostaining (E). Neuroectoderm (NE) marker (TUBB3 and NES) expression of H9 NE cells was checked by qPCR (C) and immunostaining (F). Gene expression was normalized to H9 cells differentiated in basal medium without any differentiation stimuli.

### 3.4 Discussion

As we mentioned in Chapter 2, the development of scalable systems for the expansion and differentiation of hPSCs under defined and xeno-free conditions is one of the most critical considerations for stem cell-based therapies to become a reality. Significant progress has been achieved toward culturing stem cells under defined and xeno-free conditions in 2D systems [71, 72, 170]. The work presented here describes the surface modification of xeno-free microcarriers with vitronectin, human serum albumin and UV treatment which are suitable for the expansion of hPSCs in a scalable system. Human ESCs on VN-HSA-UV coated microcarriers proliferated in E8 medium with 0.02% F-68 achieved a similar growth profile over multiple passages (more than 50 days) without compromising their high viability and the expression of pluripotency markers. When subsequently were subjected to differentiation, these cells were coaxed into lineages of the three embryonic germ layers using protocols established for 2D differentiation.

Vitronectin, which features the integrin-binding arginine–glycine–aspartic acid (RGD) motif [65], was previously shown to promote stem cell adhesion [31, 62, 72] e.g. in commercially available recombinant human VN-coated dishes. However, information is limited about translation of this strategy to 3D surfaces. In static cultures, cells are not challenged by any shear stress field due to agitation in stirred vessels. However, hESCs came off from microcarriers coated with free VN or VN with HSA in agitated suspension. After the VN and HSA were further irradiated by UV light, the coating is stable enough to support hPSC expansion

under agitation. In fact, another group also observed reduced hESC growth on full-length VN-coated microcarriers compared to culture on flat tissue culture plates layered with the same protein [168]. Based on our study, coating microcarriers with recombinant VN in the same way as for 2D surfaces was not able to sustain hPSC attachment and proliferation in a dynamic (stirred-suspension) environment. This finding illustrates that differences between 2D and 3D surfaces such as substrate curvature and the agitation-induced shear hinder the direct translation of the results from 2D culture of hPSCs to their expansion/differentiation in microcarrier bioreactor cultures.

The cell surface is typically negatively charged, so without any coating, positively charged microcarriers are thought to provide a better surface for cell attachment compared to neutrally charged microcarriers. However, in this study after coating, Plastic microcarriers outperformed Plastic Plus beads in cell seeding efficiency and cell number increase. This indicated that neutrally charged microcarriers rather than positively charged ones favor the VN-HSA-UV coating process.

E8 medium is a commercial, defined, xeno-free and low-protein medium for maintaining hPSC proliferation and pluripotency in 2D culture. However, when used in a 3D dynamic environment, the lack of some shear-protective reagents such as F68 or Tween-20 may increase cell death. Therefore, findings based on the culture of cells on microcarriers in static culture cannot be translated directly to a dynamic stirred-suspension environment.

In conclusion, our study demonstrates the engineering of xeno-free microcarriers for long-term scalable culture of hPSCs under fully defined conditions. Human PSCs were successfully maintained on VN-HSA-UV treated microcarriers in stirred-suspension vessels for multiple passages without compromising their pluripotency and proliferation. The defined, xeno-free microcarrier culture system described here may contribute to the development of hPSC bioprocesses for the production of therapeutically useful stem cells.

## 4 Xeno-Free Differentiation of hPSC towards Pancreatic Progenitor Cells

### 4.1 Introduction

As summarized in Chapter 1, diabetes is a chronic disease caused by the decrease of functional insulin-producing  $\beta$ -cells due to autoimmune destruction or insulin resistance and insufficient insulin secretion [129, 130]. Transplantation of insulin-producing islet cells from a donor pancreas could be a cure for diabetes. However, lack of sufficient donors and the side effects of the immunosuppressing regimens limit its potential. A way to overcome these problems is to derive islet cells from other sources such as human adult stem cells, ESCs, and iPSCs. Different from adult stem cells, which have limited division capacity and present challenges in their isolation, hPSCs can self-renew extensively and thus can serve as renewable sources for generating pancreatic  $\beta$ -cells.

Success of stem cell-based diabetes therapy relies on the development of efficient differentiation protocols for turning hPSCs into genetically normal and functional insulin-producing pancreatic islet cells, as well as robust bioprocesses for generating large quantities of functional progeny under xeno-free and well-defined conditions which meet clinical demand [134-138].

Similar to the embryonic pancreas development, pancreatic differentiation of hPSCs *in vitro* is usually carried out in a step-wise manner. Recently, the sequential application of growth factors and/or small molecules was shown to generate insulin/C-peptide-expressing cells from both hESCs [137, 155, 156] and

hiPSCs [138, 157]. However, in most of the protocols, the differentiation efficiency was not shown or was not optimized. From a bioprocessing point of view, only limited emphasis has been placed on cell numbers, viability and differentiation efficiency. Furthermore, none of the studies thus far were conducted under xeno-free conditions. Rather, serum and serum replacement supplements, which are typically undefined and with components of animal origin, were usually included in the differentiation medium. In addition, Matrigel was normally used as ECM coating. Such methods are not suitable for the generation of cells intended for clinical applications.

In our study, xenogeneic components used during culture and differentiation are substituted with xeno-free reagents. A stage-wise differentiation protocol which was previously established [195] is optimized during two critical stages, i.e. commitment to definitive endoderm (DE) and subsequently to posterior foregut (PF).

## **4.2 Materials and Methods**

### **4.2.1 Human PSC culture and differentiation**

The hESC line H9 (passages 30-50) and hiPSC line IMR90 (passages 50-70) were obtained from the WiCell Research Institute (Madison, WI). Cells were cultured in dishes coated with recombinant human vitronectin (Thermo Fisher, Boston, MA) and in mTeSR1 or TeSR-E8 medium (StemCell Technologies, Vancouver, BC). Cells were maintained in 5% CO<sub>2</sub>/95% air incubator at 37 °C. Medium was replaced every day, and the cells were passaged every 5–6 days.

The stage-wise differentiation procedure and stage-specific genes are shown in **Figure 4.1**. In brief, for DE differentiation, iPSCs were cultured in RPMI (GIBCO, Grand Island, NY) supplemented with 100 ng/ml activin A (R&D Systems, Minneapolis MN) and varying concentrations of Knockout™ Serum Replacement (KSR) (GIBCO, Grand Island, NY) for comparison or 1% xeno-free B27 (GIBCO, Grand Island, NY) for 4 days. Primitive gut tube (PGT) was induced by treatment with 50 ng/ml KGF (R&D Systems, Minneapolis MN), 2 μM all-*trans* retinoic acid (RA) (Sigma-Aldrich, St. Louis, MI), 200 ng/ml EGF (Sigma-Aldrich, St. Louis, MI) and 0.25 μM KAAD-cyclopamine (Toronto Research Chemicals, Toronto, Canada) in RPMI supplemented with 2% KSR or 1% xeno-free B27 (GIBCO, Grand Island, NY) for another 4 days. PGT cells were further differentiated to PF by culture with growth factors same as those used in last step but in DMEM/F12 (GIBCO, Grand Island, NY) as basal medium with 1% insulin-containing xeno-free B27 (GIBCO, Grand Island, NY).

#### **4.2.2 Reverse transcription and quantitative PCR**

Total RNA was isolated using Trizol (Invitrogen, Carlsbad, CA) according to the manufacturer's instructions, and reverse transcription (RT) was performed using the ImPromII reverse transcriptase (Promega, Madison, WI).

Quantitative PCR (qPCR) was performed using SYBR Green qPCR Kit (Thermo Scientific, Vantaa Finland, Finland) under the following conditions: Denaturation and polymerase activation at 95 °C for 15 min; amplification for 40 cycles at 94 °C for 10 s, 58–60 °C for 20 s, and 72 °C for 30 s using StepOne™ real-time PCR

system (Life Technologies, Grand Island, NY). All reactions were run in triplicates. Amplification specificity was verified by the melting curve method and gel electrophoresis. Relative gene expression was calculated by normalizing to the endogenous  $\beta$ -actin (*ACTB*) expression. The  $C_T$  for the housekeeping gene did not vary under different experimental conditions when equal amounts of RNA were used.

#### **4.2.3 Flow cytometry**

Cells were dissociated and pelleted by centrifugation at  $200\times g$  for 5 min. Cells were then fixed with 3.7% formaldehyde solution (Sigma-Aldrich) for 10 min, washed with PBS and permeabilized with Cytonin (Trevigen, Gaithersburg, MD) for 30 min before their blocking with 3% normal donkey serum (NDS; Jackson ImmunoResearch Laboratories, West Grove, PA) for 20 min. The samples were then incubated with the primary antibodies for 1 h at room temperature. Cells were washed three times with 1% NDS and incubated with appropriate DyLight secondary antibodies (Jackson ImmunoResearch Laboratories) for 1 h at room temperature. Cells were washed three times with PBS and analyzed in an Attune flow cytometer. Cells were considered as positive for a particular antigen if their emitted fluorescence level was higher than 99% of that of samples stained only with the corresponding secondary antibodies.

#### **4.2.4 Immunocytochemistry**

Cells were fixed with 4% paraformaldehyde (Sigma) in PBS, permeabilized/blocked in PBS with 0.1% Triton X-100 (Mallinckrodt Baker, Phillipsburg, NJ) and 1% bovine serum albumin (BSA; Sigma) for 30 min. Samples were incubated overnight at 4 °C with primary antibodies. After three washes with PBS, cells were incubated with appropriate DyLight secondary antibodies (Jackson ImmunoResearch Laboratories) for 1 h at room temperature. Nuclear DNA was stained with DAPI (Vectashield, Vector Laboratories, Burlingame, CA).

### **4.3 Results**

#### **4.3.1 Effects of different basal medium on the cell viability of DE differentiation stage**

Based on embryological studies of definitive endoderm (DE) formation *in vivo*, activation of TGF- $\beta$ /Nodal signaling should induce the commitment of hPSCs toward DE progeny [140]. This is accomplished with exposure to 100 ng/ml Activin A (hereby termed ‘activin’) for 3 or 4 days whereas lower concentrations of activin specify mesoderm [196]. However, little is known about the effects of basal medium on the differentiation process as in most studies diverse media have been utilized.

Therefore, we studied the effects of three different basal media during DE differentiation. A suspension of  $2 \times 10^6$  of single H9 cells was seeded on VN-coated 35-mm tissue culture dishes with 10  $\mu$ M Y-27632. Differentiation was

initiated 24 hrs post-seeding with the addition of 100 ng/ml activin in three different xeno-free basal media: RPMI + 1% xeno-free B27 (B27XF), DMEM + 1% B27XF and E6. Control medium contained RPMI, the same concentration of activin, and knockout serum replacer (KSR) at 0% (day 1), 0.2% (day 2) and 2% (day 3-4). As shown in **Figure 4.1**, cell concentration increased between 3.4- and 5.2-fold for RPMI with KSR or B27XF, DMEM with B27XF, and E6 (**Figure 4.2A**). Moreover, the fraction of cells co-expressing SOX17 and FOXA2 in RPMI with B27XF was  $64\% \pm 7\%$  (**Figure 4.2B**), which is much higher compared to cells cultured in DMEM with B27XF ( $39\% \pm 13\%$ ,  $p < 0.05$ ) or E6 ( $14\% \pm 5\%$ ,  $p < 0.05$ ). Immunostaining analysis corroborated the co-expression of SOX17 and FOXA2 with RPMI with 1% B27XF (**Figure 4.2C**). Those cells also expressed other DE specific markers such as CXCR4 (**Figure 4.3A**) and CKIT (**Figure 4.3B**).

IMR90 cells (hiPSCs) can be induced into SOX17 and FOXA2 co-positive DE cells using RPMI with 1% B27XF supplemented with 100 ng/ml activin for 4 days (**Figure 4.4A**) with a differentiation efficiency of 55% (**Figure 4.4B**).

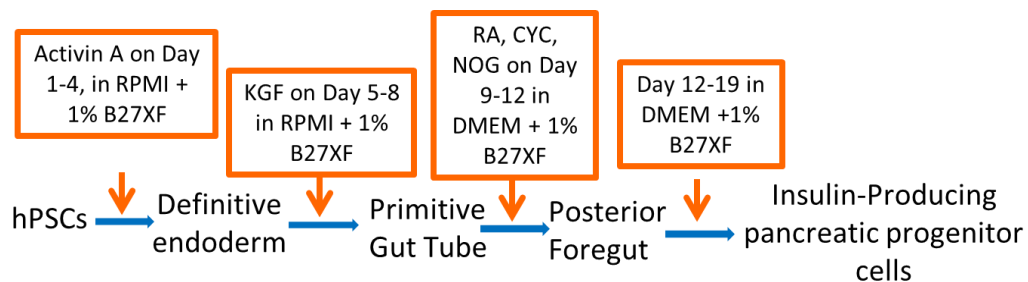


**Figure 4.1** Scheme of step-wise pancreatic differentiation protocol of hPSCs under xeno-free conditions. Activin A: 100 ng/ml; B27XF: Xeno-free B27

supplement; CYC: 0.25  $\mu$ M KAAD-cyclopamine; KGF: 50 ng/ml; RA: 2  $\mu$ M Retinoic Acid; NOG: 50 ng/ml noggin.

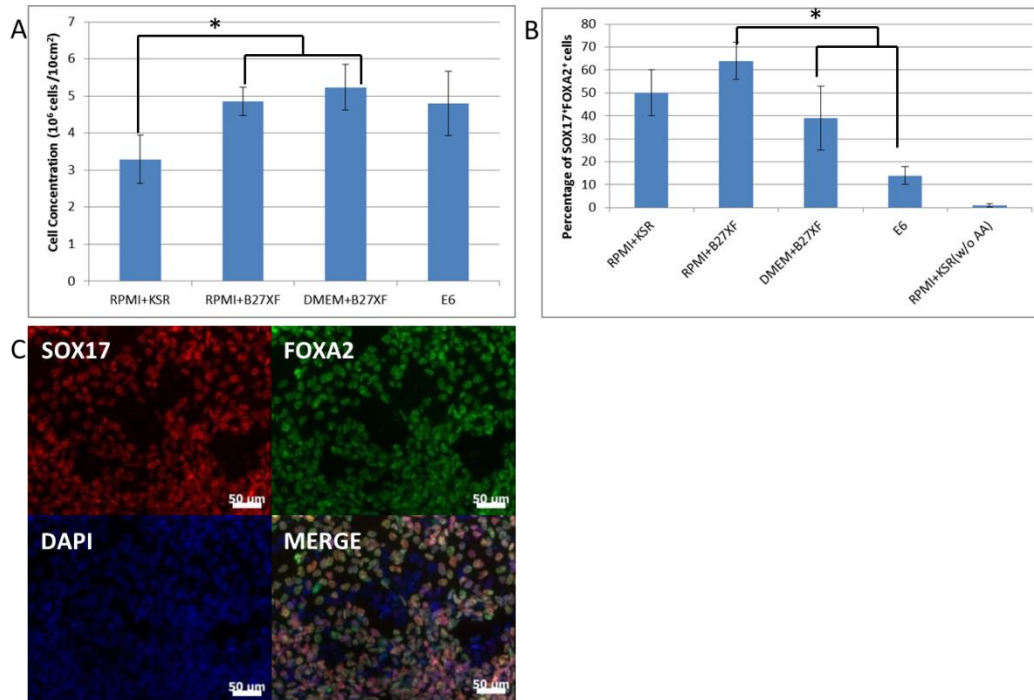


**Figure 4.2** H9 cells (hESCs) differentiated in different basal medium towards DE. Initial seeding:  $2 \times 10^6$  cells/10 cm<sup>2</sup>. Cell number was counted after 4 days of differentiation. (A) cell viability. (B) Level of co-expression of SOX17 and FOXA2. \* $p < 0.05$ . (C) Co-staining of SOX17 and FOXA2 of DE stage cells with RPMI supplemented with B27XF.

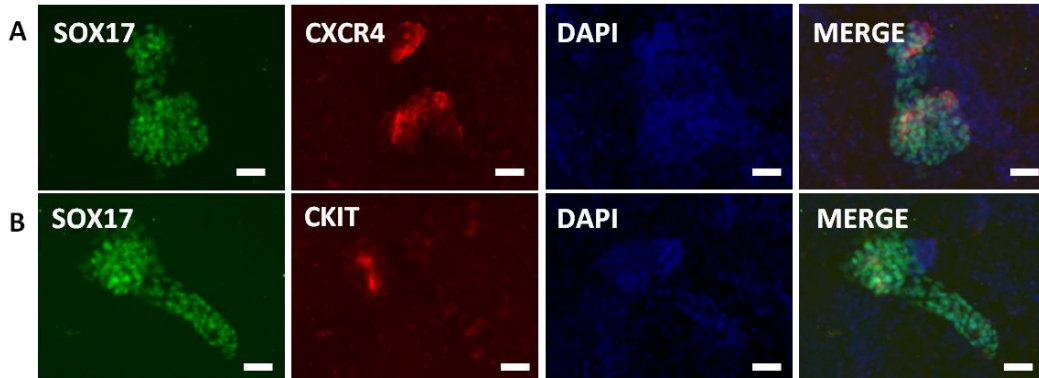


**Figure 4.3** H9 cells (hESCs) differentiated with RPMI with 1% B27XF and 100 ng/ml Activin A on vitronectin-coated dish co-stained with SOX17 and CXCR4 (A) and SOX17 + CKIT (B). Bar = 50  $\mu$ m.

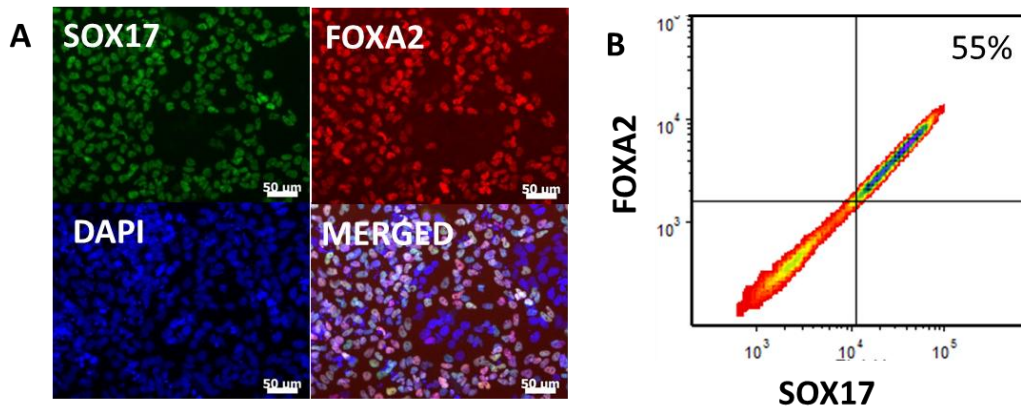


**Figure 4.4** IMR90 cells (hiPSCs) differentiated into DE cells on VN-coated dishes with RPMI containing 1% B27XF and 100 ng/ml Activin A were co-stained with SOX17 and FOXA2 (A). The co-positive percentage is shown in (B).

### 4.3.2 Differentiation of hPSCs into PGT cells

Keratinocyte growth factor (KGF, also known as FGF7), which signals through the FGFR2IIIb, is involved in specifying foregut endoderm cells [197] and was previously used to generate primitive gut tube (PGT) cells from hPSC-derived DE cells on Matrigel-coated dishes using RPMI supplemented with serum replacer. Here, the same KGF concentration (50 ng/ml) was added to RPMI with 1% B27XF to treat DE cells on VN-coated dishes for 4 more days. After 8 days of differentiation, H9 hESC-derived PGT cells co-expressed the PGT markers HNF1B and HNF4A (**Figure 4.5A**). With the same protocol, IMR90-Clone 4 hiPSCs also transitioned into HNF1B and HNF4A co-positive cells (**Figure 4.5B**).

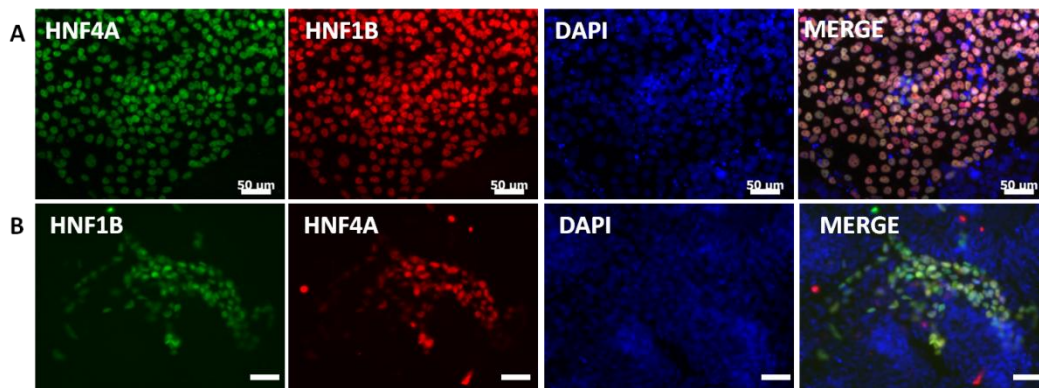


**Figure 4.5** Immunostaining of HNF4A and HNF1B of PGT stage cells differentiated in RPMI medium with B27XF and KGF on VN-coated dishes. (A) H9 hESC-derived and (B) IMR90-Clone 4 hiPSC-derived cells. Bar = 50 µm.

### 4.3.3 Directed differentiation of hPSCs into *PDX1*-expressing pancreatic progenitor cells

The expression of the pancreatic and duodenal homeobox gene 1 (*PDX1*), which is expressed in early pancreatic progenitors and later in mature  $\beta$ -cells, is a critical

check-point during pancreatic specification of hPSCs. However, unlike the differentiation to DE which is regulated predominantly by activin, subsequent commitment is governed by a more complex network of signaling pathways including KGF/FGF7 and FGF10 [148, 197], RA [198-201], BMPs [137, 198, 202], and hedgehog ligands [141, 203]. Although these factors have been utilized either separately or in combination, interaction effects are largely unexplored. This is further confounded by the use of undefined medium containing serum or serum replacer supplements.

Here, hPSC-derived PGT cells were coaxed to PDX1-expressing cells on xeno-free substrate and medium containing RA (2  $\mu$ M), CYC (0.25  $\mu$ M) and NOG (50 ng/ml). RA plays a crucial role in the patterning of foregut and pancreatic endoderm as well as in the induction of *PDX1* expression [199-201]. KAAD-Cyclopamine is an hedgehog signaling inhibitor [203]. Low levels of hedgehog signaling are required during pancreatic bud specification [141]. Noggin is a BMP antagonist, inhibiting hepatic induction after DE patterning [137, 198]. Without it, C-peptide<sup>+</sup> are not detected and secreted insulin levels are greatly diminished [204]. We studied the effects of different combinations of these factors on the PDX1 expression of differentiating cells. After a total of 12 days of differentiation, treatment with NOG, CYC, and RA or NOG and RA led to the highest percentage (30.9%  $\pm$  3.2% vs. 30.5%  $\pm$  2.7%) of PDX1<sup>+</sup> cells (**Figure 4.6A**). Immunostaining for PDX1<sup>+</sup> posterior foregut (PF) cells upon incubation with 2  $\mu$ M RA, 0.25  $\mu$ M CYC and 50 ng/ml NOG is shown in **Figure 4.6B**.

We further optimized the basal medium for the PF stage. It was found that with the same growth factors (NOG, CYC, RA) the use of DMEM + 1% B27XF yielded a significantly higher cell concentration ( $p < 0.05$ ) compared to RPMI with 1% B27XF (**Figure 4.7A**) and a higher percentage of PDX1<sup>+</sup> cells (flow cytometry, **Figure 4.7B**). IMR90-Clone 4 (IMR90) hiPSCs can also be induced into a PDX1<sup>+</sup> PF cell population with the same protocol (**Figure 4.8A**) and a differentiation efficiency of 20% (**Figure 4.8B**).

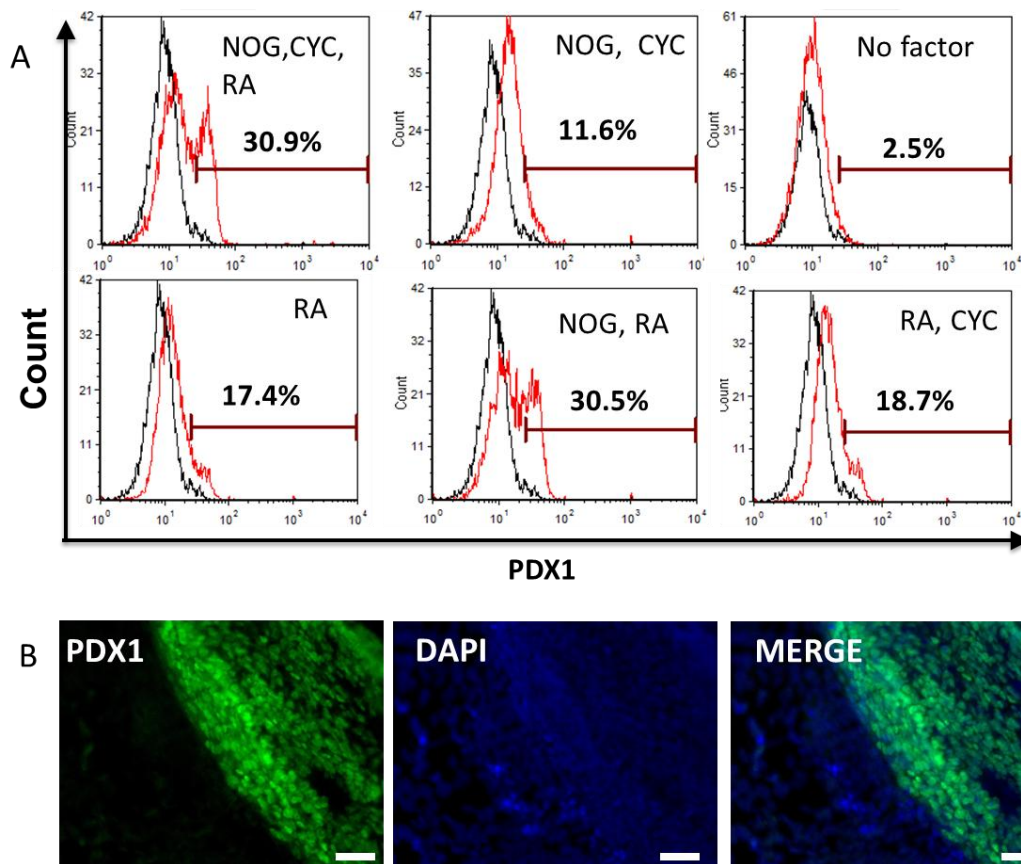


**Figure 4.6** H9 differentiated on VN-coated dishes to PF stage. (A) Flow cytometry results of differentiation with different combinations of growth factors. (B) Immunostaining of H9 cells differentiated with NOG, CYC, RA condition.

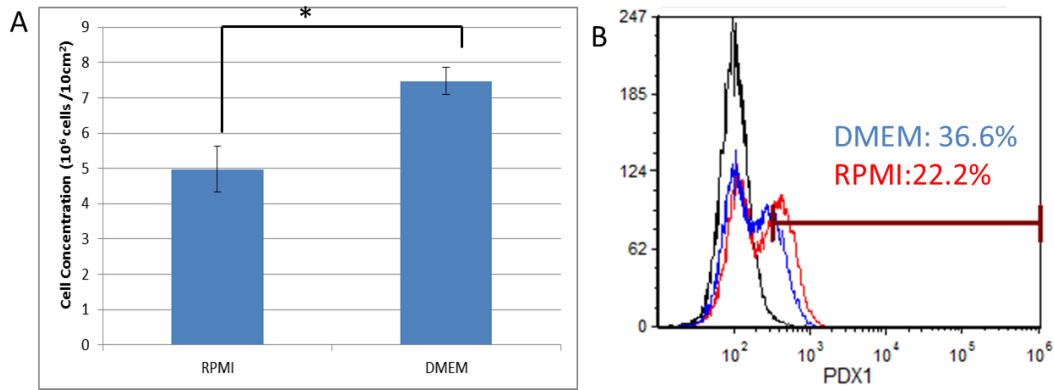


**Figure 4.7** Effect of different basal media on the induction of PDX1. (A) Comparison of cell concentration using different media. \* $p < 0.05$ . (B) Differentiation efficiency determined by flow cytometry. RPMI: RPMI with 1% B27XF; DMEM: DMEM with 1% B27XF. In both cases the culture was supplemented with NOG, CYC and RA.

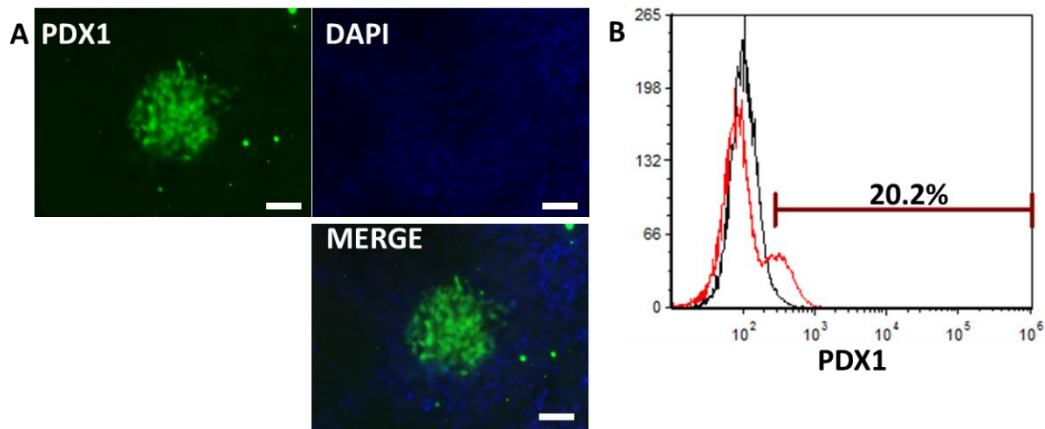


**Figure 4.8** IMR90 hiPSCs were differentiated into PF cells with DMEM containing 1% B27XF and supplemented with NOG, CYC and RA on VN-coated dishes. (A) Cells were stained for PDX1. (B) The PDX1<sup>+</sup> cell fraction is shown. Bar = 50  $\mu\text{m}$ .

#### 4.3.4 Differentiation of hPSCs into insulin-producing pancreatic progenitor cells

Furthermore, PDX1<sup>+</sup> cells derived from hPSCs were cultured in DMEM with 1% B27XF for another 7 days (for a total of 19 days of differentiation). Small patches

of cells co-expressing insulin (INS) and C-peptide were observed (about 5% of the whole population) (**Figure 4.9A**). IMR90 hiPSCs differentiated with the same method showed similar co-expression of INS and C-peptide (**Figure 4.9B**).

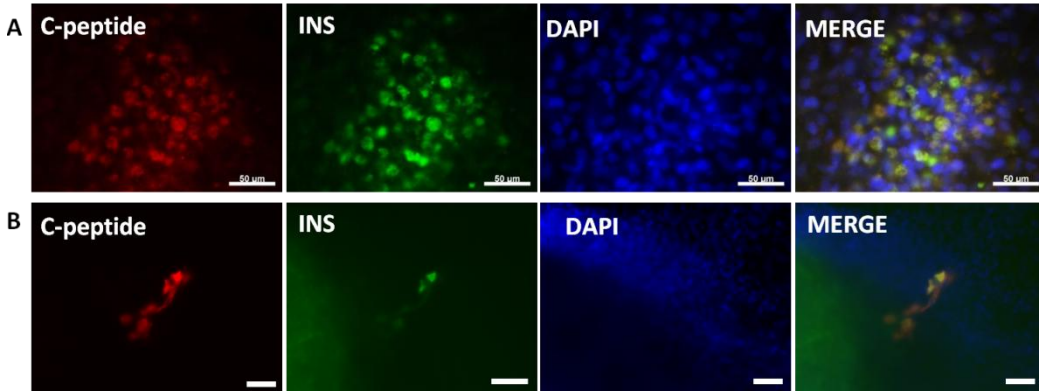


**Figure 4.9** Immunostaining of H9 hESCs (A) and IMR90 hiPSCs (B) coaxed toward pancreatic cells in DMEM with B27XF on VN-coated dishes co-expressing INS and C-peptide after 19 days of differentiation.

#### 4.4 Discussion

In this chapter, we established a xeno-free protocol to generate insulin-producing cells from hPSCs. We removed and/or substituted all the xenogeneic reagents with xeno-free components in the differentiation medium and the cell attachment substrate used during commitment to pancreatic cell progeny.

Fate specification is accompanied by changes in cell morphology and expression of stage-specific markers. Equally important is the maintenance of cell viability, especially from a bioprocessing point of view. For this reason, when we attempted to optimize the differentiation method, we focused on the marker expression level while aiming to maintain maximum cell viability. This was done by investigating the effects of different basal media on cell viability at the DE and PF stages. We

found that different basal media with the same combinations and concentrations of growth factors demonstrated different cell viability and differentiation efficiency during induction of DE and PF populations. However, the mechanism or the biological significance of the basal medium effects on cell growth, viability and differentiation efficiency need to be studied further.

The stage-wise differentiation strategy was optimized based on previous work in our lab and published literature by D'Amour *et al* [205] although some groups [206, 207] have reported challenges in replicating the findings of the latter report. We were able to induce both hESCs (H9) and hiPSCs (IMR90) into insulin-expressing cells using very similar combinations of growth factors with certain modifications. However, PDX1 is a non-specific pancreatic progenitor marker and we need to evaluate additional stage markers to better define the specific populations of differentiated cells obtained. Meanwhile, hPSC-derived pancreatic progenitor cells using the protocol reported by D'Amour gave rise to poly-hormonal insulin-producing cells which are not responsive to glucose stimulation. For this reason, existing protocols should be further tested and modified in order to better mimic functional native pancreatic  $\beta$ -cells which secrete insulin in response to changes in glucose levels.

## 5 Conclusion and Future Work

### 5.1 Impact of the work

In this work, we first demonstrated that hPSCs can be maintained on VN peptide-conjugated/pLL-treated microcarriers in stirred-suspension spinner flasks long-term (multiple passages) without compromising their pluripotency, normal karyotype, proliferation, and differentiation capacity. Cells expanded on these microcarriers can be coaxed into mesoderm lineage directly without harvesting or cell-bead separation. Therefore, the VN peptide-conjugated microcarrier culture system described is a step forward in the development of bioprocesses integrating expansion and directed differentiation of human stem cells for the production of therapeutically useful progeny. However, the beads used in this study to generate peptide-conjugated microcarriers have a high specific gravity (1.7) which made them unsuitable for agitation at lower rates (below 60 rpm). Use of more vigorous stirring exposes cells to higher shear stresses. Yet, the peptide amidation reaction via EDC/NHS coupling is complicated, with relatively low efficiency and time-consuming (~ 2 days to prepare the microcarriers).

As a result, we developed another approach to engineer polystyrene microcarrier with vitronectin, HSA and UV irradiation. In this way, we were able to prepare xeno-free VN-HSA-UV microcarriers for long-term cultivation of hPSCs comparable with peptide-conjugated peptide but with a lower specific gravity (1.09) which allow the agitation as low as 30 rpm in our spinner flasks (agitation rates are not directly translatable between systems of different size or configuration). Moreover, those microcarriers can be prepared fast (~3 hrs) and in a straightforward manner.

Lastly, a differentiation protocol to guide hPSCs into insulin-expressing pancreatic progenitor cells was developed under complete xeno-free conditions. This differentiation protocol is an important improvement as it eliminates all xenogeneic components during differentiation, which is a prerequisite for the generation of differentiated cells for clinical applications. We also optimized our method by analyzing the effects of different basal media during the DE and PF stages. Different combinations of growth factors were also tested on the differentiation to PF. Emphasis was placed in our study on the maintenance of cell viability during differentiation. Moreover, the method is reproducible and can be applied across different hPSC lines.

In conclusion, our studies provide new insights into the bioprocessing of hPSCs used for pancreatic cell therapy and provides a better understanding regarding the translation of 2D culture systems to 3D dynamic environments.

## **5.2 Outlook and future work**

In Chapter 3, we showed that VN-HSA-UV microcarriers combined with xeno-free medium are able to support long-term hPSC proliferation. In the future, systematic efforts will be necessary to identify the mechanism(s) of VN-HSA-UV coating and the interactions among the three components. Furthermore, approaches to increase the seeding efficiency of the novel microcarriers (both peptide-conjugated/pLL-treated and VN-HSA-UV microcarriers) which is lower compared to the standard Matrigel-coated beads should be considered.

Both peptide-conjugated/pLL-treated and VN-HSA-UV microcarriers are made of polystyrene, which is widely available but not biodegradable. In the future, use of biodegradable microcarriers will be advantageous for direct implantation of stem cell progeny reducing or eliminating steps of downstream separation of cells from beads and thus decreasing the overall cost. For instance, lactic/glycolic acid-based biomaterials featuring chemical groups for attaching adhesion molecules may be used to engineer such microcarriers. Non-spherical microcarriers amenable to the same surface functionalization can be considered as their use may confer advantages as others have indicated [168].

With respect to pancreatic differentiation of hPSCs, the fractions of insulin-expressing cells obtained from current *in vitro* protocols are limited (e.g., 5% of insulin<sup>+</sup> cells in our hands and ~7% in another report [205]). Therefore, more effort should be placed on the later stages of endocrine pancreatic differentiation and in particular on the maturation and expansion of insulin-expressing cells.

## Bibliography

1. Thomson, J.A., et al., *Embryonic stem cell lines derived from human blastocysts*. Science, 1998. **282**(5391): p. 1145-1147.
2. Yu, J., et al., *Induced pluripotent stem cell lines derived from human somatic cells*. Science, 2007. **318**(5858): p. 1917-20.
3. Huangfu, D.W., et al., *Induction of pluripotent stem cells from primary human fibroblasts with only Oct4 and Sox2*. Nature Biotechnology, 2008. **26**(11): p. 1269-1275.
4. Takahashi, K., et al., *Induction of pluripotent stem cells from adult human fibroblasts by defined factors*. Cell, 2007. **131**(5): p. 861-872.
5. Kehoe, D.E., et al., *Scalable Stirred-suspension Bioreactor Culture of Human Pluripotent Stem Cells*. Tissue Eng Part A, 2010. **16**(2): p. 405-21.
6. Fan, Y., et al., *Facile Engineering of Xeno-Free Microcarriers for the Scalable Cultivation of Human Pluripotent Stem Cells in Stirred Suspension*. Tissue Eng Part A, 2013.
7. Carvajal-Vergara, X., et al., *Patient-specific induced pluripotent stem-cell-derived models of LEOPARD syndrome*. Nature, 2010. **465**(7299): p. 808-12.
8. Zhang, J., et al., *A human iPSC model of Hutchinson Gilford Progeria reveals vascular smooth muscle and mesenchymal stem cell defects*. Cell Stem Cell, 2011. **8**(1): p. 31-45.
9. Jing, D., et al., *Stem Cells for Heart Cell Therapies*. Tissue Eng Part B Rev, 2008. **14**(4): p. 393-406.
10. Lock, L.T. and E.S. Tzanakakis, *Stem/Progenitor Cell Sources of Insulin-Producing Cells for the Treatment of Diabetes*. Tissue Eng, 2007. **13**(7): p. 1399-1412.
11. Kehoe, D.E., et al., *Scalable Stirred-Suspension Bioreactor Culture of Human Pluripotent Stem Cells*. Tissue Engineering Part A, 2010. **16**(2): p. 405-421.
12. Pera, M.F. and P.P. Tam, *Extrinsic regulation of pluripotent stem cells*. Nature, 2010. **465**(7299): p. 713-20.

13. Chambers, I. and S.R. Tomlinson, *The transcriptional foundation of pluripotency*. Development, 2009. **136**(14): p. 2311-22.
14. Bibikova, M., et al., *Unraveling epigenetic regulation in embryonic stem cells*. Cell Stem Cell, 2008. **2**(2): p. 123-34.
15. Rodda, D.J., et al., *Transcriptional regulation of nanog by OCT4 and SOX2*. J Biol Chem, 2005. **280**(26): p. 24731-7.
16. Boyer, L.A., et al., *Core transcriptional regulatory circuitry in human embryonic stem cells*. Cell, 2005. **122**(6): p. 947-56.
17. Boiani, M. and H.R. Scholer, *Regulatory networks in embryo-derived pluripotent stem cells*. Nat Rev Mol Cell Biol, 2005. **6**(11): p. 872-84.
18. Wang, L., et al., *Self-renewal of human embryonic stem cells requires insulin-like growth factor-1 receptor and ERBB2 receptor signaling*. Blood, 2007. **110**(12): p. 4111-9.
19. Bendall, S.C., et al., *IGF and FGF cooperatively establish the regulatory stem cell niche of pluripotent human cells in vitro*. Nature, 2007. **448**(7157): p. 1015-21.
20. Chase, L.G. and M.T. Firpo, *Development of serum-free culture systems for human embryonic stem cells*. Current Opinion in Chemical Biology, 2007. **11**(4): p. 367-72.
21. Unger, C., et al., *Good manufacturing practice and clinical-grade human embryonic stem cell lines*. Hum Mol Genet, 2008. **17**(R1): p. R48-53.
22. Welling, M. and N. Geijsen, *Uncovering the true identity of naive pluripotent stem cells*. Trends Cell Biol, 2013. **23**(9): p. 442-8.
23. Ying, Q.L., et al., *BMP induction of Id proteins suppresses differentiation and sustains embryonic stem cell self-renewal in collaboration with STAT3*. Cell, 2003. **115**(3): p. 281-92.
24. Xu, R.H., et al., *BMP4 initiates human embryonic stem cell differentiation to trophoblast*. Nat Biotechnol, 2002. **20**(12): p. 1261-4.
25. Ginis, I., et al., *Differences between human and mouse embryonic stem cells*. Developmental Biology, 2004. **269**(2): p. 360-380.

26. Xu, R.H., et al., *NANOG is a direct target of TGFbeta/activin-mediated SMAD signaling in human ESCs*. Cell Stem Cell, 2008. **3**(2): p. 196-206.
27. Vallier, L., et al., *Activin/Nodal signalling maintains pluripotency by controlling Nanog expression*. Development, 2009. **136**(8): p. 1339-49.
28. Xu, R.H., et al., *Basic FGF and suppression of BMP signaling sustain undifferentiated proliferation of human ES cells*. Nat Methods, 2005. **2**(3): p. 185-90.
29. Vallier, L., M. Alexander, and R.A. Pedersen, *Activin/Nodal and FGF pathways cooperate to maintain pluripotency of human embryonic stem cells*. J Cell Sci, 2005. **118**(Pt 19): p. 4495-509.
30. Amit, M., et al., *Clonally derived human embryonic stem cell lines maintain pluripotency and proliferative potential for prolonged periods of culture*. Dev Biol, 2000. **227**(2): p. 271-8.
31. Xu, C., et al., *Feeder-free growth of undifferentiated human embryonic stem cells*. Nat Biotechnol, 2001. **19**(10): p. 971-4.
32. Wang, L., et al., *Human embryonic stem cells maintained in the absence of mouse embryonic fibroblasts or conditioned media are capable of hematopoietic development*. Blood, 2005. **105**(12): p. 4598-603.
33. Xu, C., et al., *Basic fibroblast growth factor supports undifferentiated human embryonic stem cell growth without conditioned medium*. Stem Cells, 2005. **23**(3): p. 315-23.
34. Levenstein, M.E., et al., *Basic fibroblast growth factor support of human embryonic stem cell self-renewal*. Stem Cells, 2006. **24**(3): p. 568-74.
35. Sato, N., et al., *Maintenance of pluripotency in human and mouse embryonic stem cells through activation of Wnt signaling by a pharmacological GSK-3-specific inhibitor*. Nature Medicine, 2004. **10**(1): p. 55-63.
36. Fernandez, A., et al., *The WNT receptor FZD7 is required for maintenance of the pluripotent state in human embryonic stem cells*. Proceedings of the National Academy of Sciences of the United States of America, 2014. **111**(4): p. 1409-1414.

37. Dravid, G., et al., *Defining the role of Wnt/beta-catenin signaling in the survival, proliferation, and self-renewal of human embryonic stem cells*. Stem Cells, 2005. **23**(10): p. 1489-501.
38. Martin, M.J., et al., *Human embryonic stem cells express an immunogenic nonhuman sialic acid*. Nat Med, 2005. **11**(2): p. 228-32.
39. Garcia-Gonzalo, F.R. and J.C. Izpisua Belmonte, *Albumin-associated lipids regulate human embryonic stem cell self-renewal*. PLoS One, 2008. **3**(1): p. e1384.
40. Akopian, V., et al., *Comparison of defined culture systems for feeder cell free propagation of human embryonic stem cells*. In Vitro Cell Dev Biol Anim, 2010. **46**(3-4): p. 247-58.
41. Mallon, B.S., et al., *Toward xeno-free culture of human embryonic stem cells*. Int J Biochem Cell Biol, 2006. **38**(7): p. 1063-75.
42. Valamehr, B., et al., *Developing defined culture systems for human pluripotent stem cells*. Regenerative Medicine, 2011. **6**(5): p. 623-34.
43. Ludwig, T.E., et al., *Derivation of human embryonic stem cells in defined conditions*. Nature Biotechnology, 2006. **24**(2): p. 185-187.
44. Ludwig, T.E., et al., *Feeder-independent culture of human embryonic stem cells*. Nature Methods, 2006. **3**(8): p. 637-646.
45. Chen, G., et al., *Chemically defined conditions for human iPSC derivation and culture*. Nat Methods, 2011. **8**(5): p. 424-9.
46. Chen, G., et al., *Thermal stability of fibroblast growth factor protein is a determinant factor in regulating self-renewal, differentiation, and reprogramming in human pluripotent stem cells*. Stem Cells, 2012. **30**(4): p. 623-30.
47. Lotz, S., et al., *Sustained levels of FGF2 maintain undifferentiated stem cell cultures with biweekly feeding*. PLoS One, 2013. **8**(2): p. e56289.
48. Kumagai, H., et al., *Identification of small molecules that promote human embryonic stem cell self-renewal*. Biochemical and Biophysical Research Communications, 2013. **434**(4): p. 710-716.

49. Desbordes, S.C., et al., *High-throughput screening assay for the identification of compounds regulating self-renewal and differentiation in human embryonic stem cells*. Cell Stem Cell, 2008. **2**(6): p. 602-612.
50. Meng, G., et al., *Extracellular matrix isolated from foreskin fibroblasts supports long-term xeno-free human embryonic stem cell culture*. Stem Cells Dev, 2010. **19**(4): p. 547-56.
51. Choo, A.B., et al., *Expansion of pluripotent human embryonic stem cells on human feeders*. Biotechnology and Bioengineering, 2004. **88**(3): p. 321-31.
52. Hovatta, O., et al., *A culture system using human foreskin fibroblasts as feeder cells allows production of human embryonic stem cells*. Human Reproduction, 2003. **18**(7): p. 1404-1409.
53. Amit, M., et al., *Human feeder layers for human embryonic stem cells*. Biology of Reproduction, 2003. **68**(6): p. 2150-6.
54. Richards, M., et al., *Human feeders support prolonged undifferentiated growth of human inner cell masses and embryonic stem cells*. Nat Biotechnol, 2002. **20**(9): p. 933-6.
55. Cheng, L.Z., et al., *Human adult marrow cells support prolonged expansion of human embryonic stem cells in culture*. Stem Cells, 2003. **21**(2): p. 131-142.
56. Zhang, K., et al., *Utilization of human amniotic mesenchymal cells as feeder layers to sustain propagation of human embryonic stem cells in the undifferentiated state*. Cell Reprogram, 2011. **13**(4): p. 281-8.
57. Kim, S.J., et al., *Human placenta-derived feeders support prolonged undifferentiated propagation of a human embryonic stem cell line, SNUhES3: comparison with human bone marrow-derived feeders*. Stem Cells and Development, 2007. **16**(3): p. 421-8.
58. Miyamoto, K., et al., *Human placenta feeder layers support undifferentiated growth of primate embryonic stem cells*. Stem Cells, 2004. **22**(4): p. 433-40.

59. Escobedo-Lucea, C., et al., *Development of a Human Extracellular Matrix for Applications Related with Stem Cells and Tissue Engineering*. Stem Cell Reviews and Reports, 2012. **8**(1): p. 170-183.
60. Xu, C.H., et al., *Feeder-free growth of undifferentiated human embryonic stem cells*. Nature Biotechnology, 2001. **19**(10): p. 971-974.
61. Prowse, A.B.J., et al., *Stem cell integrins: Implications for ex-vivo culture and cellular therapies*. Stem Cell Research, 2011. **6**(1): p. 1-12.
62. Braam, S.R., et al., *Recombinant vitronectin is a functionally defined substrate that supports human embryonic stem cell self-renewal via alphavbeta5 integrin*. Stem Cells, 2008. **26**(9): p. 2257-65.
63. Manton, K.J., et al., *A chimeric vitronectin: IGF-I protein supports feeder-cell-free and serum-free culture of human embryonic stem cells*. Stem Cells Dev, 2010. **19**(9): p. 1297-305.
64. Ruoslahti, E., *The RGD story: a personal account*. Matrix Biol, 2003. **22**(6): p. 459-65.
65. Ruoslahti, E. and M.D. Pierschbacher, *New perspectives in cell adhesion: RGD and integrins*. Science, 1987. **238**(4826): p. 491-7.
66. Obara, M., M.S. Kang, and K.M. Yamada, *Site-directed mutagenesis of the cell-binding domain of human fibronectin: separable, synergistic sites mediate adhesive function*. Cell, 1988. **53**(4): p. 649-57.
67. Nishiuchi, R., et al., *Ligand-binding specificities of laminin-binding integrins: a comprehensive survey of laminin-integrin interactions using recombinant alpha3beta1, alpha6beta1, alpha7beta1 and alpha6beta4 integrins*. Matrix Biol, 2006. **25**(3): p. 189-97.
68. Humphrey, R.K., et al., *Maintenance of pluripotency in human embryonic stem cells is STAT3 independent*. Stem Cells, 2004. **22**(4): p. 522-530.
69. Baxter, M.A., et al., *Analysis of the distinct functions of growth factors and tissue culture substrates necessary for the long-term self-renewal of human embryonic stem cell lines*. Stem Cell Res, 2009. **3**(1): p. 28-38.

70. Braam, S.R., et al., *Recombinant vitronectin is a functionally defined substrate that supports human embryonic stem cell self-renewal via alpha V beta 5 integrin*. Stem Cells, 2008. **26**(9): p. 2257-2265.
71. Rodin, S., et al., *Long-term self-renewal of human pluripotent stem cells on human recombinant laminin-511*. Nat Biotechnol, 2010. **28**(6): p. 611-5.
72. Melkounian, Z., et al., *Synthetic peptide-acrylate surfaces for long-term self-renewal and cardiomyocyte differentiation of human embryonic stem cells*. Nat Biotechnol, 2010. **28**(6): p. 606-10.
73. Liu, Y., et al., *A novel chemical-defined medium with bFGF and N2B27 supplements supports undifferentiated growth in human embryonic stem cells*. Biochem Biophys Res Commun, 2006. **346**(1): p. 131-9.
74. Yap, L.Y., et al., *Defining a threshold surface density of vitronectin for the stable expansion of human embryonic stem cells*. Tissue Eng Part C Methods, 2011. **17**(2): p. 193-207.
75. Humphries, J.D., A. Byron, and M.J. Humphries, *Integrin ligands at a glance*. Journal of Cell Science, 2006. **119**(19): p. 3901-3903.
76. Leiss, M., et al., *The role of integrin binding sites in fibronectin matrix assembly in vivo*. Current Opinion in Cell Biology, 2008. **20**(5): p. 502-507.
77. Kalaskar, D.M., et al., *Characterization of the interface between adsorbed fibronectin and human embryonic stem cells*. Journal of the Royal Society Interface, 2013. **10**(83).
78. Doran, M.R., et al., *Defined high protein content surfaces for stem cell culture*. Biomaterials, 2010. **31**(19): p. 5137-42.
79. Kolhar, P., et al., *Synthetic surfaces for human embryonic stem cell culture*. J Biotechnol, 2010. **146**(3): p. 143-6.
80. Klim, J.R., et al., *A defined glycosaminoglycan-binding substratum for human pluripotent stem cells*. Nat Methods, 2010. **7**(12): p. 989-94.

81. Melkoumian, Z., et al., *Synthetic peptide-acrylate surfaces for long-term self-renewal and cardiomyocyte differentiation of human embryonic stem cells*. Nature Biotechnology, 2010. **28**(6): p. 606-U95.
82. Li, Z., et al., *Feeder-free self-renewal of human embryonic stem cells in 3D porous natural polymer scaffolds*. Biomaterials, 2010. **31**: p. 404-412.
83. Siti-Ismail, N., et al., *The benefit of human embryonic stem cell encapsulation for prolonged feeder-free maintenance*. Biomaterials, 2008. **29**: p. 3946-3952.
84. Lu, H.F., et al., *A 3D microfibrinous scaffold for long-term human pluripotent stem cell self-renewal under chemically defined conditions*. Biomaterials, 2012. **33**: p. 2419-2430.
85. Kim, J., P. Sachdev, and K. Sidhu, *Alginate microcapsule as a 3D platform for the efficient differentiation of human embryonic stem cells to dopamine neurons*. Stem Cell Research, 2013. **11**(3): p. 978-989.
86. Gerecht, S., et al., *Hyaluronic acid hydrogel for controlled self-renewal and differentiation of human embryonic stem cells*. Proc Natl Acad Sci U S A, 2007. **104**(27): p. 11298-303.
87. Kuo, Y.C. and Y.H. Chang, *Differentiation of induced pluripotent stem cells toward neurons in hydrogel biomaterials*. Colloids Surf B Biointerfaces, 2013. **102**: p. 405-11.
88. Carlson, A.L., et al., *Microfibrinous substrate geometry as a critical trigger for organization, self-renewal, and differentiation of human embryonic stem cells within synthetic 3-dimensional microenvironments*. FASEB, 2012. **26**: p. 3240-3251.
89. Gao, S.Y., et al., *Modeling the adhesion of human embryonic stem cells to poly(lactic-co-glycolic acid) surfaces in a 3D environment*. Journal of Biomedical Materials Research, 2010. **92A**: p. 683-692.
90. Chao, T.I., et al., *Poly(methacrylic acid)-grafted carbon nanotube scaffolds enhance differentiation of hESCs into neuronal cells*. Adv Mater, 2010. **22**(32): p. 3542-7.

91. Chao, T.I., et al., *Carbon nanotubes promote neuron differentiation from human embryonic stem cells*. *Biochem Biophys Res Commun*, 2009. **384**(4): p. 426-30.
92. Gerecht-Nir, S., S. Cohen, and J. Itskovitz-Eldor, *Bioreactor cultivation enhances the efficiency of human embryoid body (hEB) formation and differentiation*. *Biotechnol Bioeng*, 2004. **86**(5): p. 493-502.
93. Wang, X., et al., *Scalable producing embryoid bodies by rotary cell culture system and constructing engineered cardiac tissue with ES-derived cardiomyocytes in vitro*. *Biotechnol Prog*, 2006. **22**(3): p. 811-8.
94. Placzek, M.R., et al., *Stem cell bioprocessing: fundamentals and principles*. *J R Soc Interface*, 2009. **6**(32): p. 209-32.
95. Chen, A.K., et al., *Critical microcarrier properties affecting the expansion of undifferentiated human embryonic stem cells*. *Stem Cell Research*, 2011. **7**(2): p. 97-111.
96. Uludag, H., P. De Vos, and P.A. Tresco, *Technology of mammalian cell encapsulation*. *Adv Drug Deliv Rev*, 2000. **42**(1-2): p. 29-64.
97. Orive, G., et al., *Biocompatibility of microcapsules for cell immobilization elaborated with different type of alginates*. *Biomaterials*, 2002. **23**: p. 3825-3831.
98. Pasparakis, G. and N. Bouropoulos, *Swelling studies and in vitro release of verapamil from calcium alginate and calcium alginate–chitosan beads*. *International Journal of Pharmaceutics*, 2006. **323**: p. 34-42.
99. Erickson, G.R., et al., *Chondrogenic potential of adipose tissue-derived stromal cells in vitro and in vivo*. *Biochemical and Biophysical Research Communications* 2002. **290**: p. 763–769.
100. Jing, D., A. Parikh, and E.S. Tzanakakis, *Cardiac cell generation from encapsulated embryonic stem cells in static and scalable culture systems*. *Cell Transplantation*, 2010. **19**: p. 1397-1412.
101. Serra, M., et al., *Microencapsulation Technology: A Powerful Tool for Integrating Expansion and Cryopreservation of Human Embryonic Stem Cells*. *Plos One*, 2011. **6**(8).

102. Siti-Ismael, N., et al., *Development of a Novel Three-Dimensional, Automatable and Integrated Bioprocess for the Differentiation of Embryonic Stem Cells into Pulmonary Alveolar Cells in a Rotating Vessel Bioreactor System*. Tissue Engineering Part C-Methods, 2012. **18**(4): p. 263-272.
103. Consolo, F., et al., *Computational modeling for the optimization of a cardiogenic 3D bioprocess of encapsulated embryonic stem cells*. Biomechanics and Modeling in Mechanobiology, 2012. **11**(1-2): p. 261-277.
104. Hwang, Y.S., et al., *The use of murine embryonic stem cells, alginate encapsulation, and rotary microgravity bioreactor in bone tissue engineering*. Biomaterials, 2009. **30**(4): p. 499-507.
105. Dang, S.M., et al., *Controlled, scalable embryonic stem cell differentiation culture*. Stem Cells, 2004. **22**(3): p. 275-282.
106. Bauwens, C., et al., *Development of a perfusion fed bioreactor for embryonic stem cell-derived cardiomyocyte generation: Oxygen-mediated enhancement of cardiomyocyte output*. Biotechnology and Bioengineering, 2005. **90**(4): p. 452-461.
107. Clark, J.M. and M.D. Hirtenstein, *Optimizing culture conditions for the production of animal cells in microcarrier culture*. Ann N Y Acad Sci, 1981. **369**: p. 33-46.
108. van Wezel, A.L., *Growth of cell-strains and primary cells on microcarriers in homogeneous culture*. Nature, 1967. **216**(110): p. 64-5.
109. Varani, J., et al., *Use of recombinant and synthetic peptides as attachment factors for cells on microcarriers*. Cytotechnology, 1993. **13**(2): p. 89-98.
110. <http://www.weizmann.ac.il/plants/Milo/images/humanCellSize120116Clean.pdf>.
111. Schmidt, J.J., J. Jeong, and H. Kong, *The Interplay Between Cell Adhesion Cues and Curvature of Cell Adherent Alginate Microgels in Multipotent Stem Cell Culture*. Tissue Engineering Part A, 2011. **17**(21-22): p. 2687-2694.

112. Nie, Y., et al., *Scalable culture and cryopreservation of human embryonic stem cells on microcarriers*. Biotechnol Prog, 2009. **25**(1): p. 20-31.
113. Marinho, P.A., et al., *Xeno-free production of human embryonic stem cells in stirred microcarrier systems using a novel animal/human-component-free medium*. Tissue Eng Part C Methods, 2012.
114. Kurosawa, S., et al., *Olanzapine potentiates neuronal survival and neural stem cell differentiation: regulation of endoplasmic reticulum stress response proteins*. J Neural Transm, 2007. **114**(9): p. 1121-8.
115. Ungrin, M.D., et al., *Reproducible, ultra high-throughput formation of multicellular organization from single cell suspension-derived human embryonic stem cell aggregates*. PLoS One, 2008. **3**(2): p. e1565.
116. Torisawa, Y.S., et al., *Efficient formation of uniform-sized embryoid bodies using a compartmentalized microchannel device*. Lab on a Chip, 2007. **7**(6): p. 770-776.
117. Carpenedo, R.L., C.Y. Sargent, and T.C. McDevitt, *Rotary suspension culture enhances the efficiency, yield, and homogeneity of embryoid body differentiation*. Stem Cells, 2007. **25**(9): p. 2224-34.
118. Krawetz, R., et al., *Large-scale expansion of pluripotent human embryonic stem cells in stirred-suspension bioreactors*. Tissue Eng Part C Methods, 2010. **16**(4): p. 573-82.
119. Watanabe, K., et al., *A ROCK inhibitor permits survival of dissociated human embryonic stem cells*. Nat Biotechnol, 2007. **25**(6): p. 681-6.
120. Abbasalizadeh, S., et al., *Bioprocess development for mass production of size-controlled human pluripotent stem cell aggregates in stirred suspension bioreactor*. Tissue Eng Part C Methods, 2012. **18**(11): p. 831-51.
121. Schulz, T.C., et al., *A scalable system for production of functional pancreatic progenitors from human embryonic stem cells*. PLoS One, 2012. **7**(5): p. e37004.

122. Amit, M., et al., *Dynamic suspension culture for scalable expansion of undifferentiated human pluripotent stem cells*. Nature Protocols, 2011. **6**(5): p. 572-9.
123. Powers, D.E., et al., *Effects of oxygen on mouse embryonic stem cell growth, phenotype retention, and cellular energetics*. Biotechnology and Bioengineering, 2008. **101**(2): p. 241-254.
124. Wolfe, R.P. and T. Ahsan, *Shear stress during early embryonic stem cell differentiation promotes hematopoietic and endothelial phenotypes*. Biotechnol Bioeng, 2013. **110**(4): p. 1231-42.
125. O'Shea, K.S., *Embryonic stem cell models of development*. Anat Rec, 1999. **257**(1): p. 32-41.
126. Purpura, K.A., et al., *Systematic engineering of 3D pluripotent stem cell niches to guide blood development*. Biomaterials, 2012. **33**(5): p. 1271-80.
127. Carpenedo, R.L., et al., *Homogeneous and organized differentiation within embryoid bodies induced by microsphere-mediated delivery of small molecules*. Biomaterials, 2009. **30**(13): p. 2507-2515.
128. Ferreira, L., et al., *Human embryoid bodies containing nano- and microparticulate delivery vehicles*. Advanced Materials, 2008. **20**(12): p. 2285-+.
129. Van Hoof, D., K.A. D'Amour, and M.S. German, *Derivation of insulin-producing cells from human embryonic stem cells*. Stem Cell Research, 2009. **3**(2-3): p. 73-87.
130. Borowiak, M., *The new generation of beta-cells: replication, stem cell differentiation, and the role of small molecules*. Rev Diabet Stud, 2010. **7**(2): p. 93-104.
131. Gaur, T., et al., *Secreted frizzled related protein 1 regulates Wnt signaling for BMP2 induced chondrocyte differentiation*. Journal of Cellular Physiology, 2006. **208**(1): p. 87-96.
132. Shapiro, A.M.J., et al., *Islet transplantation in seven patients with type 1 diabetes mellitus using a glucocorticoid-free immunosuppressive regimen*. New England Journal of Medicine, 2000. **343**(4): p. 230-238.

133. Takahashi, K. and S. Yamanaka, *Induction of pluripotent stem cells from mouse embryonic and adult fibroblast cultures by defined factors*. Cell, 2006. **126**(4): p. 663-76.
134. Kroon, E., et al., *Pancreatic endoderm derived from human embryonic stem cells generates glucose-responsive insulin-secreting cells in vivo*. Nature Biotechnology, 2008. **26**(4): p. 443-452.
135. Jiang, J., et al., *Generation of insulin-producing islet-like clusters from human embryonic stem cells*. Stem Cells, 2007. **25**(8): p. 1940-53.
136. Wei, J.A., et al., *In vitro derivation of functional insulin-producing cells from human embryonic stem cells*. Cell Research, 2007. **17**(4): p. 333-344.
137. D'Amour, K.A., et al., *Production of pancreatic hormone-expressing endocrine cells from human embryonic stem cells*. Nature Biotechnology, 2006. **24**(11): p. 1392-1401.
138. Zhang, D.H., et al., *Highly efficient differentiation of human ES cells and iPS cells into mature pancreatic insulin-producing cells*. Cell Research, 2009. **19**(4): p. 429-438.
139. Kubo, A., et al., *Development of definitive endoderm from embryonic stem cells in culture*. Development, 2004. **131**(7): p. 1651-62.
140. D'Amour, K.A., et al., *Efficient differentiation of human embryonic stem cells to definitive endoderm*. Nat Biotechnol, 2005. **23**(12): p. 1534-41.
141. Hebrok, M., S.K. Kim, and D.A. Melton, *Notochord repression of endodermal Sonic hedgehog permits pancreas development*. Genes Dev, 1998. **12**(11): p. 1705-13.
142. Tian, T. and A.M. Meng, *Nodal signals pattern vertebrate embryos*. Cellular and Molecular Life Sciences, 2006. **63**(6): p. 672-685.
143. Tahamtani, Y., et al., *Stauprimide Priming of Human Embryonic Stem Cells toward Definitive Endoderm*. Cell J, 2014. **16**(1): p. 63-72.
144. Murtaugh, L.C., *Pancreas and beta-cell development: from the actual to the possible*. Development, 2007. **134**(3): p. 427-38.
145. Jorgensen, M.C., et al., *An illustrated review of early pancreas development in the mouse*. Endocrine Reviews, 2007. **28**(6): p. 685-705.

146. Pan, F.C., et al., *Retinoic acid-mediated patterning of the pre-pancreatic endoderm in Xenopus operates via direct and indirect mechanisms*. Mech Dev, 2007. **124**(7-8): p. 518-31.
147. Stafford, D. and V.E. Prince, *Retinoic acid signaling is required for a critical early step in zebrafish pancreatic development*. Current Biology, 2002. **12**(14): p. 1215-20.
148. Dessimoz, J., et al., *Pancreas-specific deletion of beta-catenin reveals Wnt-dependent and Wnt-independent functions during development*. Current Biology, 2005. **15**(18): p. 1677-83.
149. McLin, V.A., S.A. Rankin, and A.M. Zorn, *Repression of Wnt/beta-catenin signaling in the anterior endoderm is essential for liver and pancreas development*. Development, 2007. **134**(12): p. 2207-17.
150. Ober, E.A., et al., *Mesodermal Wnt2b signalling positively regulates liver specification*. Nature, 2006. **442**(7103): p. 688-91.
151. Serls, A.E., et al., *Different thresholds of fibroblast growth factors pattern the ventral foregut into liver and lung*. Development, 2005. **132**(1): p. 35-47.
152. Wells, J.M. and D.A. Melton, *Early mouse endoderm is patterned by soluble factors from adjacent germ layers*. Development, 2000. **127**(8): p. 1563-72.
153. Yasuda, M., et al., *Effects of growth factors on development of fetal islet B-cells in vitro*. Journal of Veterinary Medical Science, 2007. **69**(8): p. 807-11.
154. Cho, Y.M., et al., *Betacellulin and nicotinamide sustain PDX1 expression and induce pancreatic beta-cell differentiation in human embryonic stem cells*. Biochem Biophys Res Commun, 2008. **366**(1): p. 129-34.
155. Cai, J., et al., *Generation of homogeneous PDX1(+) pancreatic progenitors from human ES cell-derived endoderm cells*. J Mol Cell Biol, 2010. **2**(1): p. 50-60.

156. Shirasawa, S., et al., *A novel stepwise differentiation of functional pancreatic exocrine cells from embryonic stem cells*. *Stem Cells Dev*, 2011. **20**(6): p. 1071-8.
157. Maehr, R., et al., *Generation of pluripotent stem cells from patients with type 1 diabetes*. *Proc Natl Acad Sci U S A*, 2009. **106**(37): p. 15768-73.
158. Lock, L.T. and E.S. Tzanakakis, *Expansion and differentiation of human embryonic stem cells to endoderm progeny in a microcarrier stirred-suspension culture*. *Tissue Eng Part A*, 2009. **15**(8): p. 2051-63.
159. Bardy, J., et al., *Microcarrier suspension cultures for high-density expansion and differentiation of human pluripotent stem cells to neural progenitor cells*. *Tissue Eng Part C Methods*, 2013. **19**(2): p. 166-80.
160. Oh, S.K., et al., *Long-term microcarrier suspension cultures of human embryonic stem cells*. *Stem Cell Res*, 2009.
161. Fernandes, A.M., et al., *Successful scale-up of human embryonic stem cell production in a stirred microcarrier culture system*. *Braz J Med Biol Res*, 2009. **42**(6): p. 515-22.
162. Li, Y., et al., *Expansion of human embryonic stem cells in defined serum-free medium devoid of animal-derived products*. *Biotechnol Bioeng*, 2005. **91**(6): p. 688-98.
163. Lu, J., et al., *Defined culture conditions of human embryonic stem cells*. *Proc Natl Acad Sci U S A*, 2006. **103**(15): p. 5688-93.
164. Yao, S., et al., *Long-term self-renewal and directed differentiation of human embryonic stem cells in chemically defined conditions*. *Proc Natl Acad Sci U S A*, 2006. **103**(18): p. 6907-12.
165. Furue, M.K., et al., *Heparin promotes the growth of human embryonic stem cells in a defined serum-free medium*. *Proc Natl Acad Sci U S A*, 2008. **105**(36): p. 13409-14.
166. Ludwig, T.E., et al., *Derivation of human embryonic stem cells in defined conditions*. *Nat Biotechnol*, 2006. **24**(2): p. 185-7.
167. Ludwig, T.E., et al., *Feeder-independent culture of human embryonic stem cells*. *Nat Methods*, 2006. **3**(8): p. 637-46.

168. Chen, A.K., et al., *Critical microcarrier properties affecting the expansion of undifferentiated human embryonic stem cells*. *Stem Cell Res*, 2011. **7**(2): p. 97-111.
169. Marinho, P.A., et al., *Xeno-free production of human embryonic stem cells in stirred microcarrier systems using a novel animal/human-component-free medium*. *Tissue Eng Part C Methods*, 2013. **19**(2): p. 146-55.
170. Villa-Diaz, L.G., et al., *Synthetic polymer coatings for long-term growth of human embryonic stem cells*. *Nat Biotechnol*, 2010. **28**(6): p. 581-3.
171. Brafman, D.A., et al., *Long-term human pluripotent stem cell self-renewal on synthetic polymer surfaces*. *Biomaterials*, 2010. **31**(34): p. 9135-9144.
172. Mei, Y., et al., *Combinatorial development of biomaterials for clonal growth of human pluripotent stem cells*. *Nature materials*, 2010. **9**(9): p. 768-78.
173. Irwin, E.F., et al., *Engineered polymer-media interfaces for the long-term self-renewal of human embryonic stem cells*. *Biomaterials*, 2011. **32**(29): p. 6912-9.
174. Kilian, K.A., et al., *Geometric cues for directing the differentiation of mesenchymal stem cells*. *Proc Natl Acad Sci U S A*, 2010. **107**(11): p. 4872-7.
175. Engler, A.J., et al., *Matrix elasticity directs stem cell lineage specification*. *Cell*, 2006. **126**(4): p. 677-89.
176. McBeath, R., et al., *Cell shape, cytoskeletal tension, and RhoA regulate stem cell lineage commitment*. *Dev Cell*, 2004. **6**(4): p. 483-95.
177. Kehoe, D.E., et al., *Propagation of Embryonic Stem Cells in Stirred Suspension without Serum*. *Biotechnol Prog*, 2008. **24**(6): p. 1342-52.
178. Wu, J. and E.S. Tzanakakis, *Contribution of Stochastic Partitioning at Human Embryonic Stem Cell Division to NANOG Heterogeneity*. *PLoS One*, 2012. **7**(11): p. e50715.
179. Nat, R., et al., *Neurogenic neuroepithelial and radial glial cells generated from six human embryonic stem cell lines in serum-free suspension and adherent cultures*. *Glia*, 2007. **55**(4): p. 385-99.

180. Jing, D., *Investigation of the cardiogenic differentiation of human pluripotent stem cells in static cultures and stirred-suspension bioreactors*, 2010, State University of New York at Buffalo: United States -- New York. p. 188.
181. Jing, D., A. Parikh, and E.S. Tzanakakis, *Cardiac cell generation from encapsulated embryonic stem cells in static and scalable culture systems*. Cell Transplant, 2010. **19**(11): p. 1397-412.
182. McKeehan, W.L., *Use of basic polymers as synthetic substrata for cell culture*, in *Methods for preparation of media, supplements, and substrata for serum-free animal cell culture*, D.W. Barnes, D.A. Sirbasku, and G.H. Sato, Editors. 1984, Alan R. Liss, Inc.: New York. p. 209-213.
183. Ang, S.L., et al., *The formation and maintenance of the definitive endoderm lineage in the mouse: involvement of HNF3/forkhead proteins*. Development, 1993. **119**(4): p. 1301-15.
184. Sasaki, H. and B.L. Hogan, *Differential expression of multiple fork head related genes during gastrulation and axial pattern formation in the mouse embryo*. Development, 1993. **118**(1): p. 47-59.
185. Lin, L., et al., *Beta-catenin directly regulates Islet1 expression in cardiovascular progenitors and is required for multiple aspects of cardiogenesis*. Proc Natl Acad Sci U S A, 2007. **104**(22): p. 9313-8.
186. Petropoulos, H., et al., *Disruption of Meox or Gli activity ablates skeletal myogenesis in P19 cells*. J Biol Chem, 2004. **279**(23): p. 23874-81.
187. Kattman, S.J., T.L. Huber, and G.M. Keller, *Multipotent flk-1+ cardiovascular progenitor cells give rise to the cardiomyocyte, endothelial, and vascular smooth muscle lineages*. Dev Cell, 2006. **11**(5): p. 723-32.
188. Yap, L.Y., et al., *Defining a threshold surface density of vitronectin for the stable expansion of human embryonic stem cells*. Tissue engineering. Part C, Methods, 2011. **17**(2): p. 193-207.
189. Heng, B.C., et al., *Translating human embryonic stem cells from 2-dimensional to 3-dimensional cultures in a defined medium on laminin- and vitronectin-coated surfaces*. Stem Cells Dev, 2012. **21**(10): p. 1701-15.

190. Lu, H., et al., *Effects of poly(L-lysine), poly(acrylic acid) and poly(ethylene glycol) on the adhesion, proliferation and chondrogenic differentiation of human mesenchymal stem cells*. J Biomater Sci Polym Ed, 2009. **20**(5-6): p. 577-89.
191. Hughes, C.S., L.M. Postovit, and G.A. Lajoie, *Matrigel: a complex protein mixture required for optimal growth of cell culture*. Proteomics, 2010. **10**(9): p. 1886-90.
192. Lecina, M., et al., *Scalable platform for human embryonic stem cell differentiation to cardiomyocytes in suspended microcarrier cultures*. Tissue Eng Part C Methods, 2010. **16**(6): p. 1609-19.
193. Lee, J.E., et al., *Characterization of UV-irradiated dense/porous collagen membranes: morphology, enzymatic degradation, and mechanical properties*. Yonsei Med J, 2001. **42**(2): p. 172-9.
194. Yamazoe, H., T. Uemura, and T. Tanabe, *Facile cell patterning on an albumin-coated surface*. Langmuir, 2008. **24**(16): p. 8402-4.
195. Lye, T.L., *Expansion and Directed Differentiation of Human Pluripotent Stem Cells to Insulin-Producing Cells in a Stirred-Suspension Microcarrier System*, 2010, SUNY Buffalo.
196. Vincent, S.D., et al., *Cell fate decisions within the mouse organizer are governed by graded Nodal signals*. Genes Dev, 2003. **17**(13): p. 1646-62.
197. Afrikanova, I., et al., *Inhibitors of Src and focal adhesion kinase promote endocrine specification: impact on the derivation of beta-cells from human pluripotent stem cells*. Journal of Biological Chemistry, 2011. **286**(41): p. 36042-52.
198. Mfopou, J.K., B. Chen, and I. Mateizel, *Noggin, retinoids, and fibroblast growth factor regulate hepatic or pancreatic fate of human embryonic stem cells (vol 138, pg 2233, 2010)*. Gastroenterology, 2010. **139**(6): p. 2224-2224.
199. Stafford, D., et al., *A conserved role for retinoid signaling in vertebrate pancreas development*. Development Genes and Evolution, 2004. **214**(9): p. 432-41.

200. Chiang, M.K. and D.A. Melton, *Single-cell transcript analysis of pancreas development*. *Developmental Cell*, 2003. **4**(3): p. 383-393.
201. Gittes, G.K., *Developmental biology of the pancreas: a comprehensive review*. *Developmental Biology*, 2009. **326**(1): p. 4-35.
202. Mfopou, J.K., et al., *Recent Advances and Prospects in the Differentiation of Pancreatic Cells From Human Embryonic Stem Cells*. *Diabetes*, 2010. **59**(9): p. 2094-2101.
203. Lau, J., H. Kawahira, and M. Hebrok, *Hedgehog signaling in pancreas development and disease*. *Cellular and Molecular Life Sciences*, 2006. **63**(6): p. 642-52.
204. Nostro, M.C., et al., *Stage-specific signaling through TGF{beta} family members and WNT regulates patterning and pancreatic specification of human pluripotent stem cells*. *Development*, 2011. **138**(5): p. 861-71.
205. D'Amour, K.A., et al., *Production of pancreatic hormone-expressing endocrine cells from human embryonic stem cells*. *Nat Biotechnol*, 2006. **24**(11): p. 1392-401.
206. Johannesson, M., et al., *FGF4 and retinoic acid direct differentiation of hESCs into PDX1-expressing foregut endoderm in a time- and concentration-dependent manner*. *PLoS One*, 2009. **4**(3): p. e4794.
207. Semb, H., *Definitive endoderm: a key step in coaxing human embryonic stem cells into transplantable beta-cells*. *Biochem Soc Trans*, 2008. **36**(Pt 3): p. 272-5.